ABSTRACT

ANTONELLI, TIMOTHY DAVID. Population Dynamics Models for *Wolbachia* and its Host, the Dengue Vector *Aedes aegypti*. (Under the direction of Alun Lloyd and Fred Gould.)

Dengue remains an important mosquito-borne disease in many tropical and subtropical regions around the world. Controlling its primary vector, *Aedes aegypti*, has proven difficult, and attention has turned to developing novel control strategies. One such strategy is to release *Ae. aegyti* that have been infected with the bacterium *Wolbachia*. *Wolbachia* is able to spread in a population and has been shown to block the replication of dengue virus within the mosquito. Mathematical models are a useful tool in determining whether and how quickly *Wolbachia* is expected to spread. In this thesis, multiple models for *Wolbachia* and *Ae. aegypti* dynamics are developed and analyzed.

With an ordinary differential equation model for a well-mixed insect population, we examine the interactions of density-dependent population dynamics and changes in the proportion of *Wolbachia*-infected individuals. Due to maternal inheritance of *Wolbachia* and its ability to manipulate host reproduction, population genetic models are typically used to model changes in the frequency of *Wolbachia* in a population. Because changes in frequency occur on the same time scale as ecological processes, we instead develop a model that incorporates mosquito population dynamics, and we show how changes in mosquito population size can affect the spread of *Wolbachia*. In particular, the frequency threshold that must be exceeded for *Wolbachia* to spread depends on the size of the population relative to its carrying capacity. We find that suppressing the population prior to release lowers the frequency threshold, making it easier for *Wolbachia* to spread.

Developing this work further with a reaction-diffusion model, we examine how *Wolbachia* may spread spatially. We find that density dependence affects how quickly *Wolbachia* spreads in space and depends on whether it acts on the per capita emergence rate of new adults or the per capita death rate. We also examine the effects of stochastic dynamics and spatial heterogeneity

in a metapopulation model that simulates mating and dispersal. Here we find that spatial heterogeneity consistently slows spread of *Wolbachia*, and that the effect of stochasticity on spread depends on whether the fitness cost of *Wolbachia* is low or high.

We carry out an experiment for *Ae. aegypti* growth in Iquitos, Peru, where we monitor the immature life stages of individual mosquitoes over time. With a Markov chain model, we derive the likelihood of parameter values and use Bayesian methods to analyze the data. We find that the amount of time that water accumulates debris in the field increases the average amount of food in a container and that the presence of food, rather than quantity or quality, determines immature growth rates. Blocking containers by house explains little of the variation in growth rates, indicating that containers within a house do not tend to be similar in their suitability for *Ae. aeypti* growth.

We demonstrate the various ways in which mathematical models can provide meaningful insights into *Wolbachia* and *Ae. aegypti* dynamics. By combining theoretical and experimental results, we aim to paint a clearer picture of what to expect in field releases of *Wolbachia* in order to develop the most efficient strategies for suppressing pest populations like *Ae. aegypti*.

Population Dynamics Models for *Wolbachia* and its Host, the Dengue Vector *Aedes aegypti*

by
Timothy David Antonelli

A dissertation submitted to the Graduate Faculty of
North Carolina State University
in partial fulfillment of the
requirements for the Degree of
Doctor of Philosophy

Biomathematics

Raleigh, North Carolina

2015

APPROVED BY:

Kevin Gross	Andrew Binder
Alun Lloyd Co-chair of Advisory Committee	Fred Gould Co-chair of Advisory Committee

DEDICATION

To my wonderful family:

Mom, Dad, Kristen, Tyler, Daniel

BIOGRAPHY

Tim was born on a cool spring evening in Orlando, FL. His father's position in the Navy moved him all over the country until he settled among the sandy beaches of Wilmington, NC. He attended New Hanover High School, where he excelled in math and science and did not excel in things like history. He assumed this destined him to be an engineer like his father, and he got his bachelor's degree in biomedical and electrical engineering from Duke University in 2008. After two years working at a small engineering firm, he decided he really just liked math and science, and he attended North Carolina State University for a less practical and more fun combination of his interests. Beginning in fall 2015, he will be sharing his love of math and science as a professor of statistics and probability at Worcester State University.

ACKNOWLEDGEMENTS

First and foremost, I thank my co-advisors Alun Lloyd and Fred Gould, who let me blaze my own path while also keeping me focused, highlighting the key biological questions and steering me away from the many mathematical rabbit holes. Their guidance, support, and high expectations kept me interested and motivated throughout my time at NC State.

I also thank my committee members: Kevin Gross and Andy Binder, whose wide range of expertise challenged me and whose advice on the various facets of my work helped me assemble a dissertation from the many diverse projects in which I was involved. I thank Brian Reich as well, whose class and help with Bayesian methods were instrumental in the completion of the fourth chapter.

To my family, who supported me while I figured out what I wanted to do with my life, who gave me sound advice, and who constantly reminded me to not take myself too seriously.

To my biomath family, I never could have done this without you. You made me feel welcome from day one, and you were always there when I needed you. Jess, thank you for taking care of me. Your ability to put others before yourself is an inspiration. Jake, thank you for the mid-afternoon walks, and Caitlin for the many wonderful homemade treats. Greg, for never failing to put a smile on my face and a song in my head. And to Michael for showing me the ropes when I arrived and for being such a good friend throughout the years. To all the students with whom I interacted over the years: you helped create some of the fondest memories of my life, for which I will always be grateful.

To my IGERT friends: Gabe, Amanda, Molly, Sophia, Will, and Carolyn, and the faculty mentors: Fred, Alun, Yasmin, Nora, Andy, Zack, Matthew, Will, Bill. You all created such a singular graduate experience that I will always cherish and that I feel very fortunate to have been able to take a part of.

To my collaborators in Iquitos, especially Amy, Gaby, Helvio and John: thank you for all your help and for being so patient with my Spanish.

Zach and Mandy, the Monday night meals and game nights were a much needed respite. Thank you for holding me to them.

Finally, to Diego. I never could have imagined that a summer trip to Peru to study mosquitoes would change my life in so many wonderful and challenging ways. It hasn't been easy, but thank you for believing in me and giving so much to make this work. I look forward to starting this next chapter with you. I love you.

TABLE OF CONTENTS

LIST OF TABLES

LIST OF FIGURES

Chapter 1

Introduction

1.1 Background

Dengue is a mosquito-borne viral disease that affects nearly 390 million people each year (Bhatt et al., 2013). The disease can present a wide variety of symptoms ranging from fever, rash and severe joint pain to internal hemorrhaging and death. It is endemic in many dense urban tropical regions where containers with standing water serve as larval development sites for *Ae. aegypti*, the principal vector of the virus. Female *Ae. aegypti* adults are highly anthropophilic, meaning they prefer to take bloodmeals from humans rather than other warm-blooded animals, which contributes to transmission of the disease. There is currently no licensed vaccine or treatment for dengue, and so control efforts have mainly focused on controlling the mosquito population. However, traditional control methods such as insecticide and reduction of larval habitats have had limited success in controlling the disease (Morrison et al., 2008).

Recently, there has been interest in developing novel technologies, such as releasing genetically modified mosquitoes or mosquitoes that have been infected with the maternally-inherited bacterium *Wolbachia* (Gould et al., 2006). These strategies require an anti-pathogen effect as well as a gene drive mechanism that allows the gene or bacterium to spread through the population despite any fitness cost caused by its insertion. *Wolbachia* accomplishes both of these by directly blocking transmission of the dengue virus (Walker et al., 2011) and by manipulating host reproduction through a phenomenon called cytoplasmic incompatibility (CI), by which most to all offspring fail to develop when *Wolbachia*-infected males mate with wild-type females (Werren, 1997). In other words, wild-type females become partially sterile in the presence of *Wolbachia*-infected males, such that *Wolbachia*-infected females may give rise to more offspring on average. Since the bacterium is only passed from mother to offspring, this can cause the overall frequency of *Wolbachia* infection, i.e. the fraction of infected individuals, to increase in a population over time.

When the insertion of *Wolbachia* causes a fitness cost to the host, e.g. by reducing average lifespan or number of eggs laid, then there is a critical frequency of infection that must be exceeded before the driving effect of cytoplasmic incompatibility outweighs the fitness cost,

such that the frequency of *Wolbachia* increases until it is established in the population. Below this threshold, the fitness cost causes wild-type hosts to outcompete *Wolbachia*-infected hosts, and the frequency of *Wolbachia* is expected to decrease over time, which will eventually result in extinction. Determining this threshold is critically important for efforts to replace wild disease-carrying mosquito populations with those less competent to vector disease.

Mathematical models can be a useful tool in assessing the feasibility of various vector control strategies, whether the goal is population replacement, as with *Wolbachia*, or population suppression, as with the release of insects with a lethal gene (Fu et al., 2010). While many previous models for *Wolbachia* dynamics have been developed, few have included the interactions of population dynamics (e.g. logistic growth) with population genetics (e.g. the frequency of an allele in a population). Population dynamics models for *Ae. aegypti* have also been developed, but field data needed to parameterize them is still lacking.

1.2 Outline

In this dissertation, I develop and analyze mathematical models for *Wolbachia* and *Ae. aegypti* dynamics, with the goal of bettering predictions for dengue control efforts. In Chapter 2, I explore how density dependence in population dynamics affects predictions for the spread of *Wolbachia* in a well-mixed population, and I compare results to both frequency-only and other density-dependent models. In Chapter 3, I incorporate the model from Chapter 2 into a reaction-diffusion model, which also accounts for spatial spread of *Wolbachia*. I compare the results for this simple model to a simulation model with both one-dimensional and two-dimensional spatial spread, which incorporates spatial heterogeneity in *Ae. aegypti* habitat as well as stochastic population dynamics. In many cases, these models give predictions regarding whether and how quickly *Wolbachia* will spread that are different from previous models, and I attempt to generalize under what conditions results differ and in what way. In both Chapters 2 and 3, I show when density dependence helps spread of *Wolbachia* and when it inhibits spread, which has implications for optimizing release strategies.

In Chapter 4, I emphasize the importance of parameterizing models for *Ae. aegypti* with field data. I develop and perform an experiment for *Ae. aegypti* larval growth in Iquitos, Peru. I then construct a framework using a continuous-time Markov chain (CTMC) model that can be used to obtain maximum likelihood estimates for development and mortality rates, as well as make statistical inferences about larval growth in Iquitos by incorporating two Markov chain Monte Carlo (MCMC) algorithms: Metropolis sampling and Gibbs sampling. This work can be used to inform future experiments for *Ae. aegypti* dynamics in dengue-endemic regions, and may be applied more generally to other life-stage CTMC models.

1.3 Other work

In addition to my dissertation work, I also had the privilege of working with several Ph.D. students from various disciplines on the many multi-faceted issues surrounding the use of genetic engineering to control dengue. As part of an NSF IGERT grant (IGERT-1068676), we looked not only at the feasibility of these technologies, but the ethical and social implications of their use. Together, we wrote an introductory chapter to a book on the genetic control of malaria and dengue, which has been accepted for publication. This chapter is attached in Appendix F. Note that we contributed equally to this work and all authors are listed alphabetically by last name.

Chapter 2

Eco-evolutionary feedback in models for *Wolbachia* and other gene drive strategies[1]

1. The content of this chapter has been submitted for publication: Antonelli T, Robert MA, Lloyd AL. Eco-evolutionary feedback in models for *Wolbachia* and other gene drive strategies.

ABSTRACT

Mathematical models for the spread of *Wolbachia* can be broadly categorized into those that neglect population dynamics and those that include population dynamics. Those that neglect population dynamics, i.e. frequency-only models, have been important in developing theoretical insights such as the existence of a frequency threshold under certain conditions and the traveling wave solution of *Wolbachia* spatial spread. Those that include population dynamics have shown that age-structure, delay due to larval stage, and density-dependent population growth can affect whether this frequency threshold is an accurate predictor of the eventual fate of *Wolbachia* (establishment or extinction). We focus on the latter type of model and show how only two effects are required to cause the invasion threshold to depend on population size: density-dependent growth and a lifespan-shortening strain of *Wolbachia*. In this way, we isolate key factors that, when present, necessitate the inclusion of population dynamics in developing accurate models. The mathematical simplicity of our approach allows for equilibrium and stability analysis, enabling us to quantify these effects, as well as generalize to other species and gene drive systems, such as underdominance.

2.1 Introduction

There is considerable interest in modeling the dynamics of *Wolbachia* to determine the conditions under which *Wolbachia* is predicted to become established in a population. Several deterministic models have been developed to examine the effects of imperfect maternal transmission (i.e. infected females produce some uninfected offspring), incomplete cytoplasmic incompatibility (CI) (i.e. mating between infected males and uninfected females produce some viable offspring), and fitness costs on the predicted spread of *Wolbachia* in a single well-mixed population. The majority of these models neglect changes in population size (Barton, 1979; Caspari and Watson, 1959; Fine, 1978; Rasgon, 2008; Schofield, 2002; Schraiber et al., 2012; Turelli and Hoffmann, 1991). While neglecting population size is a common simplifying assumption in population genetics, it assumes that evolutionary and ecological processes occur on different time scales. Recently, however, there has been increasing awareness of the interaction between ecology and evolution in systems that exhibit "rapid" evolution (Sanchez and Gore, 2013; Schoener, 2011), which Hairston et al. (2005) defines as "a genetic change occurring rapidly enough to have a measurable impact on simultaneous ecological change." *Wolbachia*, though a heritable bacterium rather than gene, fits this description because the frequency-dependent selection for *Wolbachia*-infected insects (an evolutionary process) depends critically on its ability to induce CI, which affects the average growth rate of the population (an ecological process). Thus, these two forces are inherently tied in an eco-evolutionary feedback loop that may cause non-intuitive results not captured by frequency-only models.

Some models of *Wolbachia* include population dynamics, but they either do not compare their results to frequency-only models (Chan and Kim, 2013; Farkas and Hinow, 2010; Keeling et al., 2003), or they are highly detailed and thus less amenable to analysis or generalizations about other species or genetic systems (Hancock et al., 2011). Keeling et al. (2003) derive a system of equations to track numbers of infected and uninfected individuals using a linearly increasing density-dependent per capita death rate, but they do not examine how such density-dependent mortality affects spread, and focus instead on multiple strains and spatial dynamics.

Farkas and Hinow (2010) use a similar model, but do not specifically look at the effect of density dependence on the invasion threshold. Hancock et al. (2011) determine that density-dependent mortality can have a number of effects on the spread of *Wolbachia*, such as impacting the number of mosquitoes needed to be released and when to release them (either when the population is expanding or decreasing). They were able to perform certain analyses, such as how the frequency threshold depends on their model parameters, including a constant rate of immigration, but they also showed how simulation results disagreed with analytical results for release strategies that involve a large perturbation from the population equilibrium. Although they attribute differences between analytical and simulation results to density dependence, their model includes many other features, such as age-structure and delay due to time spent in the larval stage, and so the direct effect of density dependence is difficult to isolate. In order to answer the question of the effect of density dependence on the spread of *Wolbachia* and to generalize to other species and genetic systems, we believe that the simplest model that can reproduce these effects is preferable. Such a model can bridge the gap between frequency-only models, which are less biologically relevant, and highly detailed, system-specific models, which are difficult to analyze mathematically.

In this chapter, we aim to elucidate the impact of density dependence on the spread of *Wolbachia* by comparing two simple continuous-time models: a population dynamics model that includes density dependence and a recent frequency-only model (Schraiber et al., 2012). We first construct a population dynamics model for *Wolbachia*-infected and uninfected individuals. Next, we describe the mathematical implications of assuming a constant population size and show how this reduces the model to Schraiber et al.'s (2012) model. We then explore various release scenarios and demonstrate how results from the frequency-only model differ from the population dynamics model. Finally, using the example of underdominance, we show that the inclusion of density dependence may affect predictions for other gene drive systems that typically rely on frequency-only models.

2.2 Models

We adapt an ordinary differential equation model from Keeling et al. (2003), in which population size can vary. We assume a constant sex ratio of 1:1, such that we need only track females. *Wolbachia* is not expected to skew the sex ratio in a population of *Ae. aegypti*: although it has an asymmetric effect on the fecundity of different mating pairs based on sex and infection status, the resulting offspring are expected to be equal numbers males and females, independent of the cytoplasmic compatibility of their parents. However, *Wolbachia* is known to cause feminization of males in other species (Werren, 1997), so this assumption will need to be assessed for each host species in question.

We consider both *Wolbachia*-infected adult females, $I(t)$, and uninfected adult females, $U(t)$, in a population that is regulated by intraspecific competition in the larval stage. We do not model immature dynamics explicitly, but instead use the adult population as a proxy by considering the emergence rate of new adults, $b(N)$, to be a decreasing function of the total adult female population size, $N(t) = I(t) + U(t)$. Like Keeling et al. (2003), we neglect the delay in density dependence due to time spent in the larval stage (see Hancock et al. 2011 and Zheng et al. 2014 for more detailed models that incorporate developmental delay). We assume that adult females experience a constant per capita death rate d and that *Wolbachia* may cause an additional per capita death rate D in infected females. We further assume that *Wolbachia* may cause a reduction in the number of eggs laid, such that the average rate at which infected females lay eggs relative to uninfected females is $1 - s_f$, where $0 \leq s_f \leq 1$ ($s_f = 0$ indicates infected females lay eggs at the same rate as uninfected females). To incorporate CI, we assume that the viability of offspring from matings between infected fathers and uninfected mothers is $1 - s_h$, where $0 < s_h \leq 1$ ($s_h = 1$ represents complete CI.) As in Schraiber et al. (2012), we assume perfect maternal transmission of *Wolbachia*. The parameters are summarized in Table

Table 2.1: Parameters in frequency-only model (Schraiber et al. 2012) and population dynamics model.

	Notation	
Description	Population Dynamics Model	Schraiber et al. (2012)
Per capita emergence rate of uninfected adults when no infected individuals are present	$b(N)$	b
Per capita emergence rate of infected adults	$b(N)(1-s_f)$	b_i
Per capita death rate of infected adults	$d+D$	d_i
Per capita death rate of uninfected adults	d	d_u
Reduction in birth rate due to CI	s_h	s_h
Total fitness cost of *Wolbachia* infection	$s_T = \frac{s_f d + D}{d+D}$	$1 - \frac{d_u}{d_i}\frac{b_i}{b}$

2.1. Our model consists of the coupled differential equations in Eq. 2.1:

$$\frac{dI}{dt} = \big(b(N)(1-s_f) - (d+D)\big)I \tag{2.1a}$$

$$\frac{dU}{dt} = \left(b(N)\left(1 - s_h\frac{I}{I+U}\right) - d\right)U. \tag{2.1b}$$

Our model differs from that of Keeling et al. (2003) in that we consider a constant per capita death rate d and instead incorporate density dependence into the emergence rate, $b(N)$, in order to model competition in the larval stage rather than the adult stage. For an analysis of other forms of density dependence, including the one assumed by Keeling et al. (2003), see

Appendix A.

In order to study the relationship between the frequency of *Wolbachia* and population size, we use the quotient rule to rewrite the model in terms of the frequency of *Wolbachia* $p = I/N$ and total female population size N (see Appendix A).

$$\frac{dp}{dt} = p(1-p)\big(b(N)(s_h p - s_f) - D\big) \tag{2.2a}$$

$$\frac{dN}{dt} = \big(b(N)(1 - s_f p - s_h p(1-p)) - (d + Dp)\big)N. \tag{2.2b}$$

If we were to assume a constant population size (i.e. $dN/dt = 0$), then Eq. 2.2 would imply that

$$b(N) = \frac{d + Dp}{1 - s_f p - s_h p(1-p)}\,. \tag{2.3}$$

Thus, the emergence rate would then be independent of N and would initially increase in p. This is likely not characteristic of natural populations, in which we expect density-dependent effects to act equally on infected and uninfected mosquitoes in the larval stage (i.e. independent of p) and, by definition, to depend on population size N. Yet this is what is required mathematically to maintain a constant population size in the model. To see that this is an implicit assumption in Schraiber et al's (2012) model, we can substitute Eq. 2.3 into Eq. 2.2b and recover their model (Eq. 2.4). Parameters for our population dynamics model are described and listed with

corresponding parameters from the Schraiber et al. (2012) model in Table 2.1.

$$\frac{dp}{dt} = \frac{s_h d\, p(1-p)(p-\hat{p})}{1 - s_f p - s_h p(1-p)} \tag{2.4a}$$

$$\hat{p} = \frac{1}{s_h}\frac{s_f d + D}{d + D} \tag{2.4b}$$

Their model is therefore a specific case of the model we present in Eq. 2.2, in which the emergence rate is artificially inflated at intermediate frequencies of *Wolbachia* to compensate for fewer births due to CI.

We specify a new emergence rate that depends only on population size and not on the frequency of infected mosquitoes. For simplicity, we assume a per capita emergence rate that decreases linearly with population size and satisfies the following properties: $b(0) = b_0$ and $b(K) = d$, where $b_0 > d$, and K is the carrying capacity of the wild-type population. We further assume that the emergence rate is non-negative, since a negative emergence rate is not biologically meaningful. Thus, the formula for the emergence rate is

$$b(N) = \begin{cases} b_0\left(1 - \dfrac{N}{K}\right) + d\dfrac{N}{K}, & 0 \leq N < \dfrac{b_0 K}{b_0 - d} \\ 0, & N \geq \dfrac{b_0 K}{b_0 - d}\,. \end{cases} \tag{2.5}$$

2.3 Results

2.3.1 Single Release

We first compute the basic reproductive number for both infected (R_I) and uninfected (R_U) individuals, defined as the average number of female offspring that a female adult produces when there is no density dependence and no CI. The average lifespan of an individual with per capita death rate d is $1/d$, and the average number of female offspring that a single female

produces is the emergence rate, b, multiplied by the average lifespan. Thus,

$$R_I = \frac{b_0(1-s_f)}{d+D},\ R_U = \frac{b_0}{d}\,. \tag{2.6}$$

If we assume that the effects of *Wolbachia* on survival and fecundity are multiplicative, then we can define the total fitness cost as $s_T = 1 - w_v w_f$, where $w_v = d/(d+D)$ is the relative lifespan of infected females and $w_f = (1-s_f)$ is the relative fecundity of infected females. Thus,

$$s_T = 1 - \frac{d}{d+D}(1-s_f) = \frac{s_f d + D}{d+D}\,. \tag{2.7}$$

With the density-dependent emergence rate in Eq. 2.5, the system in Eq. 2.2 has six equilibria, the coordinates and stability of which are summarized in Table 2.2 and depicted in Figure 2.1. Note that, although p is undefined when $N = 0$, we analyze the model behavior around these points because solutions can exist arbitrarily close to $N = 0$. Also, note that the absolute size of the population is not important. Rather, the current fraction of carrying capacity is all that is needed for analysis, and so our results generalize to any population size, provided the population is large enough so that a deterministic model is appropriate.

Equilibria 2, 4, and 6 correspond to those seen in frequency-only models, where equilibrium 4 is the frequency threshold, and equilibria 2 and 6 represent the *Wolbachia*-free and *Wolbachia*-established equilibria, respectively. However, as noted by several population dynamics models (Hancock et al., 2011; Zheng et al., 2014), the dynamics are not governed by frequency alone. We are able to identify the range of initial conditions that lead to establishment when p is less than the threshold predicted by frequency-only models, as well as initial conditions that lead to extinction when p is greater than the threshold predicted by frequency-only models. The fate of *Wolbachia* depends on both initial frequency and initial population size according to the curvature of the separatrix of the system (solid line in Figure 2.1). In Figure A.7, we show how the strength of density dependence affects the degree of this curvature. If the invasion threshold were independent of population size, the separatrix would be a vertical line in p-N

Table 2.2: Equilibria (p^*, N^*) and stability conditions for population dynamics model. Entries in bold represent biologically relevant conditions that are assumed throughout and depicted in Figure 1. Stability conditions were found by analyzing the Jacobian evaluated at each point. See Appendix A for detailed stability analysis.
†: A necessary but not sufficient condition for stability.
††: A sufficient but not necessary condition for instability.

	p^*	N^*	Stable	Unstable
1.	0	0	$R_U < 1$	$\boldsymbol{R_U > 1}$
2.	0	K	$\boldsymbol{R_U > 1}$	$R_U < 1$
3.	$\frac{1}{s_h}\left(s_f + \frac{D}{b_0}\right)$	0	$R_I < 1^{\dagger}$	$\boldsymbol{R_I > 1}^{\dagger\dagger}$
4.	$\frac{s_T}{s_h}$	$\left(\frac{1 - R_I^{-1}}{1 - R_U^{-1}}\right) K$	$R_I < 1,^{\dagger}$ $s_h < s_T$	$\boldsymbol{R_I > 1},^{\dagger\dagger}$ $\boldsymbol{s_h > s_T}$
5.	1	0	$R_I < 1^{\dagger}$	$\boldsymbol{R_I > 1}^{\dagger\dagger}$
6.	1	$\left(\frac{1 - R_I^{-1}}{1 - R_U^{-1}}\right) K$	$\boldsymbol{R_I > 1}$, $\boldsymbol{s_h > s_T}$	$R_I < 1$, $s_h < s_T$

space. Under the assumption of perfect maternal transmission, most previous models determine the frequency threshold to be $\hat{p} = s_T/s_h$, which corresponds to equilibrium 4 (Chan and Kim, 2013; Farkas and Hinow, 2010; Jansen et al., 2008; Rasgon, 2008; Schofield, 2002; Schraiber et al., 2012; Turelli and Hoffmann, 1991). According to our population dynamics model, this is an underestimate when releasing infected adults into a population that is at carrying capacity. This is because the released adults will cause the population to temporarily exceed carrying capacity, and the true invasion threshold will be greater than the quantity s_T/s_h, as seen by the monotonic increase of the invasion threshold in p.

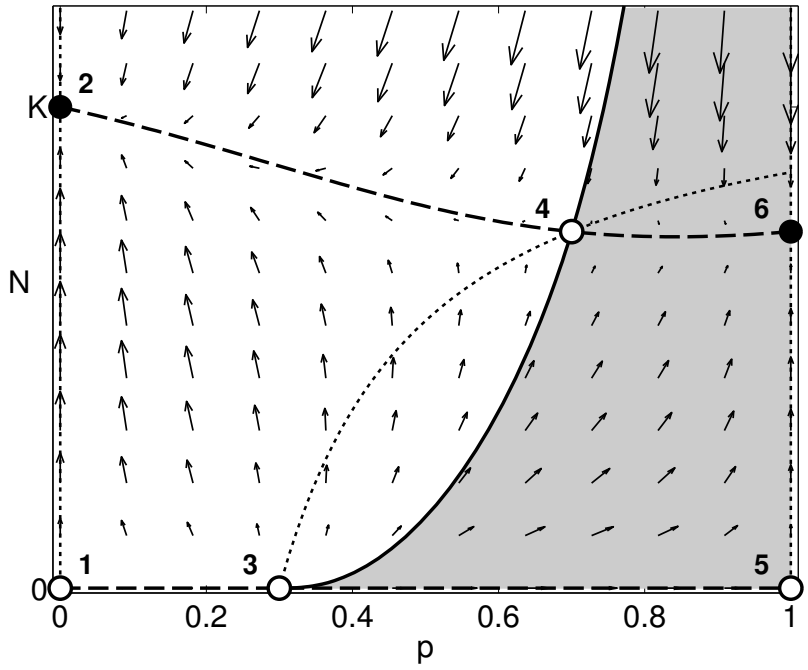

Figure 2.1: p-N phase plane of the population dynamics model for an adult insect population invaded by a *Wolbachia* strain. The intrinsic per capita emergence rate is $b_0 = 1$ day^{-1} and the per capita death rate is $d = 0.1$ day^{-1}. We assume perfect maternal transmission, a 10% fitness cost to fecundity ($s_f = 0.1$), complete CI ($s_h = 1$), and an additional per capita death rate due to infection $D = 0.2$ day^{-1}. The total fitness cost of infection is $s_T = 0.7$, and the basic reproductive numbers are $R_I = 3$ and $R_U = 10$. The dashed line represents the N-nullcline (where $dN/dt = 0$), the dotted line represents the p-nullcline (where $dp/dt = 0$), filled circles represent stable equilibria, and unfilled circles represent unstable equilibria. The solid line represents the invasion threshold, which separates the phase space into initial conditions that result in *Wolbachia* extinction (unshaded region) and initial conditions that result in *Wolbachia* establishment (shaded region). Parameter values are chosen for illustrative purposes.

On the other hand, the quantity s_T/s_h overestimates the frequency threshold for a population that has been suppressed below carrying capacity, as seen by the invasion threshold curving toward the left when $N < K$. Hancock et al. (2011) describe similar results in a population dynamics model when there is a seasonally varying carrying capacity. In a situation where the carrying capacity increases and the population level expands, e.g. a surge of new adults during a raining season, the required frequency of infected insects to release into the environment to

cause establishment of *Wolbachia* is decreased. In contrast, if the population is declining following a decrease in carrying capacity, a higher frequency of infected insects must be released. Although we do not explicitly incorporate a seasonally varying carrying capacity, one could analyze the effect by considering a population near the threshold, say equilibrium 4 in Figure 2.1. If carrying capacity is doubled, then equilibria 2, 4, and 6 move up vertically in N, while their p-coordinates remain the same, according to Table 2.2. The nullclines and separatrix also get stretched vertically. Thus, the population would momentarily be half the distance to the p-axis lower in phase space once the phase plane was rescaled to the new carrying capacity. This would make it easier to spread. Likewise, if the carrying capacity were decreased, the population would be relatively higher on the phase plane and it would be more difficult to spread, according to the curvature of the separatrix.

Although we cannot determine an analytical expression for the separatrix, we can quantify the effect of population size on the threshold in terms of relevant parameters. One measure of the degree to which population size affects the invasion threshold is the difference in the p-coordinates of equilibria 3 and 4, because the separatrix connects the two. This difference is represented by Eq. 2.8:

$$\delta = \frac{D}{s_h b_0}(R_I - 1)\,. \tag{2.8}$$

Thus, the dependence of the frequency threshold on population size is unique to lifespan-shortening strains of *Wolbachia* (i.e. $D > 0$). This is also the case for other types of density dependence (see Appendix A), and it agrees with Hancock et al. (2011) who show that the difference between emergence in an expanding versus declining population is more pronounced when the relative lifespans of infected individuals is lower, though they do not analyze the case of no lifespan-shortening. In our model, if we assume that $D = 0$, then the separatrix in Figure 2.1 is a vertical line at $\hat{p} = s_T/s_h$, which indicates that the invasion threshold is independent of population size, as assumed by frequency-only models. However, even though

the predicted fate of *Wolbachia* is the same for both types of models when $D = 0$, density dependence may still affect the transient dynamics (see Figures 2.2C and 2.2D). In addition to depending on D, the effect of density dependence on invasion threshold also depends on various density-dependent parameters and fitness costs, which is explored further in Appendix A.

To further illustrate the differences between our population dynamics model and frequency-only models, we consider the time-series solutions in Figure 2.2, where we compare predictions from our model to those of Schraiber et al. (2012) for two different release scenarios: single release into a population at carrying capacity (Figures 2.2A and 2C) and single release into a population that has been suppressed to 10% of carrying capacity (Figures 2.2B and 2.2D). Although these release scenarios explicitly violate the constant population size assumption made by frequency-only models, we include the comparison to illustrate the potential hazard of using such models to approximate realistic scenarios. Our results show that frequency-only models can underestimate the frequency threshold for release into a population at carrying capacity and overestimate the frequency threshold in suppressed populations for lifespan-shortening strains of *Wolbachia* (Figures 2.2A and 2.2B), and that density dependence can affect how quickly the system approaches equilibrium for non lifespan-shortening strains (Figures 2.2C and 2.2D).

2.3.2 Multiple Releases

We have until now considered a single release of infected insects by considering the initial condition (p_0, N_0) following release. We now consider the effect of splitting the same number of insects into multiple releases. We first consider the simplest model of *Wolbachia* with and without two features: CI combined with fecundity cost and density-dependent growth. We compare how releasing I_T total individuals split into M releases spaced τ days apart affects *Wolbachia*'s ability to spread in all four possible combinations of the presence/absence of these two effects. Using the simplest model possible allows us to construct analytical arguments—detailed in Appendix B—as to whether single or multiple releases are better in each scenario. The results are summarized in Table 2.3, where we compare the infection frequency after the

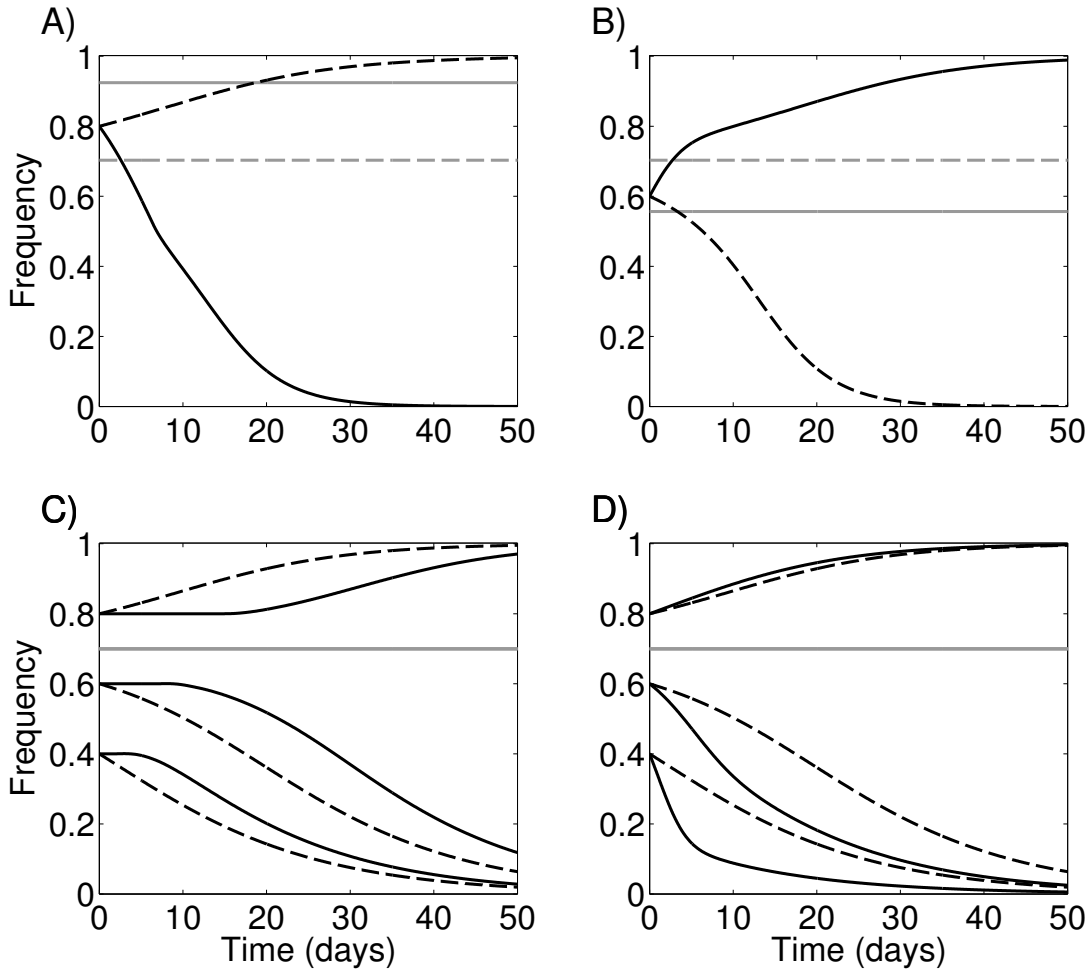

Figure 2.2: Differences in population dynamics model (solid lines) and frequency-only model (dashed lines) for the frequency of *Wolbachia* following a single release of *Wolbachia*-infected females into a population at carrying capacity (A & C) and into a population that was suppressed to 10% of carrying capacity prior to release (B & D) Frequency thresholds (gray lines) are estimated numerically for the population dynamics model and determined analytically for the frequency-only model (threshold is the same for both models in C and D). *Wolbachia* is assumed to cause a 10% fecundity cost and 67% survival cost ($s_f = 0.1$, $D = 0.2$ day^{-1}) in A and B, and a 70% fecundity cost and 0% survival cost ($s_f = 0.7$, $D = 0$) in C and D, such that the total fitness cost is 70% in all cases. Initial frequencies are A) 0.8, B) 0.6, and C) & D) 0.4, 0.6 and 0.8. For all cases, $b_0 = 1$ day^{-1}, $d = 0.1$ day^{-1} and $s_T = 0.7$.

final release for multiple releases (p_m) and single release (p_s). Analysis was possible in all cases except when both effects were present.

Table 2.3: The difference between infection frequency after final release for both single release (p_s) and multiple releases (p_m) of the same total number of infected individuals with the presence/absence of two effects: CI + fecundity cost and density dependence. Analytical results are possible for all cases except when both effects are present, as described in Appendix B. In this last case, whether single or multiple release is better in terms of increasing the infection frequency depends on the number of releases, the time between releases, the fecundity cost, and the total number of released insects.

	Density Dependence	
CI + Fecundity Cost	No	Yes
No	A) $p_m = p_s$	B) $p_m > p_s$
Yes	C) $p_m < p_s$	D) $p_m < p_s$ or $p_m > p_s$

In this simplified model with density dependence, CI, and fecundity cost (case D in Table 2.3), whether multiple or single release is better depends on the values chosen for other parameters, such as the time between releases and the total number of released insects. We demonstrate some of these scenarios in Appendix B. We differ slightly with the conclusions made by Hancock et al. (2011) as seen in their Figure 2. They state that multiple releases are more efficient when lifespan-shortening is great, and that single releases are equally efficient when lifespan-shortening is small. We demonstrate contradictions with our model to show that whether single or multiple is better in each of these cases depends on the specific parameter values being assumed. Hancock et al. (2011) do state that "the extent of the advantage [of multiple release in the case of high lifespan-shortening] depends on the precise number of introductions and the length of the gap between them" (p. 328). They further suggest some ambiguity when they state that, in the case of low lifespan-shortening, "a single introduction is an efficient means of achieving *Wolbachia* spread" (p. 328) while their Figure 2B shows the opposite to be true (this is discussed in more detail in their Appendix B).

Our goal is to show that it is difficult to make any broad conclusions in the case of single versus multiple release. Even with far fewer interacting effects, we can produce a variety of results depending on how we choose parameter values. This is the main advantage of analysis: we can pinpoint these important regions of parameter space. When we were unable to provide meaningful analysis, we simulated various scenarios to demonstrate that it is more complicated than it appears at first glance, and we thus caution against making overreaching statements regarding the direct effects of any of these factors. Certainly density dependence plays a role, as we have demonstrated elsewhere in this chapter, but it is clearly not the whole picture.

2.3.3 Underdominance

The effect of neglecting population dynamics may also be seen in other genetic systems. As an example, we demonstrate the impact of population dynamics on underdominance, which occurs in a diploid population when heterozygotes (Aa) have lower fitness than either homozygote genotype (AA or aa) (Hartl and Clark, 1989). Underdominant systems, like *Wolbachia*, are bistable, and have an allele-frequency threshold that determines which allele will become established in the population (Barton and Turelli, 2011). For this reason, underdominance has also been proposed as a possible gene drive strategy (Curtis, 1968; Davis et al., 2001; Sinkins and Gould, 2006). We construct a population dynamics model similar to Eq. 2.1 with a density-dependent emergence rate for adults of all three genotypes, and compare to a frequency-only model developed using the Moran process (Moran, 1958; Schraiber et al., 2012; see Appendix C). The results for the frequency of allele A (p_A) over time are shown for a single release of AA adults into a population of wild-type aa adults at carrying capacity (Figure 2.3A) and into a population of aa adults that was suppressed to 10% of carrying capacity prior to release (Figure 2.3B). Phase portraits can be found in Appendix C.

As in the *Wolbachia* model, the frequency-only model underestimates the frequency threshold for a single release into a population at carrying capacity and overestimates the frequency threshold for a single release into a suppressed population, once we include density-dependent

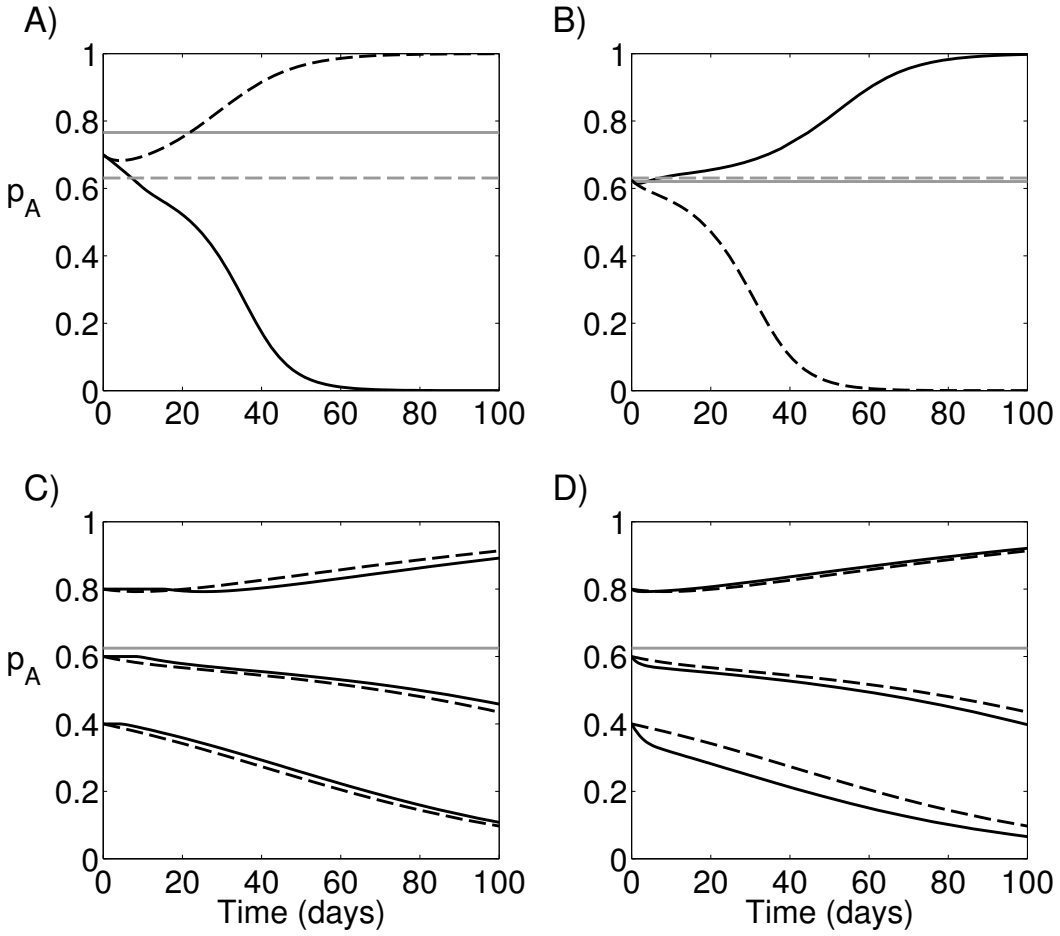

Figure 2.3: Differences in population dynamics model (solid lines) and frequency-only model (dashed lines) for the frequency of allele A versus time for a single release of AA adults into a population of aa adults at carrying capacity (A & C) and a population of aa adults that was suppressed to 10% of carrying capacity prior to release (B & D). Parameter values are chosen (for illustrative purposes) to be $s_{fAa} = 0.4$, $s_{fAA} = 0.1$, $s_{vAa} = 0.8$, $s_{vAA} = 0.3$ (A & B) and $s_{fAa} = 0.5$, $s_{fAA} = 0.2$, $s_{vAa} = s_{vAA} = 0$ (C & D), where s_f is the fecundity fitness cost and s_v is the survival fitness cost of each genotype. Gray lines represent the invasion threshold for each model, which are the same for both models in C & D. Initial frequencies are A) 0.7, B) 0.625 and C) & D) 0.4, 0.6, and 0.8. For all cases $b_0 = 1$ day^{-1} and $d = 0.1$ day^{-1}.

population dynamics and differing per capita death rates. The overestimate in the latter case is less dramatic for the case of underdominance, as the frequency threshold for a suppressed population is close to that predicted by the frequency-only model. Also like *Wolbachia*, we find that the threshold for both models is identical when the per capita death rates are equal across genotypes (i.e. $s_{vAa} = s_{vAA} = 0$), and the model simplifies enough to solve for the threshold analytically (Eq. 2.9), which is a well-known result for frequency-only models (Li, 1955):

$$\hat{p} = \frac{s_{fAa}}{2s_{fAa} - s_{fAA}}. \tag{2.9}$$

As was the case in *Wolbachia*, density dependence still affects the transient dynamics, though to a lesser degree than in *Wolbachia* (compare parts C and D in Figures 2.2 and 2.3).

2.4 Discussion

We have shown how incorporating a simple form of density dependence into continuous-time models for the spread of *Wolbachia* can cause qualitative differences in their predictions. While others have demonstrated that population dynamics impact the spread of *Wolbachia* (Hancock et al., 2011; Zheng et al., 2014), our model is the first to explicate the link to frequency-only models, as shown by the coupled p-N Eq. 2.2 and the derivation of Schraiber et al's (2012) model by assuming constant population size in our model. In addition, while previous studies have highlighted density dependence as inhibiting spread in a well-mixed population (Hancock et al., 2011), we demonstrate a release scenario (single release into a suppressed population) in which density dependence actually facilitates spread of *Wolbachia* or an underdominant gene (Figures 2.2B and 2.2B). In these cases, the population's return to carrying capacity can help drive the novel heritable factor, which is a conclusion that cannot be reached in models that neglect population dynamics.

The idea of suppressing the population prior to release is not new. This so-called "crash and release" strategy has the advantage of requiring fewer released individuals to achieve a desired

frequency (Jacups et al., 2013). However, we have shown how the frequency threshold itself may decrease for lifespan-shortening strains of *Wolbachia* when the population is suppressed. This lends more support to the crash and release strategy for lifespan-shortening strains of *Wolbachia*, although we admit that the magnitude of this effect is likely small compared to the increase in initial frequency caused by releasing the same number of individuals into a suppressed population.

Zheng et al. (2014), using a model that had density-dependent mortality instead of emergence, also showed that the invasion threshold may depend on population size. They provide formulas for upper and lower bounds on the threshold as a function of infected population size (see their Eq. 2.11), which approach a constant frequency threshold when per capita mortality in infected and uninfected individuals is the same. We provide an alternative way to quantify how the invasion threshold depends on population size (Eq. 2.8) and show how the extra mortality in infected individuals critically affects this threshold. We also show this result to be robust across different forms of density dependence, so long as density-dependent mortality interacts with *Wolbachia*-induced mortality, and that it occurs in underdominance as well (see Appendices A and C). Like Zheng et al. (2014), we find that the situation is reversed if *Wolbachia* causes a survival advantage ($D < 0$), as has been demonstrated in some infections (Dobson et al., 2004). That is, releasing into a population at carrying capacity decreases the invasion threshold, whereas suppressing the population prior to release increases the threshold, as predicted by the relative positions of equilibria 3 and 4 in Figure 2.1 when $\delta < 0$.

Another important result is that current frequency-only models underestimate the true frequency threshold when performing a single release into a population at carrying capacity. This is especially true when the total fitness cost of *Wolbachia* is high, because the predicted frequency threshold will also be high. In order to achieve the frequency threshold $\hat{p}$ with a single release into an uninfected population at carrying capacity K, one must release $\hat{p}K/(1-\hat{p})$ infected mosquitoes. This becomes prohibitively large at high frequency thresholds, and the initial population size following release, $N_0 = K/(1-\hat{p})$, would cause the frequency threshold

to be greater than s_T/s_h as predicted in most frequency-only models (at least when $D > 0$, as in Figure 2.1). Of course, one way to mitigate this effect is to perform multiple releases with the same total number of released infected adults. This allows the population to respond to a smaller perturbation before the next cohort is released, and Hancock et al. (2011) showed this to facilitate spread of *Wolbachia* in their population dynamics model of *Ae. aegypti*.

The result that large releases increase the threshold is intuitive if we consider, in our example of density-dependent emergence, that the emergence rate is zero for large populations. That is, adults die until the population decreases to a level at which new adults can emerge. During this time, if infected adults experience a greater per capita death rate than uninfected adults ($D > 0$), then the proportion of infected individuals (p) will decrease over time. Thus, the "effective" initial frequency, once new adults begin to emerge, is less than the frequency at release, which Alphey and Bonsall (2014) also showed in their model for homing endonuclease gene drive. However, the result that suppressing the population can help drive a selfish gene is more difficult to intuit, likely arising from the complicated feedback between evolutionary and ecological dynamics. The potential for such non-intuitive results stresses the importance of including interactions between ecology and evolution in mechanistic models for gene drive strategies.

Because single-release strategies involve such drastic perturbations to population size, frequency models are expected to be inaccurate in these cases. However, as previously mentioned, *Wolbachia* itself is expected to decrease population size as it spreads. This is especially true when infected and uninfected adults are near equal numbers and there is a large decrease in the emergence rate due to CI. We believe this will be particularly important when modeling spatial spread of *Wolbachia*. We agree with Schraiber et al. (2012) that "the long-term spatial dynamics [of *Wolbachia*] depend on the local dynamics" (p. 28), which is why we attempted to develop a more accurate model for the local dynamics based on population dynamics. Previous models for the spatial spread of *Wolbachia* in a homogeneous environment show a traveling wave of infection that approaches a constant speed, but they model frequency only (Barton and

Turelli, 2011; Schofield, 2002; Schraiber et al., 2012; Turelli and Hoffmann, 1991). The greatest amount of CI, and thus population reduction, will occur at the traveling wavefront, and the wave speed may be affected by various ecological effects that are neglected by frequency-only reaction-diffusion models. We believe a population dynamics model, such as the one we have proposed here, that includes the possibility of lifespan-shortening effects, can be incorporated into a reaction-diffusion equation to provide a more accurate and complete picture of the spatial spread of *Wolbachia*, and may still be sufficiently simple to allow for meaningful analysis. Although Chan and Kim (2013) provide a reaction-diffusion model with the same form of density dependence we assume here, it does not include lifespan-shortening effects, and thus results in a constant frequency threshold (see their Figure 1). Hancock and Godfray (2012) developed a density-dependent model for the spatial spread of *Wolbachia* and found that stronger density dependence helped spatial spread and spatial heterogeneity inhibited spread. This was based on only one form of density dependence, and we believe their results can be expanded to include stochastic dynamics and other forms of density dependence, like we explore in a non-spatial setting in Appendix A.

Limitations to our model include the assumption of perfect maternal transmission of *Wolbachia*, which we made in order to simplify the analysis. Although maternal transmission has been shown to be perfect in *Ae. aegypti* (Hoffmann et al., 2014; Walker et al., 2011) and near perfect in *Drosophila simulans* (Turelli and Hoffmann, 1991), this will need to be assessed for each host species and strain of *Wolbachia* in question. Hancock et al. (2011) include the possibility of imperfect maternal transmission in a more detailed model but set the default value of its rate of occurrence to 1%. Because they do not compare to the case of perfect maternal transmission, it is difficult to know how it affects the results. We feel that including it for the sake of completeness does not justify the subsequent decrease in mathematical tractability when accepted values for its rate of occurrence are near zero. As long as the frequency of maternal transmission is high, our model should provide a good approximation to the dynamics. Also, when considering release into a suppressed population, Eq. 2.8 is only one attempt to quantify

the potential benefit of prior population suppression. At small population numbers, random events may determine the outcome, such that one might prefer a stochastic model rather than a deterministic model to determine the probability of invasion. Jansen et al. (2008) developed a stochastic model for the spread of *Wolbachia*, but it assumes a constant population size, and thus would have to be expanded in order to capture the potential effects of density dependence. Finally, while we have demonstrated the effect of a specific form of density dependence (linear decrease in per capita emergence rate), our results show qualitative agreement across a number of forms of density dependence (see Appendix A). The exact form of density dependence to be used will depend on the population, however, and empirical studies into the governing dynamics will be crucial for developing more accurate models.

It is worth questioning the modeling paradigm of assuming a constant population size in density-dependent systems, especially when modeling changes in mean fitness or the release of large numbers of individuals. We have shown that a single frequency threshold for gene drive systems, such as *Wolbachia* and underdominance, may not exist when considering the interplay between evolutionary and ecological dynamics, and we encourage more wide-scale adoption of an eco-evolutionary modeling framework. This will be especially important for developing more accurate models for global health applications that seek to replace disease-carrying vector populations using these strategies.

Chapter 3

The effects of density-dependent population dynamics, spatial heterogeneity, and stochasticity on the spatial spread of *Wolbachia*

ABSTRACT

Frequency-only models have provided important insights for the spatial spread of *Wolbachia* such as the existence of a traveling wave and its dependence on dispersal and fitness parameters. In order to determine how *Wolbachia* spreads in the field, however, it is important to understand how various complexities in natural populations cause deviations from theoretical predictions that are based on simplifying assumptions such as constant population size. We develop two models to examine the effects of density-dependent growth, spatial heterogeneity in habitat, and stochasticity in population dynamics on the predicted spread of *Wolbachia*. We develop a reaction-diffusion model that can incorporate various forms of density dependence and a metapopulation model that allows for stochasticity in mating and dispersal as well as heterogeneity in patch sizes. We find that the effect of density dependence on the wave speed depends on whether it acts on the per capita emergence rate or the per capita death rate, with density dependence on the death rate making *Wolbachia* less likely to spread and slowing the wave speed when it does. We also find that spatial heterogeneity has a greater slowing effect in one-dimensional spread than two-dimensional spread and that stochasticity decreases wave speed when fitness cost is low but increases wave speed when fitness cost is high. Understanding the interaction of these effects is important for determining whether and how quickly *Wolbachia* will spread in a variety of host populations and environments.

3.1 Introduction

Dengue is a mosquito-borne virus that is estimated to infect approximately 390 million people each year (Bhatt et al., 2013). Infection with the virus can cause a wide range of symptoms, including fever, rash, joint pain, and rarely, internal hemorrhaging and death. There is no cure or vaccine for dengue, so controlling the disease requires controlling its primary vector, *Aedes aegypti* (WHO, 2014). However, traditional control methods such as insecticide and reduction of larval habitats have had very limited success in controlling the disease (Morrison et al., 2008).

Recently, there has been interest in developing novel vector control technologies, such as releasing genetically modified mosquitoes or mosquitoes that have been infected with the maternally-inherited bacterium *Wolbachia* (Gould et al., 2006). These strategies seek to either reduce the vector population or to replace it with one that is less able to transmit disease. Population replacement strategies require an anti-pathogen effect as well as a drive mechanism that allows the gene or bacterium to spread through the population despite a fitness cost (so-called "super-Mendelian" inheritance, Sinkins and Gould 2006). *Wolbachia* accomplishes both by directly blocking transmission of the dengue virus (Walker et al., 2011) and by manipulating host reproduction through a phenomenon called cytoplasmic incompatibility (CI). CI causes most to all offspring of *Wolbachia*-infected males and wild-type females to fail to develop (Werren, 1997). In other words, wild-type females become partially sterile in the presence of *Wolbachia*-infected males, so *Wolbachia*-infected females may give rise to more offspring on average. Since the bacterium is only passed from mother to offspring, this can cause the overall frequency of *Wolbachia* infection, i.e. the fraction of infected individuals, to increase in a population over time.

If *Wolbachia* infection causes a fitness cost to its host, e.g. by reducing average lifespan or number of eggs laid, then there is a critical frequency of infection that must be exceeded before the amount of cytoplasmic incompatibility outweighs the fitness cost, such that the frequency of *Wolbachia* increases until it is established in the population (it will reach 100% under perfect maternal transmission). Below this threshold, the fitness cost causes wild-type

hosts to outcompete *Wolbachia*-infected hosts, and the frequency of *Wolbachia* is expected to decrease over time to extinction. Determining this threshold is thus critically important for predicting the fate of *Wolbachia* when released into a population.

Mathematical models can be a useful aid in predicting the frequency threshold for *Wolbachia* invasion as well as the most efficient release strategies. Previous frequency-only models have shown that, when *Wolbachia* is perfectly maternally transmitted, the expected frequency threshold is equal to the total fitness cost (the number of offspring from *Wolbachia*-infected adults relative to wild-type adults when non-interacting) divided by the degree of CI (the proportion of offspring from matings between *Wolbachia*-infected males and wild-type females that are inviable) (Turelli and Hoffmann, 1991; Schofield, 2002; Jansen et al., 2008; Rasgon, 2008; Schraiber et al., 2012; Chan and Kim, 2013). However, density-dependent population dynamics can cause different outcomes from those predicted by models that track infection frequency rather than numbers of individuals (Antonelli et al., 2015, Chapter 2 of this dissertation; Hancock et al, 2011).

Partial differential equation models known as reaction-diffusion models are often used to model spatial spread in ecology (Volpert and Petrovskii, 2009). They were first used to describe the spatial spread of an advantageous gene, which was found to have a traveling wave solution with speed depending on the fitness and dispersal parameters (Fisher, 1937; Kolmogorov et al., 1937; Fife, 1979). Stokes (1976) expanded this analysis to include other reaction terms that lead to slower traveling waves. He referred to these slower waves as "pushed" because the entire wavefront drives their advancement, as opposed to Fisherian "pulled" waves, which are driven only by the leading edge. Barton (1979) showed that an underdominant system, i.e. one in which heterozygotes are at a selective disadvantage to either homozygote, can produce stable "hybrid zones" of heterozygotes that act as barriers to gene flow and move as pushed waves.

Turelli and Hoffmann (1991) used a similar reaction-diffusion model to describe the spatial spread of *Wolbachia* in *Drosophila simulans* in California but found that it underestimated the observed wave speed when realistic values for the dispersal distance were used. Lewis and

Kareiva (1993) used a similar model for a species invasion with an Allee effect, or a negative effect of low population density on the net per capita growth rate, e.g. difficulty finding a mate. *Wolbachia* is similar to both underdominance and the Allee effect in that all three possess a frequency threshold that must be exceeded locally for spread to occur, and the traveling waves for their reaction-diffusion equations all have pushed waves as asymptotic solutions. Schofield (2002) extended the spatial *Wolbachia* model to include imperfect maternal transmission which he showed to further underestimate the observed wave speed in *D. simulans*, concluding that a Gaussian dispersal kernel was not appropriate, favoring a more leptokurtic, or "fat-tailed", dispersal kernel.

The potential to use *Wolbachia* to control dengue increased when it was stably introduced into *Ae. aegypti* (McMeniman et al., 2009). Barton and Turelli (2011) expanded on the reaction-diffusion model of *Wolbachia* to look at two-dimensional spatial spread, critical release sizes and immigration, although they assumed weak CI (many viable offspring from matings between infected males and uninfected females) in their model because it allowed for an analytical solution of the wave speed. Schraiber et al. (2012) derived a model for strong CI (few viable offspring from matings between infected males and uninfected females), which is more appropriate for *Ae. aegypti*, and showed that when there is no fecundity cost, a traveling wave is produced when the frequency threshold $\hat{p}$ is less than approximately $1/2$, which agrees with earlier approximations (Turelli and Hoffmann, 1991; Barton and Turelli, 2011).

It remains an open question how population dynamics may affect the spatial spread of *Wolbachia*. Recently, Hancock and Godfray (2012) developed a density-dependent model with spatial heterogeneity in larval habitat quality and found that strong density dependence increases wave speed while spatial heterogeneity decreases wave speed. We expand upon their work by developing a reaction-diffusion model that can incorporate many different forms of density dependence, allowing us to examine the generalizability of their results. We further use this model to compare different release strategies in which the population is manipulated prior to release, affecting the probability that a traveling wave will be produced. Finally, we develop

a metapopulation model in order to examine the effect of spatial heterogeneity and stochastic population dynamics. We also demonstrate how results can differ from one-dimensional spatial models like Hancock and Godfray (2012) when modeling two-dimensional spread.

3.2 Models

3.2.1 Reaction-diffusion model

We consider a bounded region in one-dimensional space $x \in [-L, L]$ to represent an area of interest for *Wolbachia* invasion, such as the width of a city where *Wolbachia*-infected insects are to be released. In our analysis we only consider timespans over which the traveling wave of infection does not reach the boundaries $x = \pm L$, in order to avoid boundary effects. We model the density of *Wolbachia*-infected females $I(x,t)$ and wild-type females $U(x,t)$ at point x and time t with the coupled reaction-diffusion equations in Eq. 3.1:

$$\frac{\partial I}{\partial t} = \left((1 - s_f)\, b(N) - \frac{d(N)}{w} \right) I + \lambda \frac{\partial^2 I}{\partial x^2} \tag{3.1a}$$

$$\frac{\partial U}{\partial t} = \Big((1 - s_h p)\, b(N) - d(N) \Big) U + \lambda \frac{\partial^2 U}{\partial x^2}, \tag{3.1b}$$

where $\lambda = \sigma_d^2/2$ is known as the diffusion coefficient, which relates to the variance σ_d^2 of the insect's dispersal kernel. This model is similar to one used by Chan and Kim (2013), but rather than specify the form of density-dependence we consider different forms with the generalized density-dependent functions $b(N)$ and $d(N)$. These represent the per capita emergence and death rates of wild-type adults (when no *Wolbachia* is present), which depend on total population density $N = I + U$. We will consider time in units of days and non-dimensionalize space to be relative to the standard deviation of dispersal in one day, which is equivalent to setting $\lambda = 1/2$. The reaction terms on the left represent the local population dynamics. The

parameter s_f is the fitness cost to fecundity caused by *Wolbachia* infection (e.g. $s_f = 0.5$ means that *Wolbachia*-infected females lay half as many eggs per unit time as wild-type females). The parameter w is the relative lifespan of *Wolbachia*-infected females compared to wild-type females (e.g. $w = 0.5$ means that *Wolbachia*-infected females live half as long as wild-type females). The parameter s_h represents the degree of CI, and the variable $p = I/(I + U)$ is the local frequency of *Wolbachia* infection. We assume perfect maternal transmission of *Wolbachia*, which is consistent with lab experiments (Walker et al., 2011). Parameters are listed in Table 3.1 and are equal to their default values throughout unless otherwise specified.

This model is in contrast to "frequency-only" models (Barton and Turelli, 2011; Schraiber et al., 2012), which neglect population dynamics and track only one variable, the frequency of infection p, across space and time. Throughout, we will compare and contrast our results to analytical and numerical results previously obtained for frequency-only models.

Ae. aegypti experience density-dependent growth via intraspecific competition for food in the aquatic larval stage (Gilpin and McClelland, 1979; Dye, 1982). The most natural way to incorporate this into our model is to consider that the per capita emergence rate of new adults decreases with increasing population density. This neglects the delay in density dependence due to development time in the larval stage. We also consider density-dependent growth via an increase in per capita death rates with increasing population density, which is a another common way to model density dependence (Keeling et al., 2003; Farkas and Hinow, 2010; Zheng et al., 2014). We examine both linear changes in per capita growth rates, which is the commonly-used logistic growth, as well as nonlinear changes. Real systems will likely exhibit some combination of both types of density dependence, and the functional form will largely depend on the specific environment, so it is helpful to isolate the effects of each these components on the predicted wave speed.

The four forms of density dependence that we investigate are summarized in Table 3.2 and Figure 3.1, where b_0 and d_0 are the wild-type per capita intrinsic emergence and mortality rates, i.e. the rates at low densities which yield the greatest net per capita growth rate. We

Table 3.1: Parameters for reaction-diffusion model

Parameter	**Description**	**Default**	**Units**
b_0	Intrinsic per capita emergence rate	0.1 – 2 (varies)	day^{-1}
d_0	Intrinsic per capita death rate	0.005 – 0.1 (varies)	day^{-1}
K	Female carrying capacity density of wild-type population	10	adult
L	Half the total length of the spatial domain	100	-
R	Radius of release area	10	-
p_0	Initial frequency of *Wolbachia* infection after release	0.5 – 0.9 (varies)	-
q	Fraction of carrying capacity to which wild-type population is suppressed prior to release	0.1	-
s_f	Fitness cost to fecundity	0 – 0.5 (varies)	-
s_h	Degree of cytoplasmic incompatibility	1	-
w	Relative lifespan of *Wolbachia*-infected adults	0.5 – 1 (varies)	-
β	Strength of density dependence	0.5 – 4 (varies)	-

Table 3.2: Four forms of density-dependent per capita growth rates to be substituted into Eq. 3.1 to examine the effects of different forms of density dependence on the traveling wave solution of *Wolbachia* spatial spread. $N = I + U$ is the total population density at a given time and place, b_0 and d_0 are the per capita intrinsic growth rates of wild-type individuals, K is the wild-type carrying capacity, and $\beta > 0$ is a density-dependent parameter that controls the strength of density dependence in type 4.

		$b(N)$	$d(N)$
1.	Linear decrease in emergence	$\max\left\{b_0 - \frac{N}{K}(b_0 - d_0)\,,\ 0\right\}$	d_0
2.	Nonlinear decrease in emergence	$b_0\left(\frac{d_0}{b_0}\right)^{N/K}$	d_0
3.	Linear increase in death	b_0	$d_0 + \frac{N}{K}(b_0 - d_0)$
4.	Nonlinear increase in death	b_0	$d_0 + \left(\frac{N}{K}\right)^{\beta}(b_0 - d_0)$

modify the equation in type 1 to ensure that the growth rate is non-negative. The reason we do not incorporate the β parameter for nonlinear decrease in emergence (type 2) is that the stipulation that the emergence rate be non-negative limits the values of β that would be biologically realistic. K is the wild-type density carrying capacity. Notice that K only appears in the ratio N/K. Thus, we can non-dimensionalize by considering population size relative to carrying capacity, and then our results apply for any K. We include it as a parameter, even though its value does not affect the results, so that the biological interpretation is more apparent. In order to compare different forms of density dependence, we assume that the per capita death rate for wild-type adults at carrying capacity, $d(K)$, is the same across all forms. This means that the average generation time of wild-type adults at carrying capacity, which is the reciprocal of per capita death rate, is also the same. Introduced *Wolbachia*-infected adults may have shorter or longer generation times at the *Wolbachia*-established equilibrium, depending on the fitness cost of *Wolbachia* and form of density dependence.

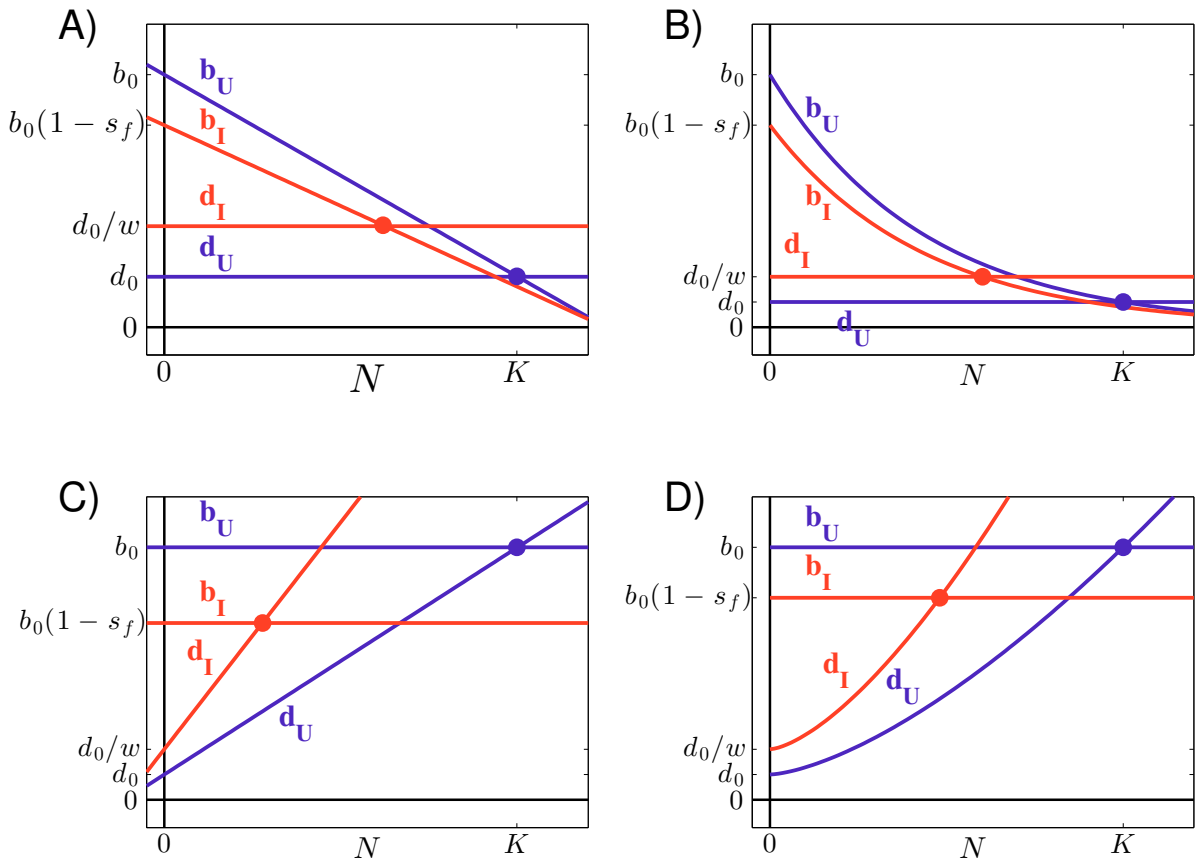

Figure 3.1: Graphs of the four forms of density dependence in Table 3.2. A) linear decrease in emergence rate, B) nonlinear decrease in emergence rate, C) linear decrease in death rate, and D) nonlinear increase in death rate with $\beta = 1.5$. Blue lines represent wild-type per capita growth rates and red lines represent *Wolbachia*-infected per capita growth rates. Blue circles represent wild-type or infection-free equilibria and red circles represent *Wolbachia*-endemic or infected equilibria. Fitness costs are exaggerated for display purposes, as many of these parameter combinations would not permit spatial spread.

We consider the "strength of density dependence" to be represented by how quickly the wild-type population returns to carrying capacity following a perturbation. We note that this definition is not entirely satisfactory, however, because the rate at which the population returns to carrying capacity depends on the size of the perturbation. For our definition we consider small

perturbations, and so this rate is represented by the slope of the net per capita growth rate evaluated at $N = K$. "Strong" density dependence may return slowly however if the system is perturbed far enough away from equilibrium—and vice-versa for "weak" density dependence—when the per capita growth rates are nonlinear (as is the case in Figure 3.1B and D). To our knowledge, there is no general consensus regarding the appropriate definition (see Herrando-Pérez, 2012 for the various uses of the term "density dependence" itself). We consider the nondimensionalized slope $dr/dx|_{x=1}$ where $r = b(x) - d(x)$ and $x = N/K$, as a measure of the strength of density dependence, which is analogous to the slope of the (non-horizontal) blue lines in Figure 3.1. This quantity is equal to $b_0 - d_0$ for the first three types of density dependence and $\beta(b_0 - d_0)$ for the last form.

3.2.2 Metapopulation Model

As a point of comparison, and to incorporate two-dimensional spread, stochastic population dynamics and spatial heterogeneity in habitat quality, we develop a discrete-time model for the spatial spread of *Wolbachia* in a metapopulation of adult insects, where we model males and females explicitly in order to incorporate stochasticity in the sex ratio over space and time.

We begin with a one-dimensional array of M patches. We consider discrete time in units of generations. Insects undergo local population dynamics based on the frequency of *Wolbachia* infection in each patch, and then a certain fraction disperse to nearest neighboring patches on either side (if not on the boundary, discussed below). An example with release of *Wolbachia*-infected *Ae. aegypti* into the central patch is shown in Figure 3.2.

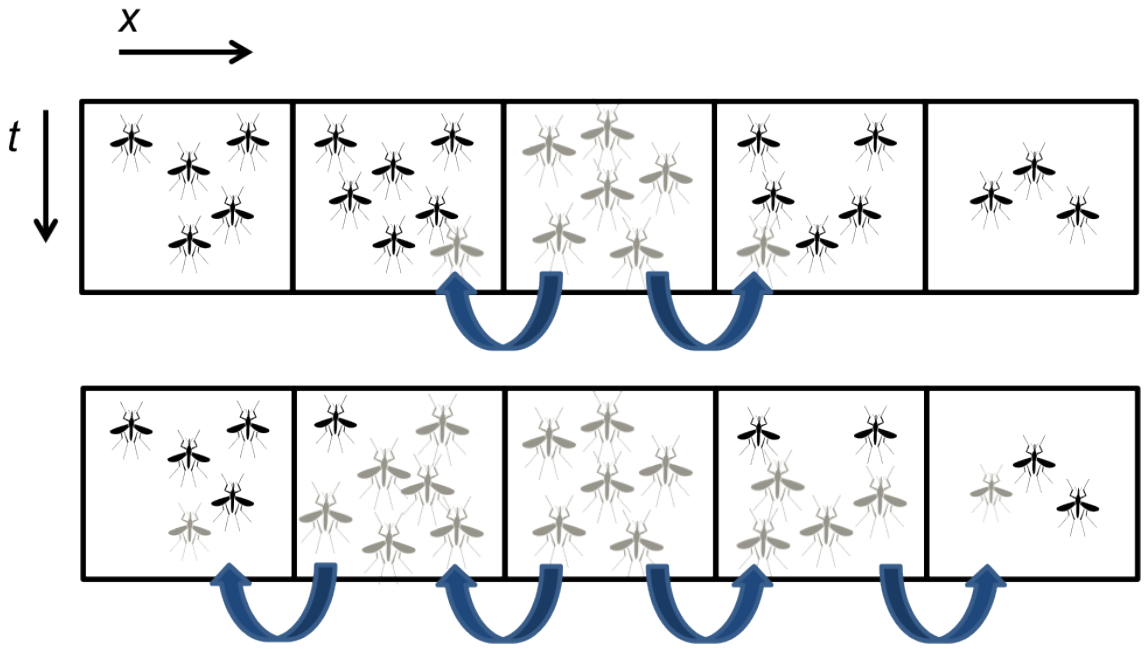

Figure 3.2: Schematic of one-dimensional spread of *Wolbachia*-infection in *Ae. aegypti* following complete *Wolbachia* infection in the central patch. Each generation, mosquitoes mate randomly, lay eggs, and a certain fraction of adults disperse to either of two nearest-neighboring patches. *Wolbachia* infection spreads locally if the frequency of infected adults is greater than the frequency threshold determined by CI and fitness cost.

In the deterministic version, i.e. solutions are uniquely determined by the initial conditions, each patch begins with K_i adults, where K_i is the carrying capacity of patch i prior to the release of *Wolbachia*. The center C patches are seeded with only *Wolbachia*-infected adults while all other patches contain only wild-type adults (half male, half female). Each female mates with a randomly selected male from the same patch and lays E eggs if uninfected and $(1-s_f)E$ eggs if infected, where s_f is the fecundity cost of *Wolbachia*. Only a fraction $1-s_h$ of eggs laid by wild-type females and fertilized by *Wolbachia*-infected males hatch due to CI, where s_h is the degree of CI as in the previous section. The frequency of *Wolbachia* infection in the next generation, $p_i(t+1)$, is determined by the ratio of *Wolbachia*-infected eggs (laid by *Wolbachia*-infected females) to the total number of eggs that hatch. The number of *Wolbachia*-infected adults in

the next generation (prior to dispersal) is then $p_i(t+1)K_i$ (half male and half female) and the number of wild-type adults is $(1-p_i(t+1))K_i$ (half male and half female). Finally, a fraction α of adults, independent of sex or infection status, disperse equally to neighboring patches on both sides. This simulates a random walk, which approaches diffusion as the distance and time between steps go to zero (Codling et al., 2008). The entire process then repeats for the next generation. Because this version is deterministic, all numbers can be fractional, reflecting the average or expectation of the dynamics. That is, if a patch has 20 adults and α is 0.1, then 1 adult (0.5 male and 0.5 female) will travel to the patch on the left and 1 adult (0.5 male and 0.5 female) will travel to the patch on the right. Adults that would disperse outside the boundary remain in the current patch.

We also consider a stochastic version of this model, in which we only have discrete numbers of insects. In the stochastic version, the number of eggs that hatch is drawn from a Poisson distribution with mean E if both parents are wild-type, $(1-s_f)E$ if laid by a *Wolbachia*-infected female, and $E(1-s_h)$ if laid by a wild-type female and fertilized by a *Wolbachia*-infected male. We assume perfect maternal transmission, so any egg laid by a *Wolbachia*-infected female gives rise to a *Wolbachia*-infected insect. We then sample K_i individuals to hatch from the available eggs using a binomial distribution with probability 1/2 to determine if the offspring is male or female. The infection frequency $p_i(t+1)$ is then updated to the resulting fraction of infected individuals. Finally, each adult disperses with probability α, and its destination is chosen at random from the nearest neighboring patches.

In both the deterministic and stochastic frameworks, the carrying capacities for each patch are drawn from a negative binomial distribution with mean μ_K and standard deviation σ_K. We choose the negative binomial distribution because it provides non-negative patch sizes that are overdispersed, meaning the variance is greater than the mean. This allows for very large patch sizes, which may be rare but have a large impact on the dynamics. Because we examine a whole range of σ_K values, we use the regular binomial distribution as an alternative when $\sigma_K^2 < \mu_K$, which is underdispersed. We vary the parameter σ_K as a measure of spatial heterogeneity in

habitat quality in order to determine its effect on the traveling wave of *Wolbachia* infection.

Finally, we expand the model to incorporate two-dimensional spatial spread by considering a grid of M x Q patches. In order to compare to the one-dimensional model, we release into C central columns and measure the linear wave speed to either side. The main difference in the two-dimensional model is that insects can migrate to any of four nearest-neighboring patches (up, down, left, right), and that the wave is more likely to be able to get around unusually large patches that are difficult to invade. The movement parameter α is set to twice as much in the two-dimensional model to account for having twice as many neighbors. This way, the same fraction are emigrating in the horizontal direction in both the one- and two-dimensional settings. We do this because the horizontal spread of "columns" of infection is the most direct extension of the one-dimensional model. In this case, the horizontal component of spread over time is the analogous wave speed to compare to the one-dimensional model.

Parameters for the metapopulation model are summarized in Table 3.3. Parameters are set to their default values unless specified otherwise.

3.3 Results

3.3.1 Reaction-diffusion Model

All results for the reaction-diffusion model were obtained using the PDE solver `pdepe` in Matlab version 8.3, which solves parabolic and elliptic PDEs using the Galerkin discretization method provided by Skeel and Berzins (1990). We also hand-coded a finite difference approximation using the Crank-Nicolson method (Crank and Nicolson, 1996), and we found similar results. The advantage to using `pdepe` is that it automates tuning the discretization parameters to ensure convergence, which can be tedious. It was thus easier to use `pdepe`, taking advantage of the fact that the reaction-diffusion equation is a parabolic PDE, to solve the equation for many different initial conditions and forms of density dependence.

Table 3.3: Parameters for metapopulation model

Parameter	**Description**	**Default**	**Units**
α	Fraction that emigrate each generation	0.1, 0.2	-
C	Number of patches or columns into which *Wolbachia*-infected adults are released	9	-
E	Number of eggs females lay each generation	50	-
K_i	Total carrying capacity in patch i	20	adult
M	Number of houses in x direction	100	house
Q	Number of houses in y direction	20	house
s_f	Fitness cost to fecundity	0 – 0.5 (varies)	-
s_h	Degree of cytoplasmic incompatibility	1	-
w	Relative lifespan of *Wolbachia*-infected adults	0.5 – 1 (varies)	-
μ_K	Mean of distribution from which K_i are drawn	20	adult
σ_K	Standard deviation of distribution from which K_i are drawn	0 – 35 (varies)	adult

Release strategies

Even if $\hat{p} < 1/2$, an initial release of *Wolbachia*-infected adults must exceed a spatial threshold for a traveling wave to be produced. This is related to the problem of determining a critical patch size, which has been extensively studied in population ecology (Skellam, 1951; Kierstad and Slobodkin, 1953) and population genetics (Slatkin, 1973; Nagylaki, 1975). If the initial release radius is too small, then the newly introduced individuals may be swamped by immigrating wild-type individuals, such that the infection dies out before getting a chance to establish and produce a traveling wave. Lewis and Kareiva (1993) determined the critical radius for two-dimensional spread of a population with an Allee effect, which has similar bistable dynamics to *Wolbachia*.

We consider the spatial threshold, or "critical bubble," for one-dimensional spread of *Wolbachia*, which represents the unstable equilibrium at which the forces of CI, fitness cost, and diffusion exactly cancel. If the initial spatial profile $p(x, 0)$ is everywhere less than the spatial profile of this bubble, then *Wolbachia* will go extinct. If $p(x, 0)$ is everywhere greater than the spatial profile, then a traveling wave of *Wolbachia* infection will be produced (Barton and Turelli, 2011). Determining this critical bubble is difficult even for the frequency-only model, and an analytic solution may not exist (Barton and Turelli, 2011). Rouhani and Barton (1987) determined the critical bubble for a similar bistable genetic model. The integral of this bubble, or "total frequency," is

$$T(\gamma) = \log\left(\frac{\sqrt{\gamma(\gamma+3)}}{3-\gamma-3\sqrt{1-\gamma}}\right), \tag{3.2}$$

where $\gamma = 2\left(\frac{1}{2} - \hat{p}\right)$ and $\hat{p} = (1 - w(1 - s_f))/s_h$ is the frequency threshold predicted by the frequency-only model (Barton and Turelli, 2011). However, Barton and Turelli (2011) found this to overestimate the minimum total frequency for the *Wolbachia* model. In particular, they found that a traveling wave could be produced for a fewer total number of released insects if they were released at the same frequency across a distance of $2R$ (a "top-hat"-like initial spatial

profile) where $2Rp_0 < T(\gamma)$.

Density-dependent population dynamics complicate the initial transient dynamics further, and so we explore a number of release scenarios numerically: 1) release of *Wolbachia*-infected females into a wild-type population at carrying capacity in order to achieve an initial infection frequency p_0, 2) release of *Wolbachia*-infected females into a wild-type population that has been suppressed to a fraction q of carrying capacity in order to achieve initial frequency p_0, and 3) release of the same number of *Wolbachia*-infected females as in the first strategy into a population that has been suppressed locally to a fraction q of carrying capacity. The first strategy is the most straightforward in that it requires it no intervention prior to release. However, it is the least likely out of the three to result in *Wolbachia* establishment. The second strategy requires fewer females (a fraction q) to be released but requires some intervention prior to release in order to suppress the population. The resulting infection frequency is the same as in the first strategy, and so differences in density-dependent effects will determine how it is better or worse than the first strategy. The last strategy involves the same number of released females as the first strategy, but the resulting initial frequency $p_0' = p_0/(p_0 + q(1 - p_0))$ will be higher than in the other two strategies since the released individuals will make up a greater proportion of the total population. The population suppression in the last two strategies only occurs in the release area. The results are shown in Figs. 3.3-3.5. We keep the *Wolbachia*-infected per capita death rate at the *Wolbachia*-infected equilibrium constant across all forms of density dependence, such that the generation time of infected individuals at carrying capacity is the same across all forms of density dependence. This allows us to attribute differences in results to the form of density dependence rather than differences in parameter values.

We see from Figures 3.3 and 3.4 that the effect of a given release strategy on the spatial spread of *Wolbachia* depends on the form of density dependence that governs the host population. The effect of these forms of density dependence on the local frequency threshold, i.e. the threshold in a non-spatial, well-mixed population, are examined in Chapter 2 and Appendix A. From Figures 2.1 and A.3, we see that both forms of density dependence lower the frequency

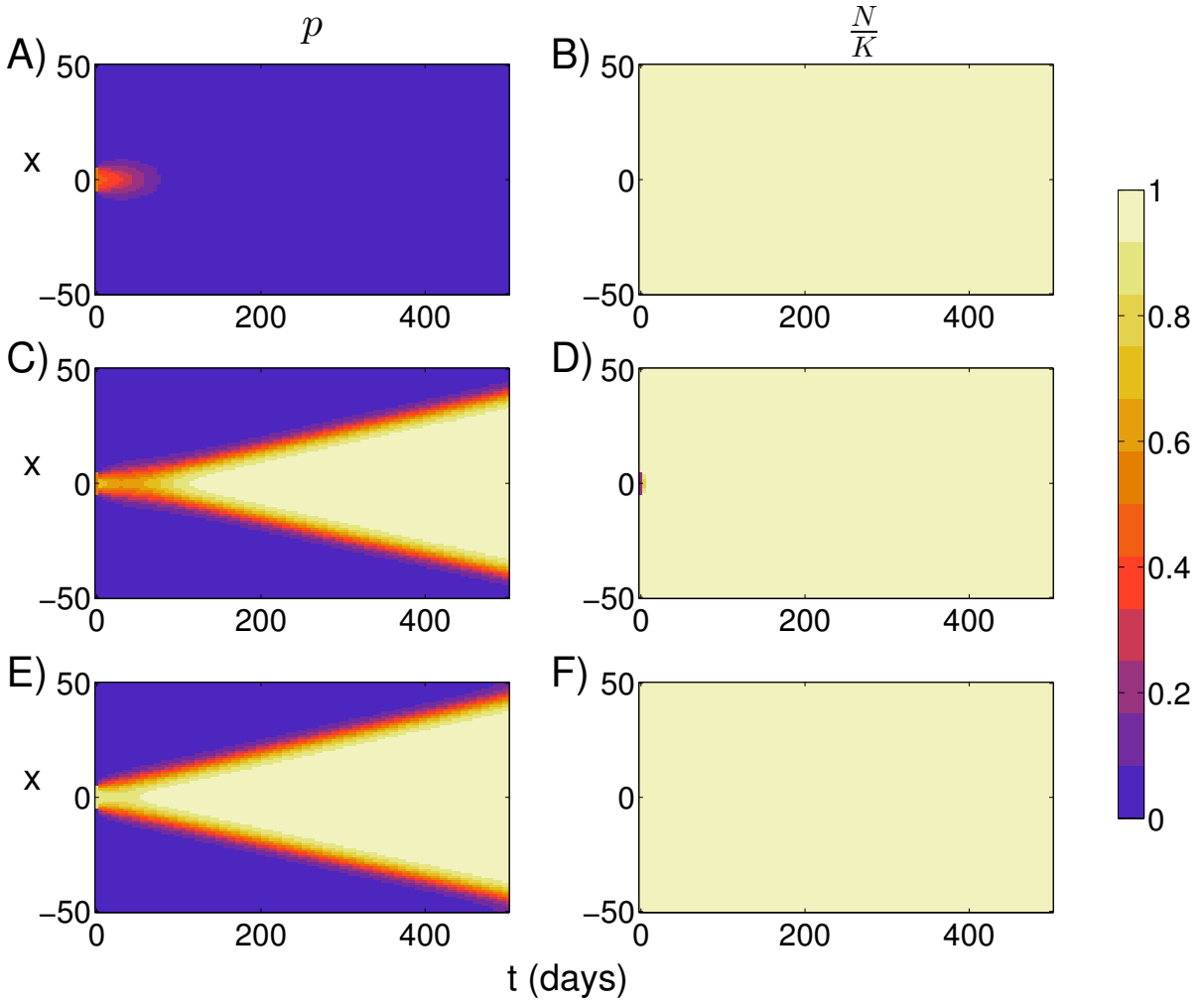

Figure 3.3: Space-time plots of infection frequency for a release radius of 5, $p_0 = 0.5$, $w = 0.7$ and type 1 density dependence (linearly decreasing per capita emergence rate). Release into carrying capacity (A, B) fails to produce a traveling wave while releasing into a population suppressed by 90% to achieve p_0 (C, D) and with the same number of individuals as in the first strategy (E, F), produce traveling waves. Frequency is shown on the left and the population size relative to wild-type carrying capacity is shown on the right. With this form of density dependence, *Wolbachia* has a negligible impact on the population size as *Wolbachia* spreads.

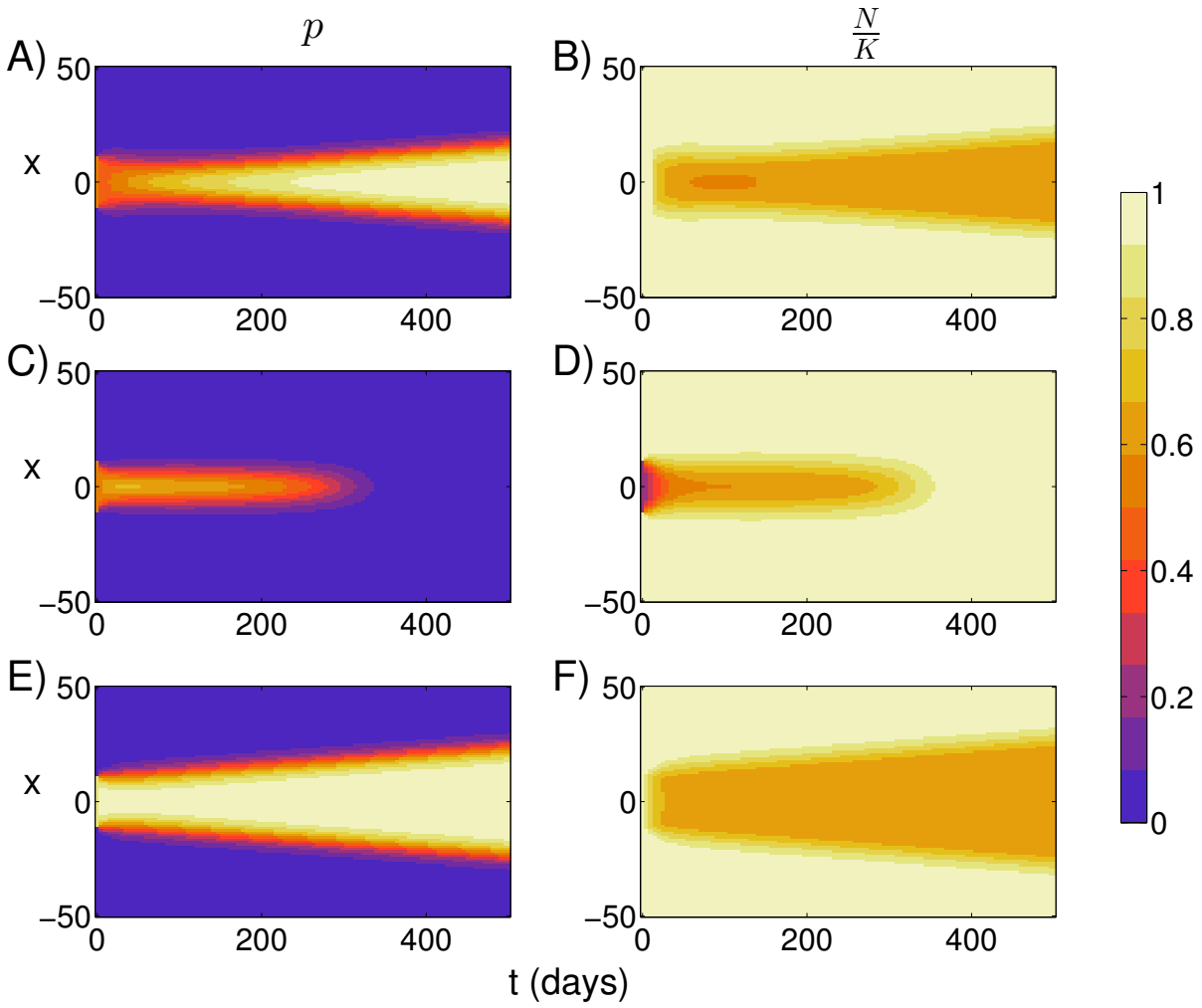

Figure 3.4: Space-time plots of infection frequency for a release radius of 11, $p_0 = 0.5$, $w = 0.7$ and type 3 density dependence (linearly increasing per capita death rate). Release into carrying capacity (A, B) produces a traveling wave while releasing into a population suppressed by 90% to achieve p_0 (C, D) fails to produce a traveling wave. Releasing into a population suppressed by 90% with the same number of individuals as in the first strategy (E, F) produces a traveling wave and does so more quickly than release into carrying capacity (A, B). Frequency is shown on the left and the population size relative to wild-type carrying capacity is shown on the right. With this form of density dependence, *Wolbachia* has a significant impact on the population size.

threshold for suppressed populations, indicating that suppressing the population prior to release should increase the chance of *Wolbachia* establishment. However, the latter form of density dependence, increasing death rate, has a lower population level at the infected equilibrium. Thus, when *Wolbachia* becomes established inside the release area, there are fewer insects to disperse outside the region and propagate the wave. Thus, the uphill gradient in population number offsets the local decrease in frequency threshold for this type of density dependence. This is the reason for the differences in Figures 3.3 and Figures 3.4 (A & C), where the efficiency of the release strategy depends on the form of density dependence. The combined strategy of suppressing the population but then releasing the same number of insects as would be required to achieve the initial frequency p_0 in a population carrying capacity appears to always be better than either of the other two strategies in producing a traveling wave (Figures 3.3 and 3.4 (E & F).

The critical patch sizes for the density-dependent *Wolbachia* model are shown in Figure 3.5 for various forms of density dependence and release strategies. The critical patch radius is determined by releasing individuals at a density to achieve p_0 into an area of length $2R$ and determining the minimum R that allows for spread (recall that in the third release strategy the number of individuals is the same as in the first release strategy but the initial frequency is higher than p_0). These are compared to the analytic prediction $R_{\text{crit}} = T(\gamma)/(2p_0)$ where $T(\gamma)$ is defined in Eq. 3.2. Although the analytical prediction is for an infinite spatial domain, we chose L large enough relative to the critical release radius such that boundary effects should not affect the results.

In contrast to what Barton and Turelli (2011) found for the frequency-only model, we find Eq. 3.2 to provide an underestimate for the critical patch radius (black dashed lines in Figure 3.5) for the density-dependent model for all but the highest release frequencies. Only the first two release strategies (blue triangles and red circles) correspond to the p_0 values on the x-axis in Figure 3.5, although they necessarily contain different numbers of released individuals, since the second (red circles) is into a population suppressed by 90%. The third release strategy

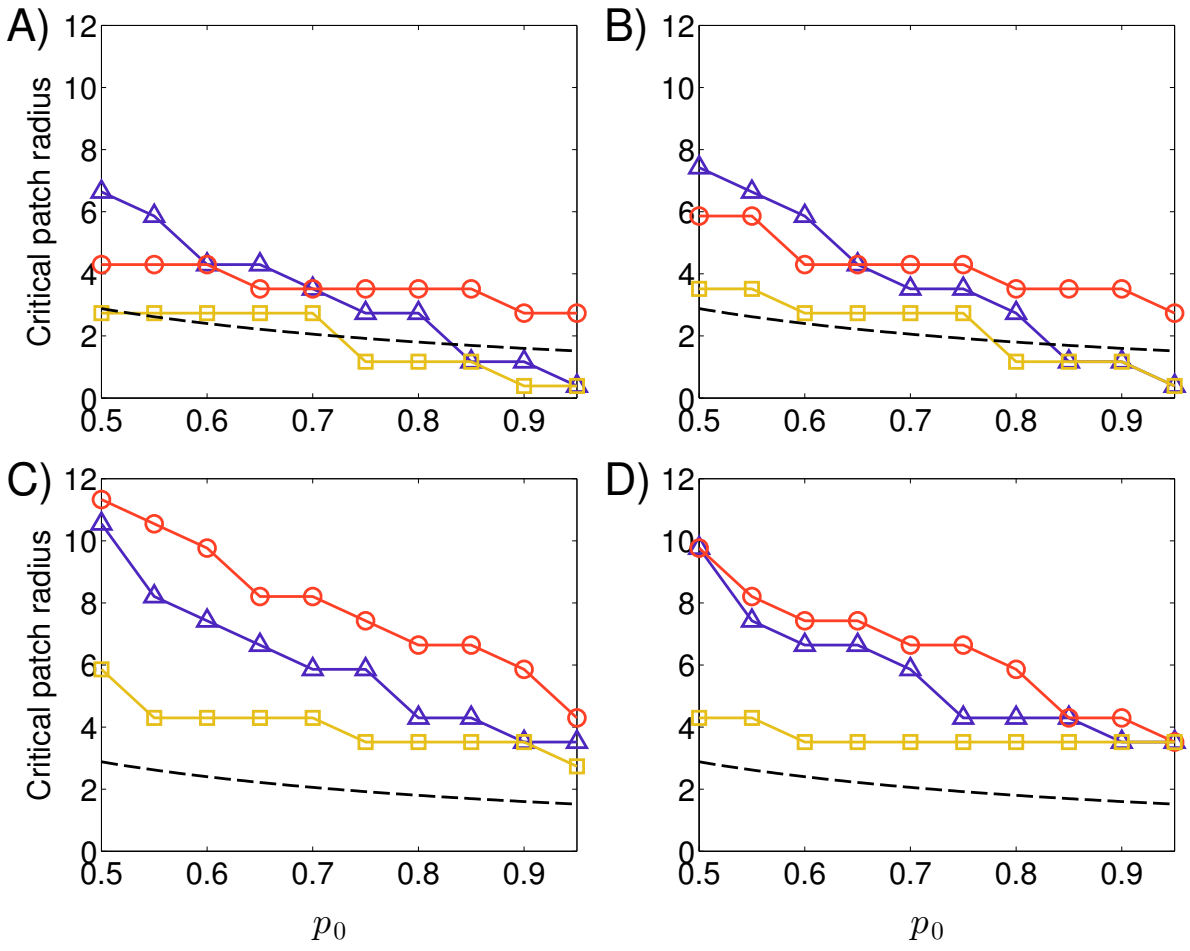

Figure 3.5: The critical patch radius R needed to obtain a traveling wave of *Wolbachia* infection for a strain that causes a 30% reduction in lifespan ($s_f = 0$, $w = 0.7$) with four types of density dependence: A) linear decrease in per capita emergence rate, B) nonlinear decrease in per capita emergence rate, C) linear increase in per capita death rate, and D) nonlinear increase in per capita death rate. *Wolbachia*-infected adults are released into a central patch of length $2R$ to achieve an initial frequency of p_0 (in all but the third release strategy). Release strategies are: release into a wild-type population at carrying capacity to obtain p_0 (blue triangles), release into a wild-type population suppressed to 10% of carrying capacity to obtain p_0 (red circles), and release into a wild-type population suppressed to 10% with the same number of mosquitoes as in the first strategy, i.e. to obtain p_0 when the population is at carrying capacity (yellow squares). The dashed line represents the analytical prediction for the frequency-only model [derived from Eq. 3.2]. The jaggedness is due to the spatial discretization and we expect these curves to be smooth for continuous space.

(yellow squares) is shown on the same graph in order to show the direct effect of suppressing the population while releasing the same number of individuals, even though the resulting initial frequency $p_0' = p_0/(p_0 + q(1-p_0)) > p_0$. Thus, the blue and red curves are for the same released number of individuals, showing that it is clearly better in all four forms of density dependence to suppress the population prior to release.

In Figures 3.5C and 3.5D, suppressing the population to achieve the same p_0 is not an efficient strategy because the resulting fewer total individuals in the release area are more easily swamped by the wild-type individuals outside the region (red triangles indicate a greater minimum release radius than blue triangles for all p_0). However, in Figures 3.5A and 3.5B, there is a tradeoff between reducing the local frequency threshold by suppressing the population and releasing a greater number of individuals (blue triangles and red circles intersect). While in the non-spatial model it is always better to suppress the population, we believe this is offset in this instance for high values of p_0 in the spatial model because releasing greater numbers of insects means more can disperse outside the release area (Antonelli et al., 2015, Chapter 2 of this dissertation). The results in the spatial model thus show a more complicated tradeoff between decreasing the local invasion threshold due to density dependence and increasing the total number of individuals that can disperse.

The release strategies depicted in Figure 3.5 affect the transient dynamics and whether or not a traveling wave will be produced. Once a traveling wave is produced, it will have the same asymptotic wave speed for all release strategies because the wave speed is governed by the fitness and dispersal parameters rather than initial conditions. In measuring wave speed for the next section, we thus use the third release strategy with a high p_0 to give the population the best possible chance to produce a traveling wave.

Asymptotic wave speed

The predicted wave speed for the frequency-only model is approximately

$$c \approx \sigma_d \sqrt{s_h d_I} \left(\frac{1}{2} - \hat{p} \right), \tag{3.3}$$

where $\sigma_d = \sqrt{2\lambda}$ is the standard deviation of adult dispersal in one day, and d_I is the per capita death rate of *Wolbachia*-infected adults (Stokes, 1976; Barton, 1979; Turelli and Hoffmann, 1991; Barton and Turelli, 2011; Schraiber et al., 2012). While in previous models d_I is constant, in some forms of density dependence we present here, d_I varies with population density. When applicable, we consider $d_I = d_N(K_I)/w$, the *Wolbachia*-infected per capita death rate at the *Wolbachia*-established equilibrium, for the approximation of wave speed, where the *Wolbachia*-established equilibrium population density K_I solves $d_N(K_I)/w = (1 - s_f)b_N(K_I)$.

We measure wave speed numerically by determining the position of a frequency contour over time (see any of the color contours in Figures 3.3 and 3.4: A, C or E). When the contour corresponding to $p = 0.9$ is increasing linearly in space with respect to time, we consider this to be the asymptotic wave speed. The results for wave speed for different forms of density dependence are shown in Figs. 3.6 - 3.7.

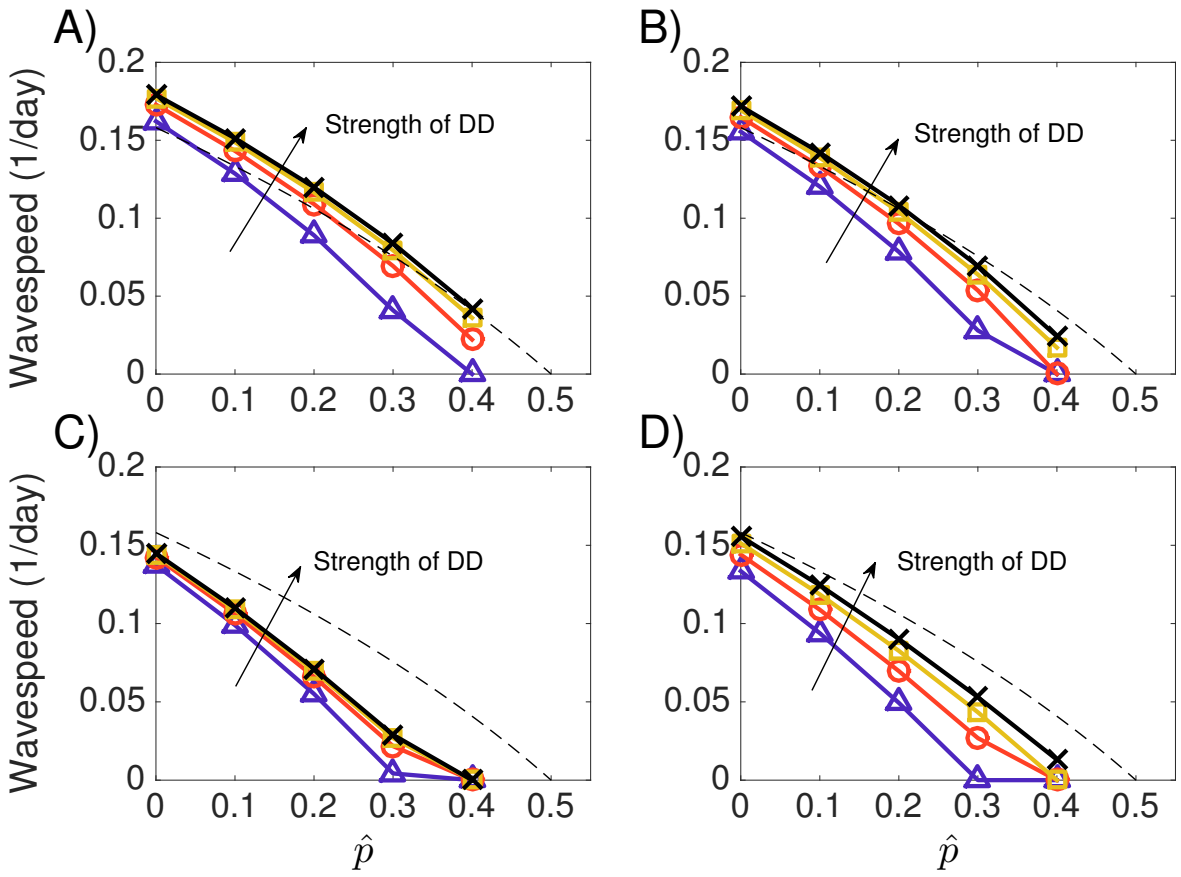

Figure 3.6: The asymptotic wave speed of the reaction-diffusion model for a lifespan-shortening strain of *Wolbachia* with four different types of density dependence: A) linear decrease in per capita emergence rate, B) nonlinear increase in per capita emergence rate, C) linear increase in per capita death rate, D) nonlinear increase in per capita death rate. The predicted frequency threshold $\hat{p} = 1 - w(1 - s_f)$ was changed by maintaing zero fecundity cost ($s_f = 0$) and adjusting the relative lifespan of *Wolbachia*-infected females w. Colors represent strength of density dependence, controlled by increasing $b_0 = 0.25, 0.5, 1, 2$ for A and B, decreasing $d_0 = 0.04, 0.02, 0.01, 0.005$ for C, and increasing $\beta = 0.5, 1, 2, 4$ for D. The order from weakest to strongest is (bottom to top) violet triangles, orange circles, yellow squares, black x's. Otherwise, $b_0 = 1$, $d_0 = 0.1$. The dashed line is the prediction by the frequency-only model [Eq. 3.3].

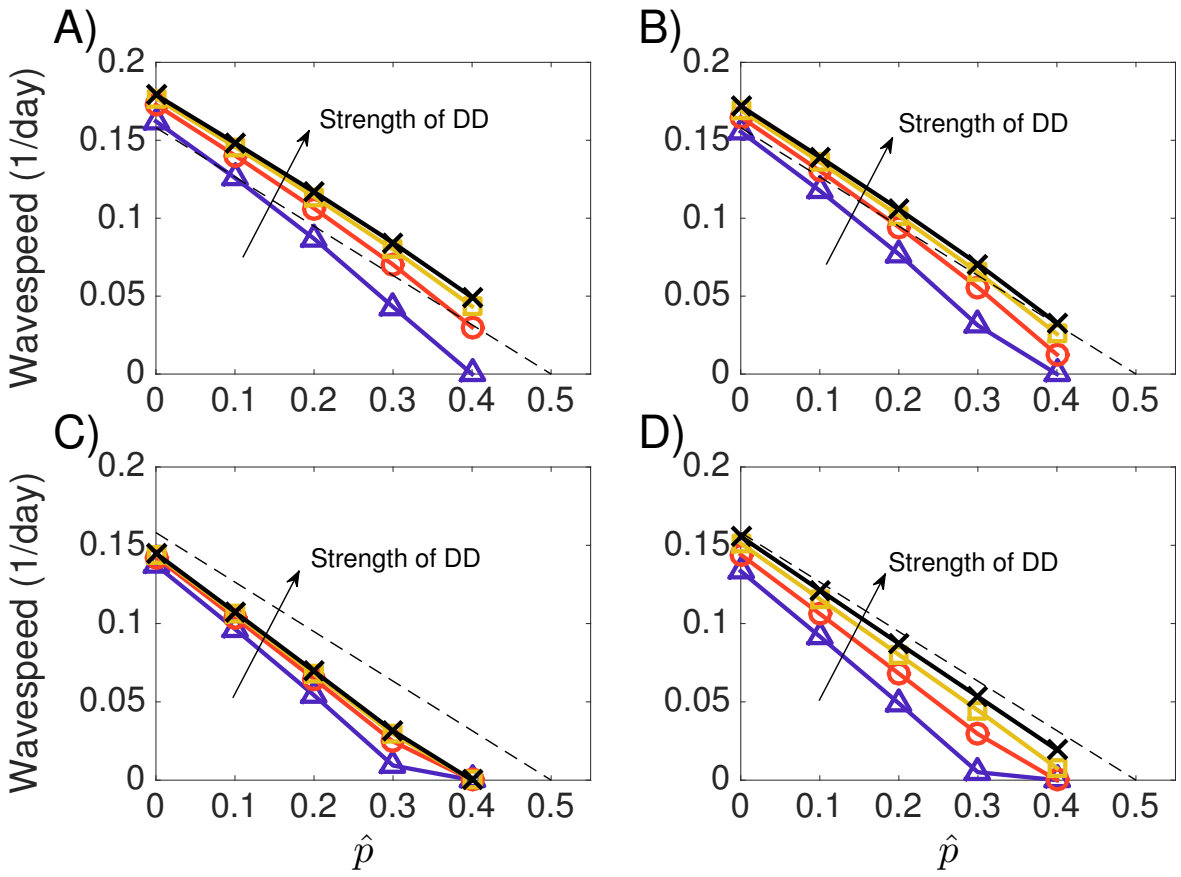

Figure 3.7: The asymptotic wave speed of the reaction-diffusion model for a non-lifespan-shortening strain of *Wolbachia* with four different types of density dependence: A) linear decrease in per capita emergence rate, B) nonlinear increase in per capita emergence rate, C) linear increase in per capita death rate, D) nonlinear increase in per capita death rate. The predicted frequency threshold $\hat{p} = 1 - w(1 - s_f)$ was changed by maintaing zero fitness cost to survival ($w = 0$) and adjusting the fecundity cost of *Wolbachia*-infected females s_f. Colors represent strength of density dependence, controlled by increasing $b_0 = 0.25, 0.5, 1, 2$ for A and B, decreasing $d_0 = 0.04, 0.02, 0.01, 0.005$ for C, and increasing $\beta = 0.5, 1, 2, 4$ for D. The order from weakest to strongest is (bottom to top) violet triangles, orange circles, yellow squares, black x's. Otherwise, $b_0 = 1$, $d_0 = 0.1$. The dashed line is the prediction by the frequency-only model [Eq. 3.3].

3.3.2 Metapopulation model

Wave speed for the metapopulation model was measured by considering the total number of patches invaded over time and performing linear regression on the portion where the asymptotic wave speed was assumed to be reached. This portion was from 5% of patches beyond the release patches to 90% of patches, which was selected to exclude both the initial transient dynamics and the dynamics at the boundary $x = \pm L$ from the analysis. In this region, the number of invaded patches over time was roughly linear, and represents two times the average wave speed since the wave propagates in both directions. Thus, we use linear regression to estimate the slope to determine the average wave speed, as shown in Figure 3.8.

The wave speed depends strongly on fitness cost, spatial dimension, spatial heterogeneity, and stochasticity in population dynamics, as seen in Figure 3.9. For each value of patch size standard deviation σ_K, we run the model 100 times with different spatial configurations, chosen by drawing the size of each patch from either the negative binomial or binomial distribution with mean μ_K and standard deviation σ_K and determine the resulting wave speed. The variance in wave speed across replicates thus depends on the variance in spatial configurations for the deterministic model and the variance in spatial configurations and population dynamics in the stochastic model.

In Figure 3.9 we see that increased spatial heterogeneity in patch carrying capacity decreases the average speed at which a wave of *Wolbachia* infection travels through the metapopulation. This agrees with results from a previous deterministic one-dimensional model (Hancock and Godfray, 2012) and previous analytic results (Barton, 1979; Nagylaki, 1975; Barton and Turelli, 2011), although we also look at the effect of stochastic population dynamics and two-dimensional spatial spread. In a one-dimensional array of patches, the deterministic model predicts a faster wave speed than the stochastic model when the fitness cost is low. This is likely because, when the fitness cost is low, the deterministic model consistently produces enough *Wolbachia*-infected individuals that disperse into neighboring populations to exceed the frequency threshold. The stochastic model produces the same number on average, but varies across replicates. The repli-

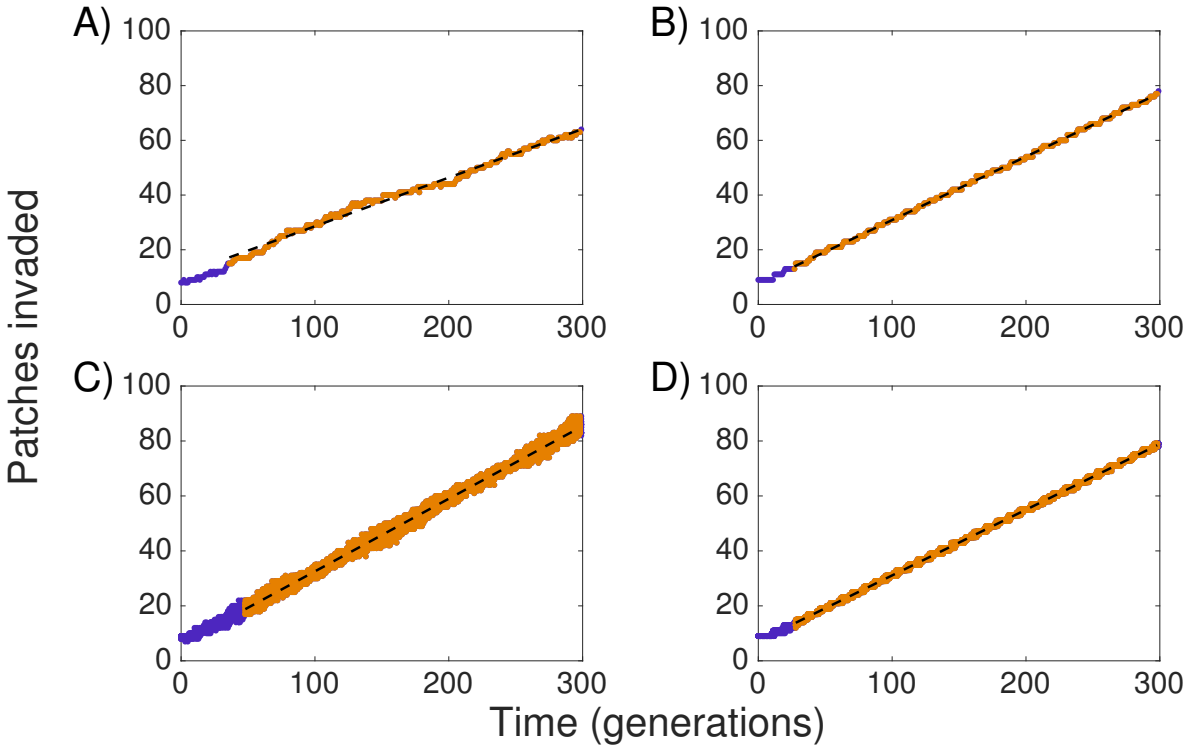

Figure 3.8: Number of patches invaded over time for A) stochastic 1-D, B) deterministic 1-D, C) stochastic 2-D and D) deterministic 1-D settings with *Wolbachia* causing 90% relative fitness ($c = 0.9$), complete cytoplasmic incompatibility, $s_h = 1$, horizontal movement parameter $\alpha = 0.1$, and patch size standard deviation $\sigma_K = 5$. The orange (light) points mark the region used for linear regression to determine wave speed, which avoids regions with transient dynamics or boundary effects. The width of the plots in C and D are due to the number of invaded patches for each of the 20 rows at each time point.

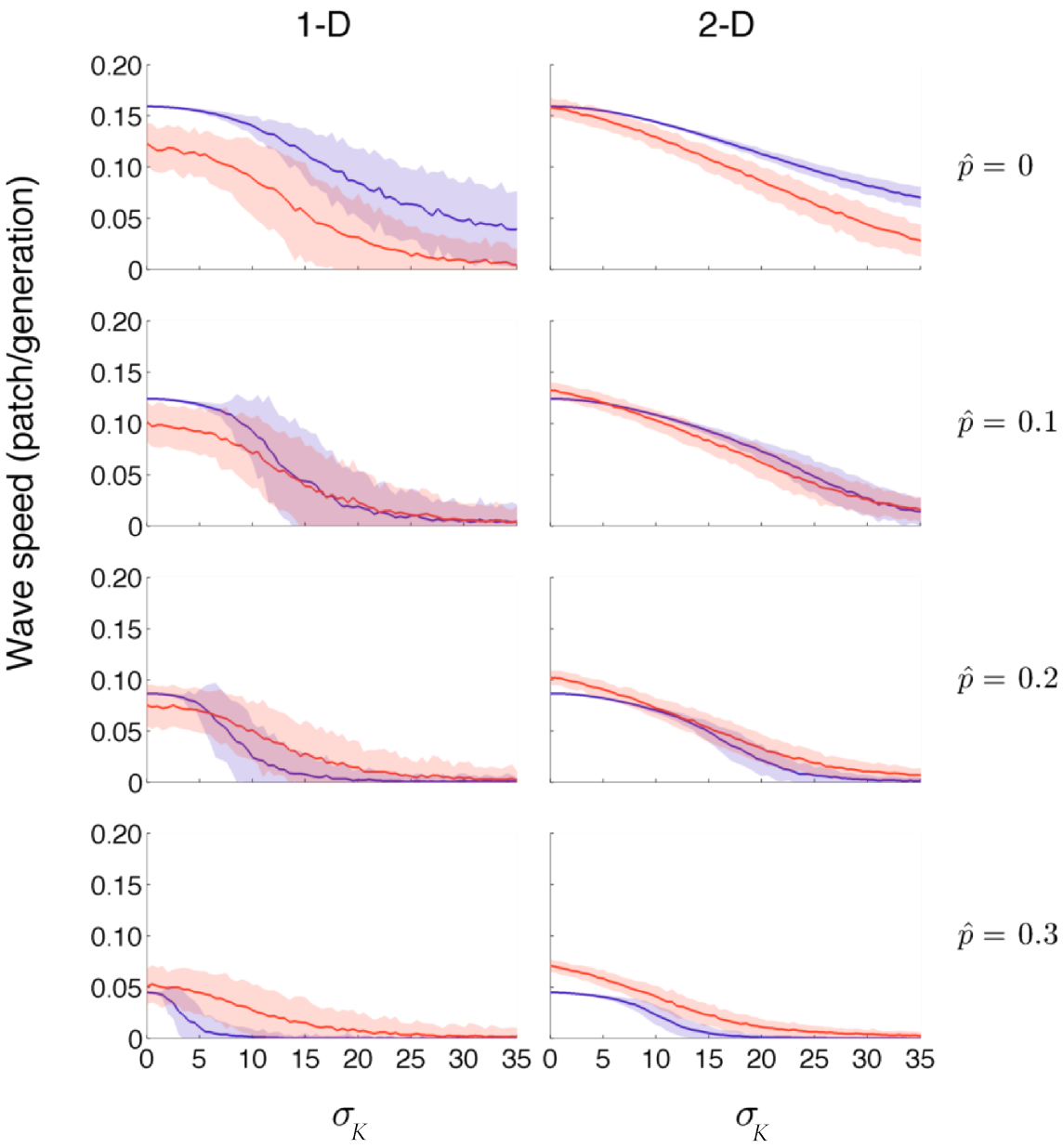

Figure 3.9: Average wave speed (solid lines) +/- one standard deviation across 100 replicates. Each replicate contains patches with carrying capacities drawn randomly with mean $\mu_K = 20$ and standard deviation σ_K (drawn independently for each replicate) and is run with deterministic (blue, dark) or stochastic (red, light) population dynamics.

cates in which the stochastic model underproduces end up nearer the frequency threshold, and these replicates are disproportionately penalized because frequency dynamics are much slower near the threshold. Thus, even when the frequency threshold is 0 (top row of Figure 3.9), such that a traveling wave is inevitable, its progress is slowed considerably more when a stochastic event underproduces than it is sped up when a stochastic event overproduces, and the net result is an average decrease in wave speed relative to the deterministic model.

The stochastic two-dimensional model also produces a slower wave speed on average than the deterministic model when there is no fitness cost (top right of Figure 3.9). However, in a spatially homogeneous environment ($\sigma_K = 0$), the stochastic model wave speed approaches that of the deterministic model, unlike in the case of one-dimensional spread. We expect this is due to "slower" rows receiving extra *Wolbachia*-infected immigrants from more quickly spreading neighboring rows, which speeds up the overall invasion wavefront. However, it is not immediately clear in that case why the difference between stochastic and deterministic predictions becomes more pronounced as σ_K increases.

3.4 Discussion

It may be possible to exploit certain aspects of density-dependent population dynamics to further the chance that *Wolbachia* will spread in a population. In particular, for all the forms of density dependence examined here, we find that suppressing the population prior to the release of a fixed number of *Wolbachia*-infected mosquitoes increases the chance of a stable wave of *Wolbachia* infection traveling through space. There are both population genetics (frequency) and population dynamics (density) effects here. We found previously with a non-spatial model that suppressing the population prior to release of a lifespan-shortening strain of *Wolbachia* causes not only a lower critical release number but also a lower critical release frequency. That is, the frequency threshold itself is lowered when a lifespan-shortening strain is released into a suppressed population. This effect does not appear as strong in the spatial model, as evidenced by the blue triangles and red circles in Figure 3.5. In fact, suppressing the population prior to

release when density dependence acts on the per capita death rate appears to *raise* the critical frequency required in the release patch (red circles), although it still lowers the critical number (yellow squares). This is likely because the decrease in the local frequency threshold is offset by the disproportionate effect of wild-type immigrants from outside the release area when the population in the release area is small. This may be mitigated by suppressing a larger area than the release area, thus reducing the ability of wild-type immigrants to flood the release area before a traveling wave has been produced.

Density dependence also affects the asymptotic speed that a traveling wave reaches, depending on how strong it is, and whether it acts on the per capita emergence or death rate. In general, the stronger density dependence, the higher the wave speed. Figs. 3.6 and 3.7 indicate that density dependence may actually increase the wave speed beyond the frequency-only prediction when density dependence acts on the emergence rate. This result agrees with what Hancock and Godfray (2012) found with a model that included density-dependent larval mortality, which is most analogous to the decrease in per capita emergence rate in our simpler model. However, it appears to only occur when fitness cost is low and not at all when density dependence acts on the death rate. With density-dependent mortality, the wave speed approaches the frequency-only prediction but never exceeds it (Figure 3.6D and 3.7D). One potential reason for these differences is that the *Wolbachia*-established equilibrium population density is more sensitive to the fitness parameters. For the same parameters, the *Wolbachia*-established equilibrium population densities are higher when density dependence acts on the emergence rate than on the death rate. This does not explain the difference in wave speeds when there is no fitness cost, however, because the population density at the *Wolbachia*-established equilibrium is equal to K for both types of density dependence.

One reason for the difference in wave speeds when there is no fitness cost may be that, at the traveling wave front, the most CI and thus population suppression occurs. When density dependence affects the emergence rate, this decrease in population density at the wavefront causes the rate of emergence of new adults to increase. This may speed up the increase in

frequency in both space and time, especially when density dependence is strong. On the other hand, when density dependence affects the death rate, adults at the traveling wave front experience increased lifespans, slowing the replacement of wild-type with *Wolbachia*-infected adults. Note that we have also used the per capita death rate at the *Wolbachia*-established equilibrium as the approximation for the frequency-only wave speed (dashed lines in Figs. 3.6 and 3.7), which is only experienced by adults once the traveling wave has passed. A more appropriate approximation may be to use the per capita death rate corresponding to the population density at the front of the traveling wave, i.e. the trough where mixing causes CI to reduce the population density to a local minimum. We do not know of a way to determine this population density analytically, although it could be determined numerically. The effects of density dependence do not appear to depend on whether the fitness cost of *Wolbachia* is to longevity (Figure 3.6) or fecundity (Figure 3.7). This is an interesting contrast to the non-spatial results in Antonelli et al. (2015, Chapter 2 of this dissertation), in which lifespan-shortening was necessary to observe any difference in the invasion threshold.

Hancock and Godfray (2012) showed how spatial heterogeneity slowed wave speed and strong density dependence increased wave speed. We have shown how the effect of strength of density dependence generalizes to other forms of density dependence (linear/nonlinear decrease in per capita emergence rate and linear/nonlinear increase per capita death rate). In short, "stronger" density dependence does increase wave speed. However, the wave speed relative to analytic predictions and the critical patch size both depend on the form of density dependence. We show how wave speed can exceed that of the frequency-only prediction when density dependence acts on the emergence rate (Figure 3.6) but not when it acts on the death rate (Figure 3.7), in which case the analytic approximation always overestimates the wave speed. Furthermore, while our results agree with Hancock and Godfray (2012) that spatial heterogeneity consistently slows spread, we show how the degree to which it slows spread depends on one- or two-dimensional spread, stochasticity and fitness cost (Figure 3.9).

Jansen et al. (2008) analyzed the stochastic spread of *Wolbachia* in a non-spatial model

with constant population size N, and Barton and Rouhani (1991) performed a similar analysis on a model of underdominance, but both analyze the probability of establishment for small introductions; thus, it is difficult to compare to our results for large releases to theirs. We find, overall, that stochastic dynamics create slower spread than predicted by deterministic models when fitness cost is low, and faster than predicted by deterministic models when fitness cost is high.

While the relative differences have important implications for spread of *Wolbachia* infection in the field, it is important to note that all the predicted wave speeds are rather slow for practical purposes even when fitness cost of *Wolbachia* is low, as has been previously noted (Schraiber et al., 2012). However, while previous models have focused on some of the constraints of using a lifespan-shortening strain (Schraiber et al., 2012), we demonstrate that it may be equally useful as a non-lifespan-shortening strain. The asymptotic wave speed does not appear to be strongly affected by whether the *Wolbachia* strain is lifespan-shortening (Figure 3.6) or not (Figure 3.7) so much as it depends on the type and strength of density dependence.

We have shown how density dependence, stochasticity in population dynamics, and spatial heterogeneity affect the spread of *Wolbachia*. Density dependence may either help or hurt the spread of *Wolbachia*, depending on where in the life cycle of the insect in question it acts. Stochasticity in population dynamics can decrease the average spread in a one-dimensional spatial environment, although it can prevent wave barriers in highly heterogeneous environments when there is a fitness cost. Stochasticity may also increase average wave speed in two-dimensional environment where patches can benefit from neighbors in which invasion of *Wolbachia* is more successful by chance.

Understanding the contributions of all three factors will be important for selecting the best strains of *Wolbachia* and release strategies based on their effects on host fitness and the host's population dynamics. While frequency-only models have provided useful approximations and valuable theoretical insights, we have expanded here on how density dependence, stochasticity and spatial heterogeneity cause deviations from theoretical predictions, in hopes of better

informing how *Wolbachia* may spread when intentionally released for global health strategies.

Chapter 4

Bayesian inference for *Aedes aegypti* immature growth in field containers in Iquitos, Peru

ABSTRACT

Aedes aegypti larvae often develop in field containers with standing water in which detritus accumulation is thought to support microorganisms that serve as a food source; however, the relationship between detritus accumulation and larval nutrition remains unclear. We performed an experiment in Iquitos, Peru to determine the effect of detritus accumulation in water-filled containers on *Ae. aegypti* larval growth. We developed three versions of a stochastic model for the progression of *Ae. aegypti* through its life stages and used continuous-time Markov chain theory to derive the likelihood of field parameter values given observed larval trajectories. Using Bayesian model selection, we determined the best version of the model: this contains different development rates among larval instars when food is present, the possibility that food is depleted, and increased mortality under starvation conditions. We estimated the posterior distributions of parameters governing development, mortality and rate of food depletion, and we used the last to infer the distribution of food accumulation in buckets left out for varying lengths of time. We found that immature dynamics were primarily determined by the presence or absence or food, regardless of quantity. While older water had more food on average, water as new as two days in the field was able to support larvae through third and fourth instars, and the average development rate when food was present was the same for old and new water. Despite a slight increase in average food accumulation for containers left in the field for longer periods of time, there is a large amount of variance indicating that all the factors that contribute to food accumulation are yet to be uncovered. This warrants further study into the elusive mechanisms of food accumulation in the field, which play a crucial role in vector ecology, but are still incompletely understood.

4.1 Introduction

Dengue is a mosquito-borne viral disease that affects nearly 390 million people each year (Bhatt et al., 2013). The disease can present a wide variety of symptoms ranging from fever, rash and severe joint pain to internal hemorrhaging and death. It is endemic in many tropical regions where it is transmitted primarily by one species of mosquito, *Aedes aegypti*. *Ae. aegypti* is an efficient vector in dense urban environments due in part to female adults' preference for feeding on humans and the larvae's ability to develop, pupate, and emerge in a variety of artificial containers that collect standing water (Ponlawat and Harrington, 2005; Scott et al., 2000). There is currently no vaccine or treatment for dengue, and so control efforts revolve around controlling the vector population.

Mathematical models can be a useful tool in assessing the feasibility of various vector control strategies, especially novel techniques involving the release of genetically modified mosquitoes that seek to either suppress the native population or replace it with a population less able to transmit the disease (Gould et al., 2006). In order to make accurate predictions, detailed knowledge of *Ae. aegypti* ecology in dengue-endemic regions is crucial.

A number of models for *Ae. aegypti* dynamics have been previously developed. Gilpin and McClelland (1979) developed a deterministic model based on laboratory studies for changes in larval weight and available food, in which mosquitoes pupate once both a minimum development time and weight have been reached. The portion of the model corresponding to pupation is often referred to as the "window model" because larval weight, when plotted versus time, must cross a rectangular "pupation window" before larvae are expected to pupate (Carpenter, 1984; Gimnig et al., 2002; Romeo Aznar et al., 2014). The more detailed models CIMSiM (Focks et al., 1993) and Skeeter Buster (Magori et al., 2009) were later developed for *Ae. aegypti* dynamics, and both incorporate the Gilpin and McClelland (1979) equations for growth in the immature stages and the window model for pupation.

Romeo Aznar et al. (2014) recently criticized the window model for being descriptive rather than theoretical. They propose a multi-compartment model for the time to pupation in which

the waiting times in each compartment are exponentially distributed. This is similar to the compartmental model that Gilpin and McClelland (1979) initially considered, in which compartments corresponded to observable life stages: eggs, four aquatic larval stages known as instars, which are separated by molts of the exoskeleton, the pupal stage, and the adult stage. Gilpin and McClelland (1979) ultimately dismissed the instar model, however, due to its inability to account for "weight, larval age and food density" (p. 365). Romeo Aznar et al. (2014) address this last issue by considering that compartments can be either of two types: food-sensitive or food-independent. The transition rates out of the food-sensitive compartments depend on food availability whereas the rates out of food-independent compartments do not. This is an important next step in incorporating food dynamics into a compartmental model; however, the compartments do not appear to correspond to anything biological, serving rather as a mathematical convenience, and the number of compartments becomes a free parameter that can be used to better fit the data. Thus, we find their model to also be more descriptive (statistical) than theoretical (mechanistic). While both types of models are useful, we believe a mechanistic model in which the compartments correspond to observable states is preferable in terms of understanding the biological dynamics and making predictions.

We propose a model for immature *Ae. aegypti* growth like the one that Gilpin and McClelland (1979) originally proposed, in which compartments correspond to instars and pupae. With such a model, we can obtain more information than just time to emergence by observing each larva's progression through the various stages over time over time. This model also has the advantage of tracking instars, which are easily determined in the field with a microscope, rather than "dry weight", which requires that larvae be sacrificed to measure. While Gilpin and McClelland's (1979) preliminary model did not incorporate food dynamics, an important component of the overall dynamics, we can include them by considering transition probabilities conditioned on the availability of food in the larval habitat.

We performed an experiment in Iquitos, Peru to determine immature *Ae. aegypti* growth in the field. Rather than control the amount of food in containers, we allowed containers to

accumulate detritus in the field for controlled periods of time. Liver powder, yeast/protein mixtures or fish food are typically used for food in the lab, but it is difficult to know what this corresponds to in the field. The different durations of accumulation time we refer to throughout as "water age." By observing the life histories of larvae placed in those containers and comparing them to our model we are able to estimate development and mortality rates and infer food levels in those containers. We use Bayesian model selection to determine the best-fit version of the model, and we use Markov chain Monte Carlo (MCMC) to approximate the posterior distribution of parameters governing immature dynamics, which was then used to infer the distribution of food in containers in Iquitos.

4.1.1 Materials and Methods

Experimental Setup

Iquitos, Peru is a city with a population of approximately 350,000 situated in the Amazonian rainforest. Dengue has been endemic in the city since the 1990s when the virus was thought to have been reintroduced following reinvasion of *Ae. aegypti* in the 1960s (Morrison et al., 2010). The dynamics of both dengue and *Ae. aegypti* have been studied in Iquitos for over a decade, and control efforts are ongoing, but epidemics of the disease continue to occur roughly annually (Morrison et al., 2004, 2010; Stoddard et al., 2014). Skeeter Buster, a detailed stochastic model of *Ae. aegypti* was parameterized to simulate the mosquito population's dynamics in Iquitos with the goal of better understanding the effect of various control efforts (Magori et al., 2009). This has proved difficult in part because of the lack of understanding about food accumulation in containers and how it impacts larval growth. Xu et al. (2010) found that Skeeter Buster was particularly sensitive to parameters governing larval dynamics, and Walsh (2011) found that the model was unable to predict larval survival and the distribution of instars within containers in Tapachula, Mexico when parameterized using local weather data. We chose Iquitos as a site where a model of larval instars and a simple field experiment could help elucidate an important but still poorly understood process.

We set up a randomized complete block design with subsampling that used ten houses as blocking factors, two levels of water age within each house, and five replicates within each water treatment (see Figure 4.1). Ten houses in the northern region of Iquitos, Peru were selected, and two four-gallon buckets were placed in the open outside each house and filled with tap water from that house. The first bucket in each house (treatment A) was left to accumulate debris for five weeks and was visited every two to three days to remove any mosquito eggs, larvae or pupae. The second bucket in each house (treatment B) was left to accumulate detritus for two days. While the specific relationship between the accumulation of detritus in containers and larval nutrition is still not entirely understood, higher accumulation is thought to support a greater quantity of microorganisms on which mosquito larvae feed (Merritt et al., 1992; Ponnusamy et al., 2008). These two treatment levels approximate extremes for containers in the field that are found to have water standing for varying lengths of time, and thus serve as a proxy for different food levels, since food is not controlled. At the end of the accumulation phase, all twenty buckets (two from each house) were transported to the laboratory. Buckets were covered with plastic wrap to prevent spillage during transport.

In the laboratory, the sides of each bucket were scraped with a wooden stirrer in order to free any attached organic matter such as algae or detritus, and the water was stirred in order to evenly distribute the organic matter. Once the water was well mixed, five 15-mL Falcon conical centrifuge tubes (Fisher Scientific, Houston, Texas) were filled with 13 mL of water from each bucket, as depicted in Figure 4.1.

Ae. aegypti eggs were identified and collected using a paper towel from household containers at various sites in Iquitos. Paper towel strips containing eggs were then placed together in a tap water bath at ambient outdoor temperature ($\sim 26^{o}$ C) and left overnight to hatch. All larvae used in the experiment hatched within 12 hours of each other. One neonate larva, selected at random, was placed into each of the 100 centrifuge tubes representing all house-treatment-replicate combinations (10 houses $\times$ 2 treatments $\times$ 5 replicates), as shown in Figure 4.1. The reason for isolating larvae was to be able to uniquely identify the life history of each larva.

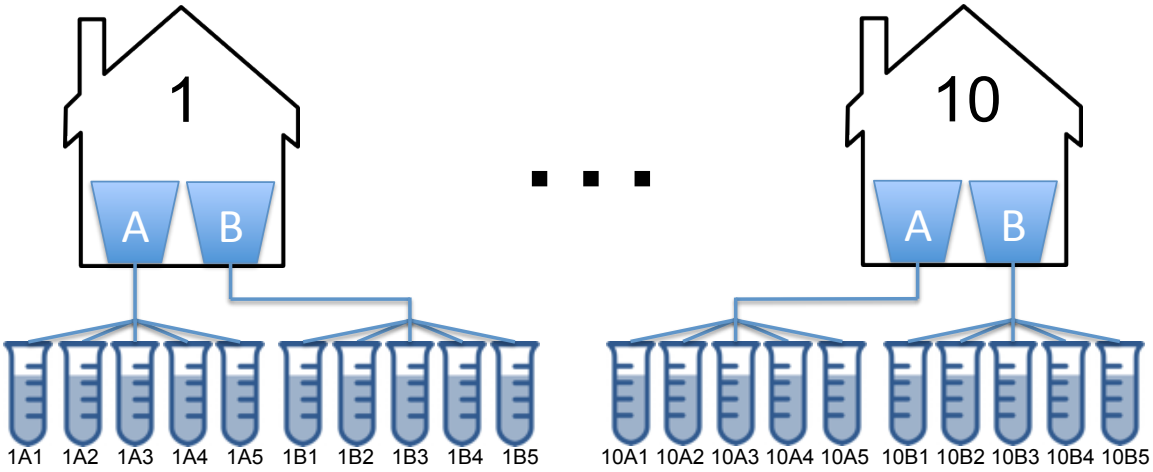

Figure 4.1: The hierarchical structure of the experiment. Old (A) and new (B) water treatments are blocked by houses, and there are five immature replicates for each bucket.

This, however, neglects the effects of intraspecific competition in field containers which typically contain multiple larvae at a time. Competition among *Ae. aegypti* larvae for food in containers plays an important role in larval growth (Barbosa et al., 1972; Dye, 1982; Walsh et al., 2011), and its effect on population dynamics in Iquitos warrants further attention, but it was beyond the scope of the present study.

Centrifuge tubes containing larvae were stored upright in polystyrene blocks placed outdoors on a surface 1m above ground. They were left uncapped in order to allow gas exchange between water and air, simulating field conditions, and were covered with mosquito netting to prevent oviposition or predation. Evaporation was minimal, but each centrifuge tube was replenished with drinking water (Agua de Mesa Tropical, Iquitos) each day to maintain a constant volume of 13 mL without affecting detritus content.

4.1.2 Data Collection

Individuals were removed from each centrifuge tube daily using a disposable pipette and placed in a drop of cold water on a microscope slide in order to slow their movement. Each individual's life stage (first instar, second instar, third instar, fourth instar, or pupa) was recorded using a

Zarbeco MiScope handheld digital microscope (Zarbeco, Randolph, New Jersey) and afterward they were returned to the centrifuge tube. The pipette was rinsed with bottled water between each observation to avoid transferring any organic material between centrifuge tubes. Life stages and mortality were recorded at 24-hr intervals for 18 days, which was found to be a sufficient length of time for all individuals to either emerge or die in a previous laboratory experiment using the same methods (data not shown). While both laboratory and field experiments have shown that *Ae. aegypti* can survive in immature stages under starvation conditions for up to forty days (Gilpin and McClelland, 1979; Southwood et al., 1972), we considered that this would be rare and chose instead to maximize the accumulation time of buckets in treatment A given the time constraint of the entire experiment. Adult mosquitoes were sacrificed upon emergence to prevent the risk of dengue transmission.

4.1.3 Data Processing

During the accumulation phase, one of the buckets was accidentally emptied, and so all data from that house were discarded. Thus, we considered only 9 houses in our final analysis. Also, three larvae were accidentally injured during observation, so the data following those points were discarded.

Ae. aegypti immature development rates increase approximately linearly with temperature in the range 15-32°C (Gilpin and McClelland, 1979). We obtained data for the daily minimum and maximum air temperature in Iquitos over the course of our experiment (NCDC, 2015), and we used an approximation by Focks et al. (1993) to convert air temperature to water temperature. We determined that the water temperature was between 23.9°C (SD: 0.75°C) and 30.9°C (SD: 0.49°C). Assuming that temperature varied sinusoidally between these two extremes each day, and because we observed life stages at 24-hr intervals, this means that the inferred growth rates are equivalent to those at a constant water temperature of 27.4°C. Thus, in order to compare to *Ae. aegypti* immature development at temperature T, one would need to multiply our results by the conversion factor $(T - 13.4^{\circ}\text{C})/(27.4^{\circ}\text{C} - 13.4^{\circ}\text{C})$, where 13.4°C

is the critical temperature determined by Gilpin and McClelland (1979) at which the linearly extrapolated development rate hits zero.

4.2 Model

We use a continuous-time Markov chain (CTMC) to model the changes in life stage of an individual over time (Figure 4.2). Each individual starts as a newly hatched first instar (1) and then progresses through the immature stages, first to fourth instar (1-4) and pupa (5), until reaching either of two absorbing states, adulthood (6) or death (7). The times at which each individual transitions as well as the state to which it transitions are stochastic, with probabilities determined by rates r_i and μ_i.

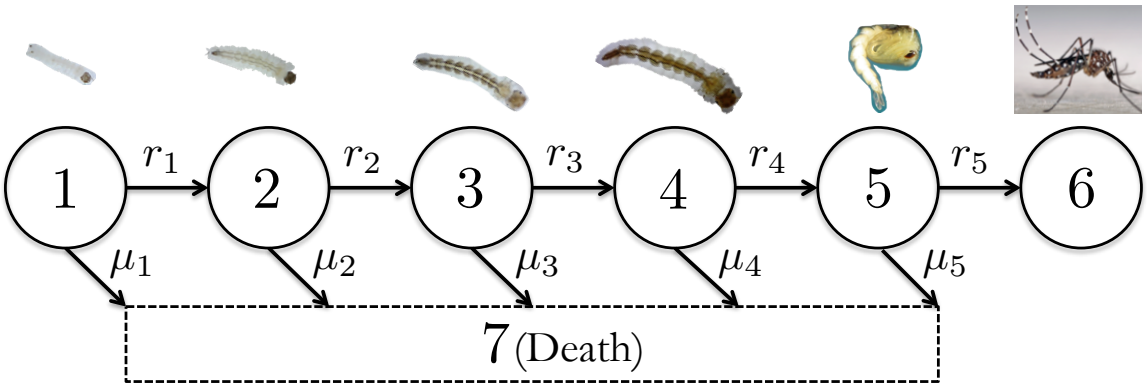

Figure 4.2: Continuous-time Markov chain for immature *Ae. aegypti* growth. An individual transitions from its current state to any of the possible next states indicated by arrows. The next state and time of transition are stochastic, occurring with probabilities determined by transition rates (arrow labels). States are first through fourth instars (1-4), pupa (5) and adult (6).

We consider three versions of this model, which contain either three or four parameters. Having more parameters will enable us to better fit the model to our dataset but runs the risk of overfitting the data. We used the Bayesian deviance information criterion (DIC) to determine the best model to use given our dataset as it both selects for models that better fit the data,

and penalizes them for having extra parameters.

In the first version of this model, when food is available, all development rates r are assumed to be the same and all mortality rates μ_f are the same. This implies that the expected duration in each life stage is the same, which may not be the most biologically realistic assumption, since *Ae. aegypti* are expected to spend more time in the fourth instar and pupal stage (Christophers, 1960), but it reduces the complexity of the model, which facilitates analysis and implementation in Bayesian routines. When food is depleted, we assume the development rate becomes zero, and the mortality rate for all stages assumes a new value, μ_v.

The second version is the same as the first, except that we assume that the mortality rate is zero when food is available. Thus, larvae develop until food is depleted, at which point they starve until they die.

The third version is the same as the second, with no mortality when food is available, except that there are two different developments rates: one for the first three instars, r_1, and one for fourth instars and pupae, r_2. This is meant to reflect the expected difference in time spent in the later stages. We again assume that all development rates become zero and the mortality rate becomes nonzero when food is depleted.

In all three versions, we model the transition from food-available conditions to starvation by assuming each container has an initial amount of food that is depleted as the mosquito develops and is not replenished. We assume that the waiting time until food runs out in each container is an exponentially distributed random variable with rate parameter λ, such that the average waiting time until food runs out is $1/\lambda$. Thus, we expect containers with greater amounts of food to have lower values of λ. This neglects any changes in the depletion rate as larvae grow, but it is a first step in including food dynamics.

4.2.1 Model analysis

We consider the stochastic process $\{X(t), t \geq 0\}$, where $X(t)$ is the stage of an individual at time t (Cox and Miller, 1965). Thus, $X(t)$ can take on values $\{1, 2, \ldots, 7\}$. We write the

transition probabilities for each of the three models as

$$P_{ij}(t, t+\Delta t) = \Pr\{X(t+\Delta t) = j \,|\, X(t) = i\}, \quad i, j = 1, 2, \ldots, 7. \tag{4.1}$$

Eq. 4.1 indicates that the probability of observing an individual in state j at time $t+\Delta t$, given that it is observed in state i at time t can be summarized as an element (in the i^{th} row and j^{th} column by convention) of a 7×7 matrix. The elements of this matrix, $\boldsymbol{P}$, known as the transition matrix, depend on both time t and the interval of observation Δt. Its elements are probabilities and therefore must be between 0 and 1. We can intuitively solve for some of the elements; for example, we know that individuals cannot regress from one stage to any previous stage so $P_{ij} = 0$ for all $i > j$. Also, both the adult stage and death are so-called absorbing states in this model, meaning once an individual enters them, it cannot leave. This implies that P_{66} and P_{77} are equal to one. We can solve for the rest of the elements of $\boldsymbol{P}$ for each model using the forward Kolmogorov equations (see Appendix D).

Given observations $\vec{x} = (x_0, x_1, x_2, \ldots, x_n)$ at equally spaced observation times $\vec{t} = (0, \Delta t, 2\Delta t, \ldots, n\Delta t)$, we can thus derive the likelihood of our model parameters $\vec{\theta}$, which is equal to the joint probability of the observed transitions:

$$L(\vec{\theta} \,|\, \vec{x}) = p(\vec{x} \,|\, \vec{\theta}) = P_{x_0 x_1}(0, \Delta t) P_{x_1 x_2}(\Delta t, 2\Delta t) \cdots P_{x_{n-1} x_n}\big((n-1)\Delta t, n\Delta t\big), \tag{4.2}$$

where $\vec{\theta} = (r, \mu_f, \mu_v, \lambda)$ for model 1, (r, μ_v, λ) for model 2, and $(r_1, r_2, \mu_v, \lambda)$ for model 3.

To determine the treatment means of the parameters, we consider the linear mixed-effects model

$$\log \theta_{ij} = \nu_{i\theta} + H_{j\theta} + \varepsilon_{ij\theta} \tag{4.3}$$

for each of the rates θ in the model, i.e. $\log r_{ij} = \nu_{ir} + H_{jr} + \varepsilon_{ijr}$, $\log \mu_{v,ij} = \nu_{i\mu_v} + H_{j\mu_v} + \varepsilon_{ij\mu_v}$, and so on. Here, $i = \text{A, B}$ represents the treatment and $j = 1, \ldots, 9$ represents the house. We are most interested in the treatment means $\nu_{i\theta}$, but also include random effects due to the house into which the treatments are blocked. We assume $H_{j\theta} \sim \mathcal{N}(0, \sigma^2_{H\theta})$ and $\varepsilon_{ij\theta} \sim \mathcal{N}(0, \sigma^2_{\varepsilon\theta})$. Thus, the

statistical model is comprised of both fixed effects $\vec{\phi} = (\nu_{Ar}, \nu_{Br}, \sigma^2_{Hr}, \sigma^2_{\varepsilon r}, \ldots, \nu_{A\lambda}, \mu_{B\lambda}, \sigma^2_{H\lambda}, \sigma^2_{\varepsilon\lambda})$ and random effects $\vec{\psi} = (H_{1r}, \ldots, H_{9r}, \ldots, H_{1\lambda}, \ldots, H_{9\lambda})$. We model the logged rates $\log \theta_{ij}$ because all rates in the model must be non-negative. We back-transform them once analysis is complete in order to interpret them biologically.

Using Bayes' rule, we can write the posterior distribution, i.e. the conditional probability distribution given the data, of all the parameters $\vec{\Theta} = (\vec{\theta}, \vec{\phi}, \vec{\psi})$:

$$\begin{aligned} p(\vec{\Theta} \,|\, \vec{x}) &\propto p(\vec{x} \,|\, \vec{\Theta})\, p(\vec{\Theta}), \\ &\propto p\big(\vec{x} \,|\, \vec{\theta}\big)\, p\big(\vec{\theta} \,|\, \vec{\phi}, \vec{\psi}\big)\, p\big(\vec{\psi} \,|\, \vec{\phi}\big)\, p\big(\vec{\phi}\big) \end{aligned} \tag{4.4}$$

where the constant of proportionality simply ensures that the posterior is a proper distribution in $\vec{\Theta}$ and thus integrates to one over the entire parameter space. Since we can solve for the likelihood function $p\big(\vec{x} \,|\, \vec{\theta}\big)$ for each of the three models (Eq. 4.2), we can use Markov chain Monte Carlo (MCMC)[1] to sample from the posterior distribution, given prior distributions of the fixed effects $p\big(\vec{\phi}\big)$. The terms $p(\vec{\theta} \,|\, \vec{\phi}, \vec{\psi})$ and $p(\vec{\psi} \,|\, \vec{\phi})$ come from Eq. 4.3 and the assumption $H_{j\theta} \sim \mathcal{N}(0, \sigma^2_{H\theta})$, $\varepsilon_{ij\theta} \sim \mathcal{N}(0, \sigma^2_{\varepsilon\theta})$, respectively. We evaluate Eq. 4.4 at many points using a combination of Metropolis and Gibbs sampling to estimate the posterior distribution (see Appendix E).

4.3 Results

4.3.1 Data summary

The life stage trajectories for each individual are shown in Figure 4.3. Barring a few exceptions like 5A (house 5, old water) and perhaps 6A, the life history of the individual appears to be well determined by the initial condition of the water, which is the same for all five replicates

[1] Note that the Markov chain in Monte Carlo sampling (MCMC) is not the same as the Markov chain in our *Ae. aegypti* immature growth model (CTMC). In the former, the Markov chain is over the continuous parameter space, and in the latter, the Markov chain is over the discrete state-space of the various life stages.

(although they are isolated). There appears to be some blocking effect in house 5, i.e. both buckets do slightly better than average for their treatment, but none for house 2. 2A was the only treatment that gave rise to adult *Ae. aegypti*, but 2B provided poorer than average conditions for larval growth.

We also find a high amount of mortality for treatment A. From Figure 4.3 we see that treatment A allowed for greater development on average than treatment B, but the majority of individuals in treatment A still died as second or third instars. *Ae. aegypti* fared surprisingly well in water that was only left to accumulate detritus for two days (B). Larvae were able to survive for roughly ten days, and some grew to third and fourth instars. It is extremely unlikely that larvae possess enough reserves upon hatching to survive this long, let alone molt two to three times, which requires an increase in mass. Previous lab experiments raising larvae in drinking water (in Iquitos) and tap water with no food added (in the lab) resulted in all first instars dying within 24-48 hrs (data not shown). This suggests containers with standing water in Iquitos start with a suitable baseline of food to sustain *Ae. aegypti* larvae. Even when isolated after two days so that no more detritus can accumulate, microorganisms appear abundant enough to sustain *Ae. aegypti* through several stages of development in small amounts of water. Thus, containers in the field with relatively new water and more water per larva may house *Ae. aegypti* larvae until more detritus can accumulate, providing more suitable conditions for pupation and emergence. In the lab, *Ae. aegypti* have been found to survive up to 40 days without food and then pupate once food is added (Gilpin and McClelland, 1979).

4.3.2 Model Selection

We use the deviance information criterion (DIC) as a measure of how good a fit the model is to the data with a penalty for a greater "effective number of parameters." In contrast to the frequentist Akaike information criterion (AIC), which penalizes for actual number of parameters, the inclusion of prior distributions in Bayesian inference tends to reduce the amount of overfitting. Therefore, effective number of parameters is used as a more appropriate measure

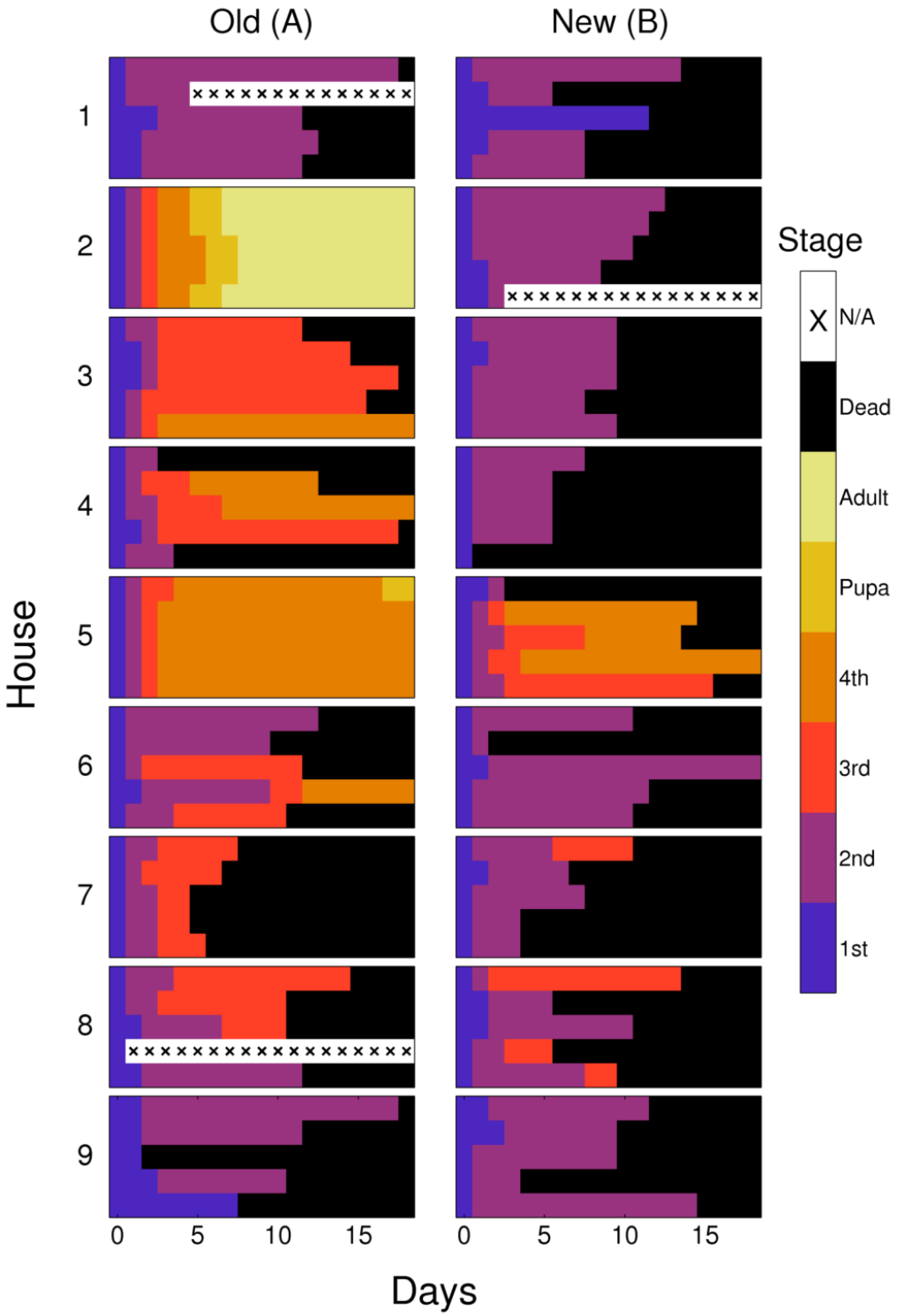

Figure 4.3: The distribution of life stages in water from each bucket. Each row within the 18 panels represents one of the five individuals exposed to water from that treatment. N/A values are where individuals that were accidentally injured during observation were removed from analysis.

of model complexity (Gelman et al., 2013). DIC values for the three models we considered are summarized in Table 4.1. We calculated the average value across several MCMC chains and report the MCMC error as 2 times the standard error of the mean. Models with lower DIC are preferable and any difference greater than about 7 is considered substantial (Spiegelhalter et al., 2002). We find substantial differences in DIC values (ΔDIC) that indicate model 3 is the best model out of the three that we considered for our Iquitos data. We thus consider only model 3 for the rest of our results.

Table 4.1: DIC values for the three model versions

Model	Description	Number of Parameters	DIC	ΔDIC
1.	Background mortality, one development rate	4	1125.11 ± 0.73	42.4
2.	No background mortality, one development rate	3	1121.19 ± 0.32	38.5
3.	No background mortality, two development rates	4	$1082.73 \pm 6.3 \times 10^{-4}$	0

4.3.3 MCMC results

We developed a function in MATLAB v. 8.3 to implement the hybrid Gibbs-Metropolis algorithm detailed in Appendix E. An initial "burn-in" period is run to allow time for the chains to converge to the posterior distributions. The posterior distributions of the four rate parameters (r_1, r_2, $1/\mu_v$ and $1/\lambda$) are shown in Figure 4.4. We use $1/\mu_v$ as a measure of "starvation resistance," similar to Arrivillaga and Barrera (2004), which represents the average amount of time an individual survives once food is depleted. We use $1/\lambda$, which is the expected waiting time until food runs out, as a proxy for the amount of food in a container (a constant depletion rate would imply that twice the waiting time means there was twice as much food in the container). The mean acceptance ratio was 0.249 (SD: 0.0037).

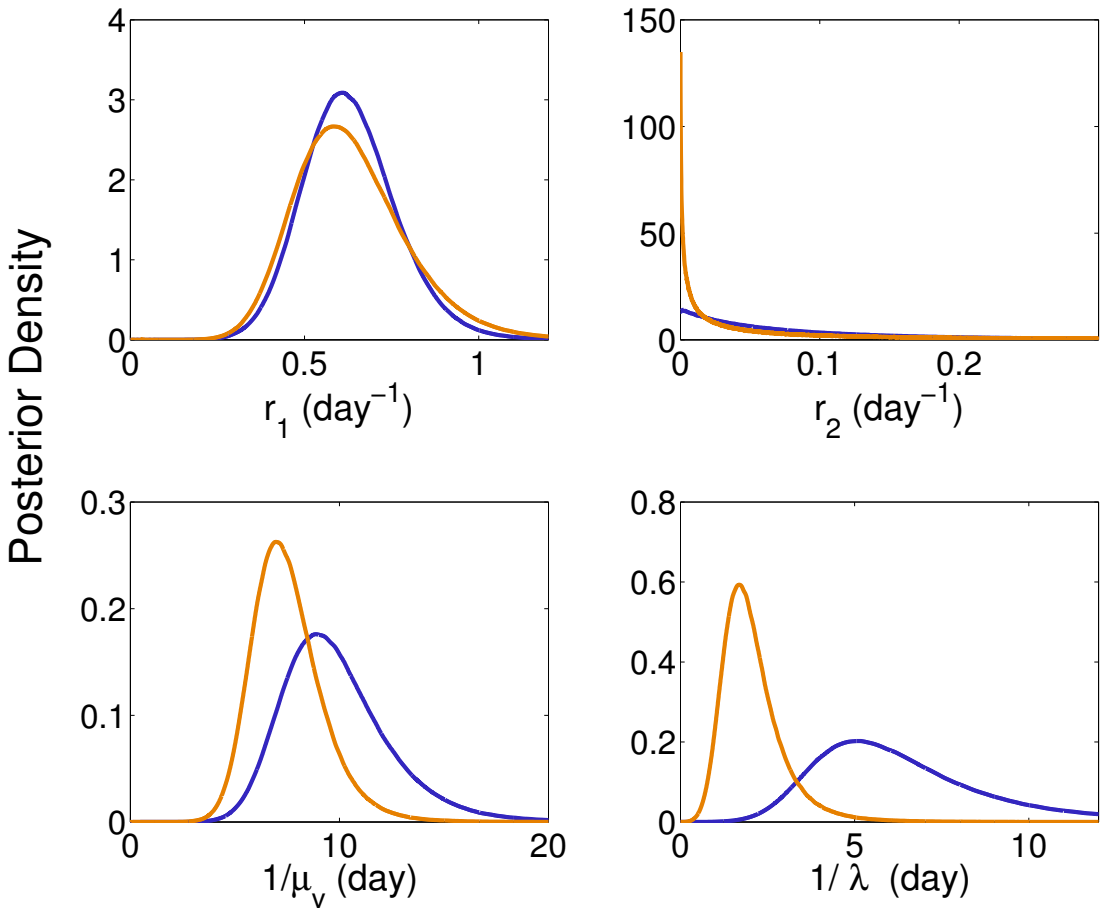

Figure 4.4: Posterior distributions for treatment means (dark = old water, light = new water) of the model parameters. 500,000 MCMC points were sampled following a burn-in of 2,000. Note the difference in horizontal scales.

The convergence diagnostics for each of the rate parameters are shown in Figures 4.5-4.8. Despite significant autocorrelation in some of the rate parameters, especially r_2, the Gelman-Rubin statistics indicate convergence to the true posterior distribution.

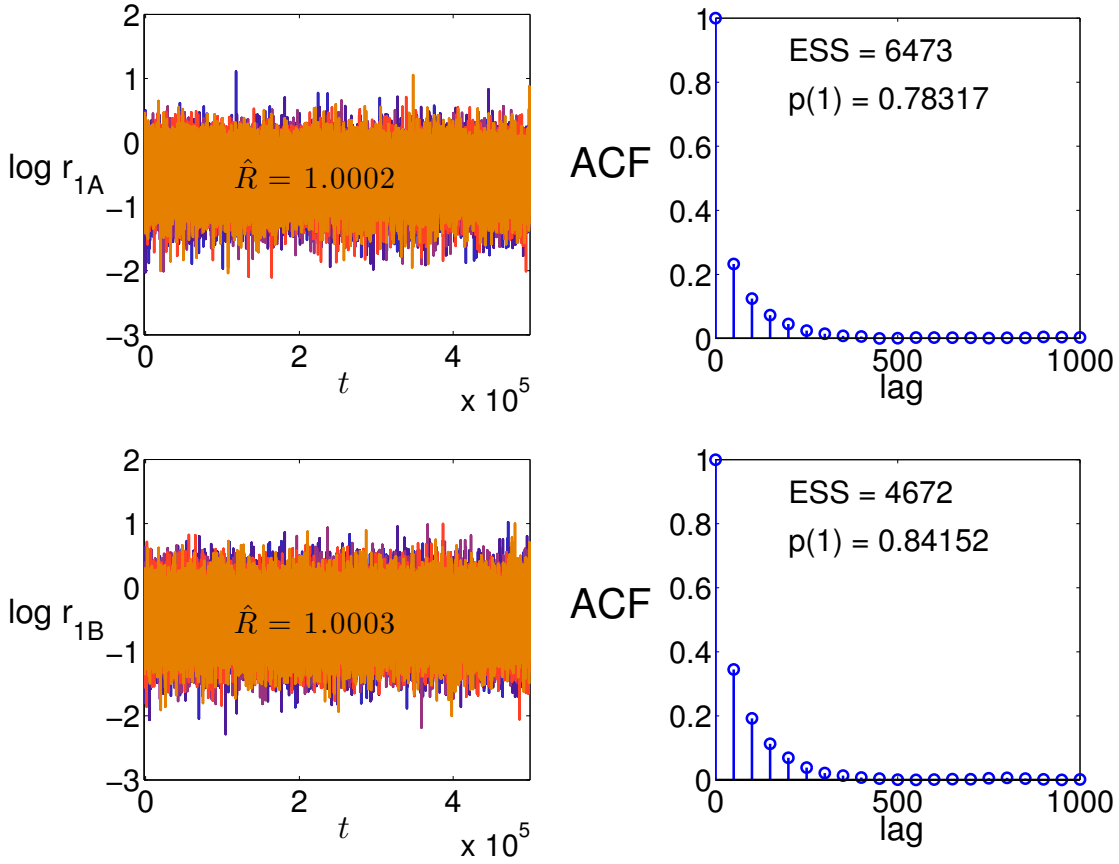

Figure 4.5: Convergence diagnostics for $\log r_1$. Five chains of 500,000 points were run with randomly selected starting values and a burn-in period of 2,000 points. Gelman-Rubin statistics, $\hat{R}$, indicate convergence when less than 1.1. Autocorrelation functions (ACF) show the ℓ-lag autocorrelation for each parameter, averaged across the five chains. The effective sample size (ESS) represents the approximate number of independent samples based on all ℓ-lag autocorrelation values (approximated using the first 2,000 ℓ-lag values). The 1-lag autocorrelation is displayed as $p(1)$.

We chose flat priors for all parameters except for $\log r_2$, as shown in Figure 4.9. We deter-

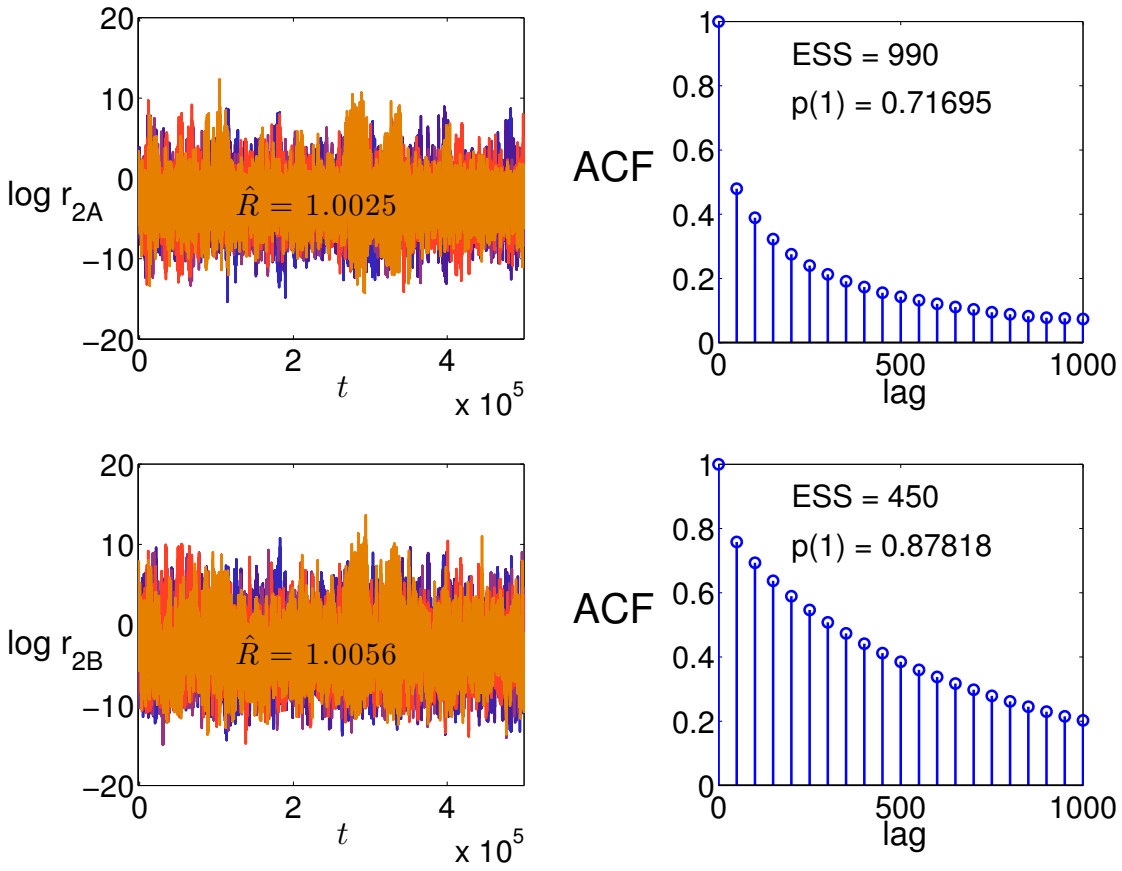

Figure 4.6: Convergence diagnostics for $\log r_2$. Five chains of 500,000 points were run with randomly selected starting values and a burn-in period of 2,000 points. Gelman-Rubin statistics, $\hat{R}$, indicate convergence when less than 1.1. Autocorrelation functions (ACF) show the ℓ-lag autocorrelation for each parameter, averaged across the five chains. The effective sample size (ESS) represents the approximate number of independent samples based on all ℓ-lag autocorrelation values (approximated using the first 2,000 ℓ-lag values). The 1-lag autocorrelation is displayed as $p(1)$.

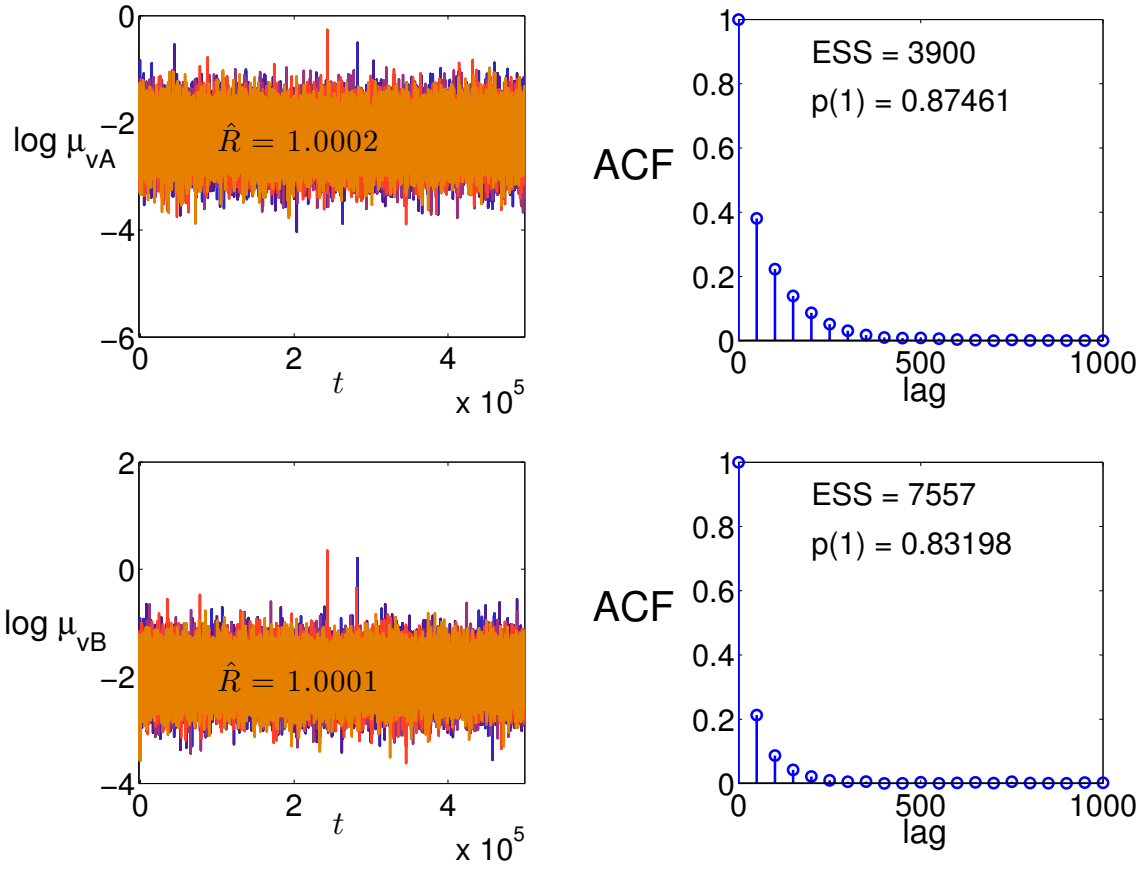

Figure 4.7: Convergence diagnostics for $\log \mu_v$. Five chains of 500,000 points were run with randomly selected starting values and a burn-in period of 2,000 points. Gelman-Rubin statistics, $\hat{R}$, indicate convergence when less than 1.1. Autocorrelation functions (ACF) show the ℓ-lag autocorrelation for each parameter, averaged across the five chains. The effective sample size (ESS) represents the approximate number of independent samples based on all ℓ-lag autocorrelation values (approximated using the first 2,000 ℓ-lag values). The 1-lag autocorrelation is displayed as $p(1)$.

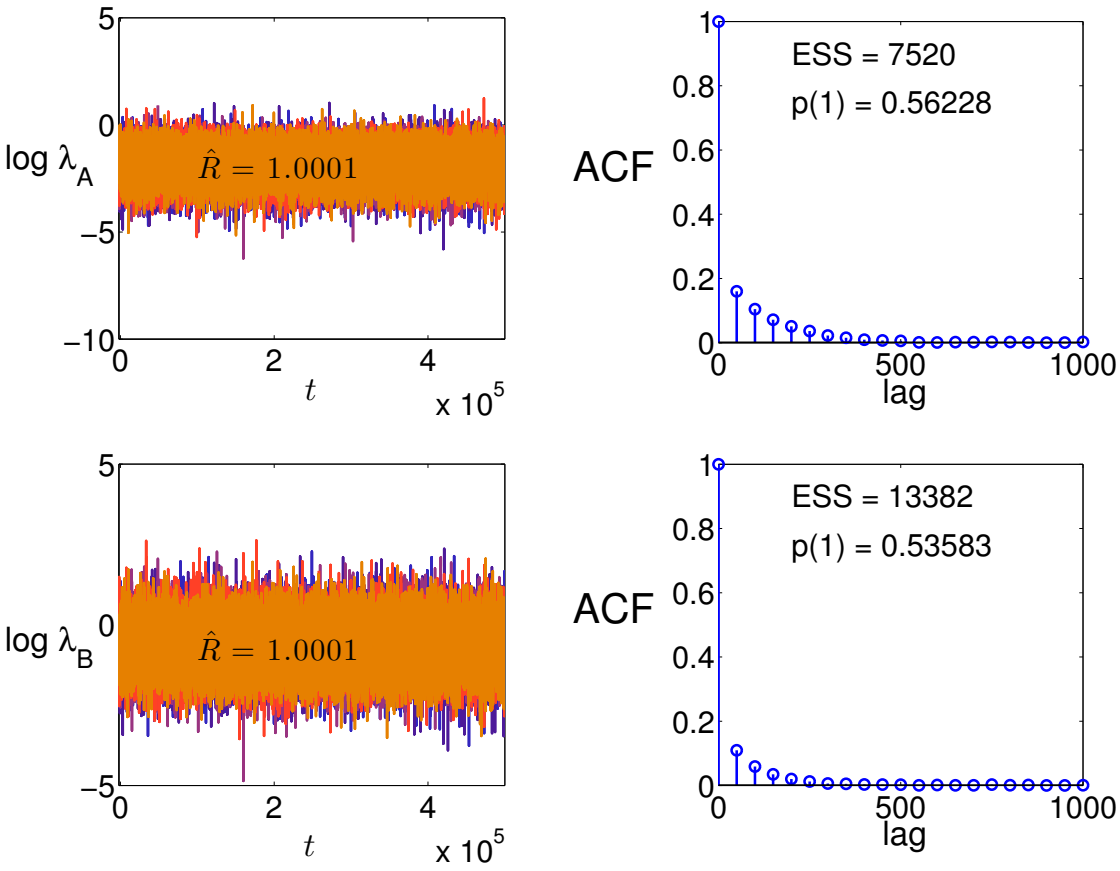

Figure 4.8: Convergence diagnostics for $\log \lambda$. Five chains of 500,000 points were run with randomly selected starting values and a burn-in period of 2,000 points. Gelman-Rubin statistics, $\hat{R}$, indicate convergence when less than 1.1. Autocorrelation functions (ACF) show the ℓ-lag autocorrelation for each parameter, averaged across the five chains. The effective sample size (ESS) represents the approximate number of independent samples based on all ℓ-lag autocorrelation values (approximated using the first 2,000 ℓ-lag values). The 1-lag autocorrelation is displayed as $p(1)$.

mined there was not enough data for fourth instars and pupae to accurately estimate $\log r_2$, especially in treatment B. We left the parameter in the model, however, because its inclusion resulted in a lower DIC than the other models which omitted the parameter. The fourth instar and pupal stage for *Ae. aegypti* have been shown to last an average of 2 days in the lab when food is abundant (Christophers, 1960). This corresponds to an average r_2 of 0.5 For variance parameters, we used an inverse-gamma prior with $a = 0.01$, $b = 0.01$, and for rate parameters other than $\log r_2$ we used a normal prior with $\mu = 0$, $\sigma^2 = 100$. . We thus chose a normal prior for $\log r_2$ with $\mu = \log(0.5)$, $\sigma^2 = 10$, which facilitated convergence to the posterior distribution without imposing too much prior information. These priors along with the marginal posterior distributions of logged rates are shown in Figure 4.9

The posterior estimates for the house-to-house variance $\sigma^2_{H\theta}$ and the error variance $\sigma^2_{\varepsilon\theta}$ are shown in Table 4.2. The uncertainty in the posterior estimates of the variance parameters was too high to determine whether or not there was a blocking effect on buckets in the same house.

Table 4.2: Mean and 2.5^{th} and 97.5^{th} percentiles of posterior distributions for variance parameters

Parameter	$p_{0.025}$	$\bar{p}$	$p_{0.975}$
$\sigma^2_{Hr_1}$	0.0094	0.107	0.158
$\sigma^2_{\varepsilon r_1}$	0.0094	0.0937	0.3591
$\sigma^2_{Hr_2}$	0.0227	14.74	114
$\sigma^2_{\varepsilon r_2}$	0.0197	18.10	156.5
$\sigma^2_{H\mu_v}$	0.0096	0.1239	0.5522
$\sigma^2_{\varepsilon\mu_v}$	0.0081	0.0755	0.3142
$\sigma^2_{H\lambda}$	0.0155	0.4551	1.966
$\sigma^2_{\varepsilon\lambda}$	0.0553	0.7008	2.306

Water age in containers does not appear to have much of an effect on the development rate

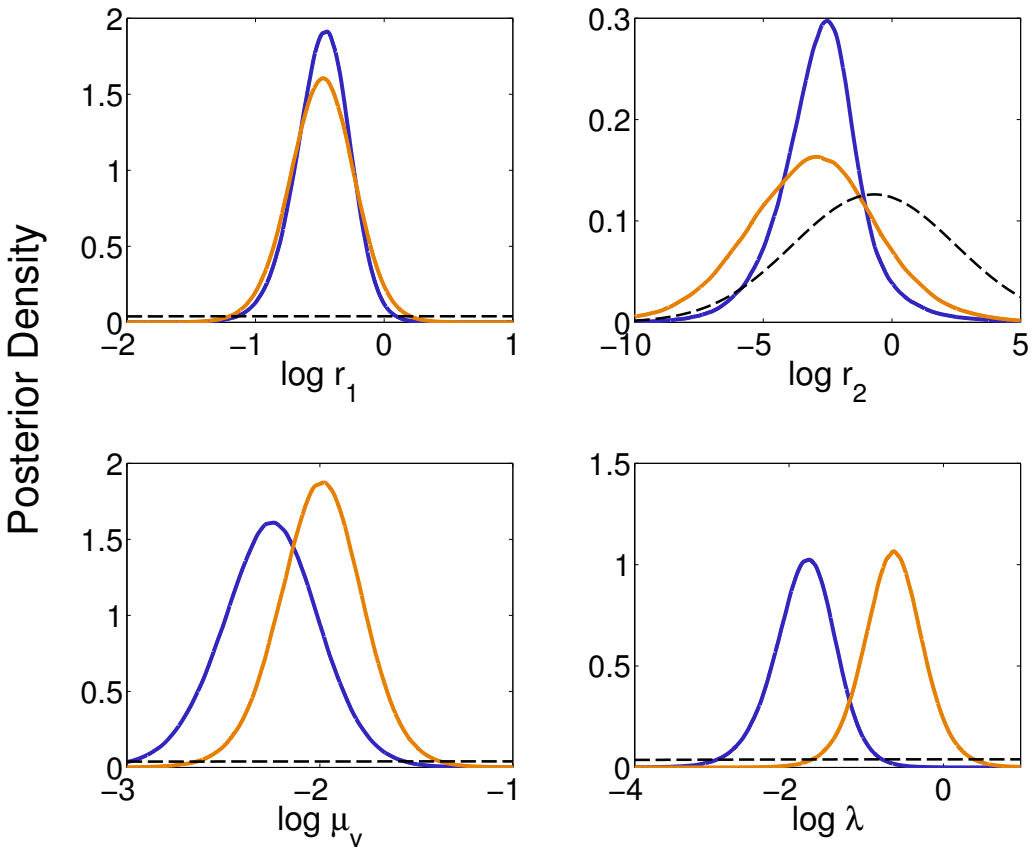

Figure 4.9: Marginal posterior distributions of logged rates for treatments A (dark) and B (light). Prior distributions (black dashed lines) are shown for comparison

of immatures. The posterior mean $\bar{r}_{1A}$ is 0.63 day^{-1} with symmetric 95% credible interval—meaning r_{1A} has an equal chance of being above or below the interval—(0.39, 0.93) day^{-1}. The estimate for r_{1B} is similar: $\bar{r}_{1B} = 0.63$ day^{-1} with symmetric 95% credible interval (0.36, 1.0) day^{-1}. Based on the posterior means of r_1 we expect first through third instars to spend 1.7 (1.1, 2.6) days in old water and 1.7 (1.0, 2.6) days in new water on average, which is longer than lab estimates of 1 day at 28^{o}C (Christophers, 1960).

Water age does appear to affect the amount of food in a container, as inferred by the average time to its depletion $1/\lambda$ (bottom right of Figure 4.4, A: 6.62 (2.77, 14.6) days, B: 2.08 (0.085, 4.32) days. However, there is considerable overlap in the marginal posterior distributions for $1/\lambda$, and even water that is only two days old has enough food to accommodate larvae. Containers in the field therefore likely start out with more food than is currently assumed by detailed models like Skeeter Buster. Currently, tap water in Iquitos is non-potable and could potentially host a number of micro-organisms that may provide a suitable habitat for *Ae. aegypti*, even when the water is relatively fresh.

Older water appears to slightly increase resistance to starvation ($1/\mu_v$) according to Figure 4.4, A: 9.85 (5.80, 16.1) days, B: 7.55 (4.77, 11.5), although again there is considerable overlap. We would expect an increase in starvation resistance for older containers if greater amounts of food in a container led to greater lipid reserves, allowing immatures to survive longer during starvation. This is included in the model by Gilpin and McClelland (1979), and was hypothesized to be the reason that Arrivillaga and Barrera (2004) observed greater starvation resistance in third instars exposed to higher food levels.

There is too much uncertainty in the estimates for r_2 to make any conclusions regarding the effect of age of water on this development rate, A: 3.05 (0.00214, 6.12) day^{-1}, B: 8.08 (2.99×10^{-4}, 13.1) day^{-1}. This is likely because there was insufficient data on the development of fourth instars and pupae, although the DIC indicated that model 3 was a better enough fit to the data to justify the parameter's inclusion.

4.4 Discussion

Our analysis shows that *Ae. aegypti* immature dynamics in food-scarce containers in Iquitos are determined almost entirely by the presence or absence of food, rather than quality or quantity. Despite a lack of understanding of what exactly constitutes food in containers, our model is able to infer the relative amount of food in containers with a CTMC that switches rates once food in a container is depleted. Development rates of immature *Ae. aegypti* in the field do not appear to depend on the amount of food, and they were equivalent for containers in the field for two days and five weeks. Starvation mortality rates showed a slight dependence on water age, suggesting increased food availability allows for a greater accumulation of lipid reserves on which the immature can survive once food is depleted.

Surprisingly, water left outdoors for only two days was capable of producing third and fourth instars, even after preventing further accumulation of detritus in the container. Detailed container models for *Ae. aegypti*, such as CiMSIM (Focks et al., 1993) and Skeeter Buster (Magori et al., 2009), that assume little to no food in containers initially and regular food input (e.g. daily) should be reassessed when modeling Iquitos in order to capture the high amount of variation observed in the field.

We also remark that there was a lower amount of survival than expected across all containers: only five of the ninety individuals survived to emergence. While some field studies report similar survival proportions (Seawright et al., 1977; Southwood et al., 1972), Walsh et al. (2011) found that survival in field containers was closer to 60%. We allowed treatment A containers to accumulate detritus in the field for up to five weeks and removed any mosquitoes found during the accumulation phase that could deplete food resources and contribute to delayed density dependence (see Walsh et al., 2013), so we expected larval survival to be closer to this proportion. This discrepancy may be due to the lower amount of water volume per larva used in this experiment. While 13 mL of water was sufficient to ensure close to 100% survival in an earlier lab experiment used to test this setup (data not shown), it is clear that food levels available in the field are much lower than those used in the lab. The low water volume per larva could

approximate high larval density conditions in the field if we assume that larvae in a container compete equally for food. Then we could consider that each larva has an effective volume of food available. For example, Seawright et al. (1977) found 4.3% survival in a field container that had 7 L of water and 500 larvae, which amounts to 14 mL of water per larvae. However, our results are more variable: rather than finding 5.6% survival in all containers we find 100% in one and 0 in 17, for an average of 5.6%. The greater variability among containers than within containers suggest that the probability of emergence is largely determined by food accumulation, and it is the food accumulation that is highly variable rather than the life stage trajectories of each larva within a container.

By using DIC to assess the suitability of several CTMC models, we were able to narrow down the most important components of immature dynamics in the field: food-present and food-absent regimes, stochastic waiting time until food depletion, and distinct development rates for early and late immature stages. Although Gilpin and McClelland (1979) found there to be some background mortality (death even in food-abundant conditions), we found that it was not a necessary parameter in our model for Iquitos, and that including background mortality did not provide a better enough fit to the data to justify the extra parameter.

The fact that water age affected amount of food in the containers (lower right panel of Figure 4.4) but not growth rates agrees with Gilpin and McClelland (1979), who noted that larval weight trajectories were "independent of food density and larval number" (p. 368). In other words, as long as there is food present, *Ae. aegypti* tend to consume at their maximum efficiency. The switch to starvation conditions likely happens abruptly as we have modeled it here (see Appendix D). In the field, however, food may be replenished and the transition rates may switch back to a food-present regime. This could be incorporated into our model, given a better understanding of how often food in containers is replenished in the field.

Although it is difficult to parameterize with field data, we feel that the Gilpin and McClelland (1979) equations for food and larval weight are a good model for what is occurring in the field, with the availability of food dictating the overall dynamics. Although they initially

assume that the food consumption rate depends on the amount of food available, they conclude that this rate saturates at a very low level. We believe it is somewhat simpler in that the consumption rate is constant regardless of the quantity of food. Rather, it is only the presence or absence of food that determines the dynamics. Otherwise, we should see a difference in r_1 for treatment A and treatment B, considering that the posterior distributions for λ indicate that treatment A contains more food on average.

A major drawback to the model by Gilpin and McClelland (1979) is that it is difficult to obtain weight data directly, although it could be inferred from length measurements (see Christophers, 1960). We believe the CTMC immature stage model developed here can track the same process and be more easily informed with immature stage trajectories, which are directly observable in the field. More work should be done, however, to determine the relationship between the expected waiting time until food is depleted and the initial amount of food in a container. It may be possible to use a less dispersed random variable such as a gamma random variable to help link the time of switching to the initial amount of food in the container. However, a better understanding of the functional form of food depletion over time will be necessary to convert depletion time to initial food level.

Future work includes modifying the CTMC model to include further biological complexities. For example, the current model assumes that the duration of each life stage is exponentially distributed, which is likely not the case. Exponential waiting times are a necessary component of the CTMC model because it preserves the memoryless property of a Markov chain. However, we can add a chain of hidden states within stages to decrease the dispersion of the waiting time, which then becomes a gamma-distributed random variable. This technique has been used with epidemic models to decrease the variance in the infectious period (Anderson and Watson, 1980; Lloyd, 2001) and has been recently proposed for *Ae. aegypti* larval dynamics (Romeo Aznar et al., 2014). The disadvantage is that the hidden states are not observable, and so the likelihood may be more difficult to derive, though it may still be possible with hidden Markov model theory.

A future experiment should include a larger volume for individual mosquitoes to account for the typically low levels of food in the field. It should also be designed to observe larvae for a longer period of time, up to forty days. This can help estimate the starvation resistance and how it varies across containers in the field. This was not feasible in our experiment given the time allotted to the food accumulation phase, but we note that several immature *Ae. aegypti* had neither died nor emerged at the end of the experiment, so potentially important information about the maximum starvation time was discarded.

We have provided a simple CTMC model for immature *Ae. aeygpti* growth in containers in Iquitos that has led to new insights. Further field experiments on *Ae. aegypti* ecology will be necessary to determine the various interactions of food accumulation in buckets, larval growth and density dependence, in order to develop more accurate models. Likewise, both simple and complex models can help identify sources of variation and uncertainty that can inform future experimental design. This iterative process will be necessary in understanding *Ae. aegypti* ecology to the level of detail required to effectively control vector populations and suppress dengue transmission in endemic regions.

REFERENCES

Alphey, N. and M. Bonsall, 2014. Interplay of population genetics and dynamics in the genetic control of mosquitoes. Journal of The Royal Society Interface 11:1–12.

Anderson, D. and R. Watson, 1980. On the spread of a disease with gamma distributed latent and infectious periods. Biometrika 67:191.

Arrivillaga, J. and R. Barrera, 2004. Food as a limiting factor for *Aedes aegypti* in water-storage containers. Journal of Vector Ecology 29:11–20.

Barbosa, P., T. M. Peters, and N. C. Greenough, 1972. Overcrowding of mosquito populations: responses of larval *Aedes aegypti* to stress. Environmental Entomology 1:89–93.

Barton, N. H., 1979. The dynamics of hybrid zones. Heredity 43:341–59.

Barton, N. H. and S. Rouhani, 1991. The probability of fixation of a new karyotype in a continuous population. Evolution 45:499.

Barton, N. H. and M. Turelli, 2011. Spatial waves of advance with bistable dynamics: cytoplasmic and genetic analogues of *Allee effects*. The American Naturalist 178:E48–75.

Bhatt, S., P. W. Gething, O. J. Brady, J. P. Messina, A. W. Farlow, C. L. Moyes, J. M. Drake, J. S. Brownstein, A. G. Hoen, O. Sankoh, M. F. Myers, D. B. George, T. Jaenisch, G. R. W. Wint, C. P. Simmons, T. W. Scott, J. J. Farrar, and S. I. Hay, 2013. The global distribution and burden of dengue. Nature 496:504–07.

Carpenter, S. R., 1984. Experimental test of the pupation window model for development of detritivorous insects. Ecological Modelling 23:257–64.

Caspari, E. and G. Watson, 1959. On the evolutionary importance of cytoplasmic sterility in mosquitoes. Evolution 13:568–70.

Chan, M. H. T. and P. S. Kim, 2013. Modelling a *Wolbachia* invasion using a slow-fast dispersal reaction-diffusion approach. Bulletin of mathematical biology 75:1501–23.

Chib, S. and E. Greenberg, 1995. Understanding the Metropolis-Hastings algorithm. The American Statistician 49:327–35.

Christophers, S. R., 1960. *Aëdes aegypti*: The Yellow Fever Mosquito. Cambridge University Press.

Codling, E. A., M. J. Plank, and S. Benhamou, 2008. Random walk models in biology. Journal of the Royal Society Interface 5:813–34.

Cox, D. and H. Miller, 1965. The theory of stochastic processes. Wiley.

Crank, J. and P. Nicolson, 1996. A practical method for numerical evaluation of solutions of partial differential equations of the heat-conduction type. Advances in Computational Mathematics 6:207–26.

Curtis, C. F., 1968. Possible use of translocations to fix desirable genes in insect pest populations. Nature 218:368–69.

Davis, S., N. Bax, and P. Grewe, 2001. Engineered underdominance allows efficient and economical introgression of traits into pest populations. Journal of theoretical biology 212:83–98.

Dobson, S. L., W. Rattanadechakul, and E. J. Marsland, 2004. Fitness advantage and cytoplasmic incompatibility in *Wolbachia* single- and superinfected *Aedes albopictus*. Heredity 93:135–42.

Dye, C., 1982. Intraspecific competition amongst larval *Aedes aegypti*: food exploitation or chemical interference? Ecological Entomology 7:39–46.

Farkas, J. Z. and P. Hinow, 2010. Structured and unstructured continuous models for *Wolbachia* infections. Bulletin of mathematical biology 72:2067–88.

Fife, P. C., 1979. Mathematical aspects of reacting and diffusing systems. Spinger-Verlag, New York.

Fine, P. E. M., 1978. On the dynamics of symbiote-dependent cytoplasmic incompatibility in culicine mosquitoes. Journal of Invertebrate Pathology 30:10–18.

Fisher, R. A., 1937. The wave of advance of advantageous genes. Annals of Human Genetics 7:355–369.

Focks, D., D. G. Haile, E. Daniels, and G. A. Mount, 1993. Dynamic life table model for *Aedes aegypti* (Diptera: Culicidae): analysis of the literature and model development. Journal of medical entomology 30:1003–17.

Fu, G., R. S. Lees, D. Nimmo, D. Aw, L. Jin, P. Gray, T. U. Berendonk, H. White-Cooper, S. Scaife, H. Kim Phuc, O. Marinotti, N. Jasinskiene, A. A. James, and L. S. Alphey, 2010. Female-specific flightless phenotype for mosquito control. Proceedings of the National Academy of Sciences of the United States of America 107:4550–54.

Gelfand, A., 1990. Sampling-based approaches to calculating marginal densities. Journal Of The American Statistical Association 85:398–409.

Gelman, A., J. B. Carlin, H. S. Stern, D. B. Dunson, A. Vehtari, and D. B. Rubin, 2013. Bayesian data analysis. 3rd ed. CRC Press, Boca Raton, FL.

Gelman, A., G. Roberts, and W. Gilks, 1996. Efficient Metropolis jumping rules. Pp. 599–607, *in* J. M. Bernando, J. O. Berger, A. P. Dawid, and A. F. M. Smith, eds. Bayesian statistics. Oxford University Press.

Geman, S. and D. Geman, 1984. Stochastic relaxation, Gibbs distributions, and the Bayesian restoration of images. IEEE Transactions on Pattern Analysis and Machine Intelligence 6:721–41.

Gilpin, M. E. and G. A. H. McClelland, 1979. Systems analysis of the yellow fever mosquito *Aedes aegypti*. Fortschritte der Zoologie 25:355–88.

Gimnig, J. E., M. Ombok, S. Otieno, M. G. Kaufman, J. M. Vulule, and E. D. Walker, 2002. Density-dependent development of *Anopheles gambiae* (Diptera: Culicidae) larvae in artificial habitats. Journal of medical entomology 39:162–72.

Gould, F., K. Magori, and Y. Huang, 2006. Genetic strategies for controlling mosquito-borne diseases. American Scientist 94:238.

Hairston, N. G., S. P. Ellner, M. a. Geber, T. Yoshida, and J. a. Fox, 2005. Rapid evolution and the convergence of ecological and evolutionary time. Ecology Letters 8:1114–27.

Hancock, P. A. and H. C. J. Godfray, 2012. Modelling the spread of *Wolbachia* in spatially heterogeneous environments. Journal of the Royal Society Interface 9:3045–54.

Hancock, P. A., S. P. Sinkins, and H. C. J. Godfray, 2011. Population dynamic models of the spread of *Wolbachia*. The American naturalist 177:323–33.

Hartl, D. and A. Clark, 1989. Principles of population genetics. Sinauer, Sunderland, MA.

Hastings, W. K., 1970. Monte Carlo sampling methods using Markov chains and their applications. Biometrika 57:97–109.

Herrando-Pérez, S., S. Delean, B. W. Brook, and C. J. A. Bradshaw, 2012. Density dependence: an ecological tower of babel. Oecologia 170:585–603.

Hoffmann, A. A., I. Iturbe-Ormaetxe, A. G. Callahan, B. L. Phillips, K. Billington, J. K. Axford, B. Montgomery, A. P. Turley, and S. L. O'Neill, 2014. Stability of the *w*Mel *Wolbachia* infection following invasion into *Aedes aegypti* populations. PLoS Neglected Tropical Diseases 8:e3115.

Jacups, S. P., T. S. Ball, C. J. Paton, H. Petrina, S. A. Ritchie, and P. H. Johnson, 2013. Operational use of household bleach to crash and release *Aedes aegypti* prior to *Wolbachia*-infected mosquito release. Journal of medical entomology 50:344–51.

Jansen, V. A. A., M. Turelli, and H. C. J. Godfray, 2008. Stochastic spread of *Wolbachia*. Proceedings of the Royal Society of London B: Biological sciences 275:2769–76.

Keeling, M. J., F. M. Jiggins, and J. M. Read, 2003. The invasion and coexistence of competing *Wolbachia* strains. Heredity 91:382–88.

Kierstad, H. and L. B. Slobodkin, 1953. The size of water masses containing plankton bloom. The Journal of Marine Research 12:141–47.

Kolmogorov, A. N., I. G. Petrovsky, and N. S. Piskunov, 1937. Etude de l'équation de la diffusion avec croissance de la quantité de matiere et son application à un probleme biologique. Mosc. Univ. Bull. Math 1:1–25.

Lewis, M. and P. Kareiva, 1993. Allee dynamics and the spread of invading organisms. Theoretical Population Biology 43:141–58.

Li, C. C., 1955. The stability of an equilibrium and the average fitness of a population. The American Naturalist 89:281–95.

Lloyd, A. L., 2001. Realistic distributions of infectious periods in epidemic models: changing patterns of persistence and dynamics. Theoretical population biology 60:59–71.

Magori, K., M. Legros, M. E. Puente, D. Focks, T. W. Scott, A. L. Lloyd, and F. Gould, 2009. Skeeter Buster: a stochastic, spatially explicit modeling tool for studying *Aedes aegypti* population replacement and population suppression strategies. PLoS Neglected Tropical Diseases 3:e508.

McMeniman, C. J., R. Lane, and B. Cass, 2009. Stable introduction of a life-shortening *Wolbachia* infection into the mosquito *Aedes aegypti*. Science 323:141–44.

Merritt, R. W., R. H. Dadd, and E. D. Walker, 1992. Feeding behavior, natural food, and nutritional relationships of larval mosquitoes. Annual review of entomology 37:349–76.

Metropolis, N., A. W. Rosenbluth, M. N. Rosenbluth, A. H. Teller, and E. Teller, 1953. Equation of state calculations by fast computing machines. The Journal of Chemical Physics 21:1087.

Moran, P. A. P., 1958. Random processes in genetics. Mathematical Proceedings of the Cambridge Philosophical Society 54:60.

Morrison, A. C., K. Gray, A. Getis, H. Astete, M. Sihuincha, D. Focks, D. Watts, J. D. Stancil, J. G. Olson, P. Blair, and T. W. Scott, 2004. Temporal and geographic patterns of *Aedes aegypti* (Diptera: Culicidae) production in Iquitos, Peru. Journal of medical entomology 41:1123–42.

Morrison, A. C., S. L. Minnick, C. Rocha, B. M. Forshey, S. T. Stoddard, A. Getis, D. Focks, K. L. Russell, J. G. Olson, P. J. Blair, D. M. Watts, M. Sihuincha, T. W. Scott, and T. J. Kochel, 2010. Epidemiology of dengue virus in Iquitos, Peru 1999 to 2005: interepidemic and epidemic patterns of transmission. PLoS neglected tropical diseases 4:e670.

Morrison, A. C., E. Zielinski-Gutierrez, T. W. Scott, and R. Rosenberg, 2008. Defining challenges and proposing solutions for control of the virus vector *Aedes aegypti*. PLoS medicine 5:e68.

Nagylaki, T., 1975. Conditions for the existence of clines. Genetics Pp. 595–615.

NCDC, 2015. Climate data online. http://www7.ncdc.noaa.gov/CDO/cdo.

Plummer, M., N. Best, K. Cowles, and K. Vines, 2006. CODA: convergence diagnosis and output analysis for MCMC. R News 6.

Ponlawat, A. and L. C. Harrington, 2005. Blood feeding patterns of *Aedes aegypti* and *Aedes albopictus* in Thailand. Journal of Medical Entomology 42:844–49.

Ponnusamy, L., N. Xu, G. Stav, D. M. Wesson, C. Schal, and C. S. Apperson, 2008. Diversity of bacterial communities in container habitats of mosquitoes. Microbial ecology 56:593–603.

Rasgon, J. L., 2008. Using predictive models to optimize *Wolbachia*-based strategies for vector-borne disease control. Advances in experimental medicine and biology 627:114–25.

Romeo Aznar, V., M. S. De Majo, S. Fischer, D. Francisco, M. A. Natiello, and H. G. Solari, 2014. A model for the development of *Aedes* (Stegomyia) *aegypti* as a function of the available food. Journal of theoretical biology 365C:311–24.

Rouhani, S. and N. H. Barton, 1987. Speciation and the shifting balance in a continuous population. Theoretical Population Biology 31:465–92.

Sanchez, A. and J. Gore, 2013. Feedback between population and evolutionary dynamics determines the fate of social microbial populations. PLoS biology 11:e1001547.

Schoener, T. W., 2011. The newest synthesis: understanding the interplay of evolutionary and ecological dynamics. Science (New York, N.Y.) 331:426–29.

Schofield, P., 2002. Spatially explicit models of Turelli-Hoffmann *Wolbachia* invasive wave fronts. Journal of theoretical biology 215:121–31.

Schraiber, J. G., A. N. Kaczmarczyk, R. Kwok, M. Park, R. Silverstein, F. U. Rutaganira, T. Aggarwal, M. A. Schwemmer, C. L. Hom, R. K. Grosberg, and S. J. Schreiber, 2012. Constraints on the use of lifespan-shortening *Wolbachia* to control dengue fever. Journal of theoretical biology 297:26–32.

Scott, T. W., P. H. Amerasinghe, A. C. Morrison, L. H. Lorenz, G. G. Clark, D. Strickman, P. Kittayapong, and J. D. Edman, 2000. Longitudinal studies of *Aedes aegypti* (Diptera: Culicidae) in Thailand and Puerto Rico: blood feeding frequency. Journal of medical entomology 37:89–101.

Seawright, J. A., D. A. Dame, and D. E. Weidhaas, 1977. Field survival and ovipositional characteristics of *Aedes aegypti* and their relation to population dynamics and control. Mosquito News 37:62–70.

Sinkins, S. P. and F. Gould, 2006. Gene drive systems for insect disease vectors. Nature reviews. Genetics 7:427–35.

Skeel, R. D. and M. Berzins, 1990. A method for the spatial discretization of parabolic equations in one space variable. SIAM Journal on Scientific and Statistical Computing 11:1–32.

Skellam, J. G., 1951. Random dispersal in theoretical populations. Biometrika 38:196–218.

Slatkin, M., 1973. Gene flow and selection in a cline. Genetics 75:733–56.

Southwood, T. R. E., G. Murdie, M. Yasuno, R. J. Tonn, and P. M. Reader, 1972. Studies on the life budget of *Aedes aegypti* in Wat Samphaya, Bangkok, Thailand. Bulletin of the World Health Organization 46:211–26.

Souto-Maior, C., J. S. Lopes, E. Gjini, C. J. Struchiner, L. Teixeira, and M. G. M. Gomes, 2014. Heterogeneity in symbiotic effects facilitates *Wolbachia* establishment in insect populations. Theoretical Ecology 8:53–65.

Spiegelhalter, D. J., N. G. Best, B. P. Carlin, and A. van der Linde, 2002. Bayesian measures of model complexity and fit. Journal of the Royal Statistical Society Series B: Statistical Methodology 64:583–639.

Stoddard, S. T., H. J. Wearing, R. C. Reiner, A. C. Morrison, H. Astete, S. Vilcarromero, C. Alvarez, C. Ramal-Asayag, M. Sihuincha, C. Rocha, E. S. Halsey, T. W. Scott, T. J. Kochel, and B. M. Forshey, 2014. Long-term and seasonal dynamics of dengue in Iquitos, Peru. PLoS Neglected Tropical Diseases 8:19–21.

Stokes, A. N., 1976. On two types of moving front in quasilinear diffusion. Mathematical Biosciences 31:307–15.

Tierney, L., 1994. Markov chains for exploring posterior distributions. The Annals of Statistics 22:1701–1728.

Turelli, M. and A. A. Hoffmann, 1991. Rapid spread of an inherited incompatibility factor in California *Drosophila*. Nature 353:440–42.

Volpert, V. and S. Petrovskii, 2009. Reaction-diffusion waves in biology. Physics of Life Reviews 6:267–310.

Walker, T., P. H. Johnson, L. A. Moreira, I. Iturbe-Ormaetxe, F. D. Frentiu, C. J. McMeniman, Y. S. Leong, Y. Dong, J. Axford, P. Kriesner, A. L. Lloyd, S. A. Ritchie, S. L. ONeill, and A. A. Hoffmann, 2011. The *w*Mel *Wolbachia* strain blocks dengue and invades caged *Aedes aegypti* populations. Nature 476:450–53.

Walsh, R. K., 2011. Assessing the impact of density dependence in natural larval populations of container inhabiting mosquitoes, *Aedes aegypti* and *Aedes albopictus*. Ph.D. thesis, North Carolina State University.

Walsh, R. K., C. L. Aguilar, L. Facchinelli, L. Valerio, J. M. Ramsey, T. W. Scott, A. L. Lloyd, and F. Gould, 2013. Regulation of *Aedes aegypti* population dynamics in field systems: quantifying direct and delayed density dependence. The American journal of tropical medicine and hygiene 89:68–77.

Walsh, R. K., L. Facchinelli, J. M. Ramsey, J. G. Bond, and F. Gould, 2011. Assessing the impact of density dependence in field populations of *Aedes aegypti*. Journal of Vector Ecology 36:300–07.

Werren, J. H., 1997. Biology of *Wolbachia*. Annual review of entomology 42:587–609.

WHO, 2014. Dengue and severe dengue: fact sheet no. 117.

Xu, C., M. Legros, F. Gould, and A. L. Lloyd, 2010. Understanding uncertainties in model-

based predictions of *Aedes aegypti* population dynamics. PLoS neglected tropical diseases 4:e830.

Zheng, B., M. Tang, and J. Yu, 2014. Modeling *Wolbachia* spread in mosquitoes through delay differential equations. SIAM Journal on Applied Mathematics 74:743–70.

APPENDICES

Appendix A

Eco-evolutionary dynamics of *Wolbachia*: Effect of different forms of density dependence

We start with a more general form of the equations for I, the number of *Wolbachia*-infected females, and U, the number of wild-type females (Eq. 2.1):

$$\frac{dI}{dt} = (b_i - d_i)I \tag{A.1a}$$

$$\frac{dU}{dt} = \left(b_u\left(1 - s_h\frac{I}{I+U}\right) - d_u\right)U. \tag{A.1b}$$

We define p, the frequency of *Wolbachia*, to be $p = I/(I+U)$ and N to be the total female population size $N = I + U$. We can then find dp/dt using the quotient rule and dN/dt as the sum of Eq. A.1a and Eq. A.1b.

$$\frac{dp}{dt} = \frac{(I+U)\frac{dI}{dt} - I\left(\frac{dI}{dt} + \frac{dU}{dt}\right)}{(I+U)^2} \tag{A.2a}$$

$$\frac{dN}{dt} = \frac{dI}{dt} + \frac{dU}{dt} \tag{A.2b}$$

Substituting in Eq. A.1 and simplifying yields the system of equations in Eq. A.3, which is a more general form of Eq. 2.2 in Chapter 2.

$$\frac{dp}{dt} = p(1-p)\Big(b_i - b_u(1 - s_h p) - (d_i - d_u)\Big) \tag{A.3a}$$

$$\frac{dN}{dt} = \Big(b_i p + b_u(1 - p - s_h p(1-p)) - (d_i p + d_u(1-p))\Big)N. \tag{A.3b}$$

Per capita emergence and death rates b_i, b_u, d_i, d_u may all be functions of N (we have omitted

function notation, e.g. $b_i(N)$, for readability). If one assumes density dependence acts only on the death rate, then there must be *Wolbachia*-induced mortality, i.e. $d_i \neq d_u$, in order for the equations to be coupled, due to the $d_i - d_u$ term in Eq. A.3a. In addition, density-dependent mortality must interact with *Wolbachia*-induced mortality. If, for example, $d_i(N) = d_u(N) + \alpha$, rather than $d_i(N) = d_u(N)(1+\alpha)$, then the dependence on N will cancel out and the equations will not be coupled (see Sections A.2 and A.3).

Even if density dependence acts only on the emergence rate, as we have assumed in Chapter 2, so long as the difference in emergence rates scales with density dependence, i.e. $b_i(N) = (1 - s_f)b_u(N)$, then in order for the invasion threshold to depend on N, we must still have $d_i \neq d_u$. Otherwise, b_u will factor out of Eq. A.3a and total population size will affect the time course of invasion (see Figs. 2.2C and 2.2D) but not the invasion threshold itself, which will reduce to $\hat{p} = \frac{s_f}{s_h}$. The coupling between p and N is what ultimately causes the invasion threshold to depend on N, and will thus depend on the specific form of density dependence assumed.

To illustrate this, we take a more detailed look at four forms of density dependence. We begin with the type assumed in the text, linear decrease in per capita emergence rate (Section A.1). We then examine two forms of linearly increasing per capita death rate: one in which density-dependent mortality interacts with *Wolbachia*-induced mortality (Section A.2), and one in which the two types of mortality act independently (Section A.3). Finally, we look at a nonlinear form of density-dependent per capita mortality (Section A.4).

A.1 Linear decrease in per capita emergence rate

We focus first on the type of density dependence assumed in Chapter 2, linear decrease in per capita emergence rate with population size. That is,

Table A.1: Per capita density-dependent emergence and death rates for the type of density dependence assumed in Chapter 2.

	I	U
$b(N)$	$(1-s_f)\left(b_0\left(1-\frac{N}{K}\right)+d\frac{N}{K}\right)$	$\left(b_0\left(1-\frac{N}{K}\right)+d\frac{N}{K}\right)$
$d(N)$	$d+D$	d

The rates are depicted graphically in Figure A.1:

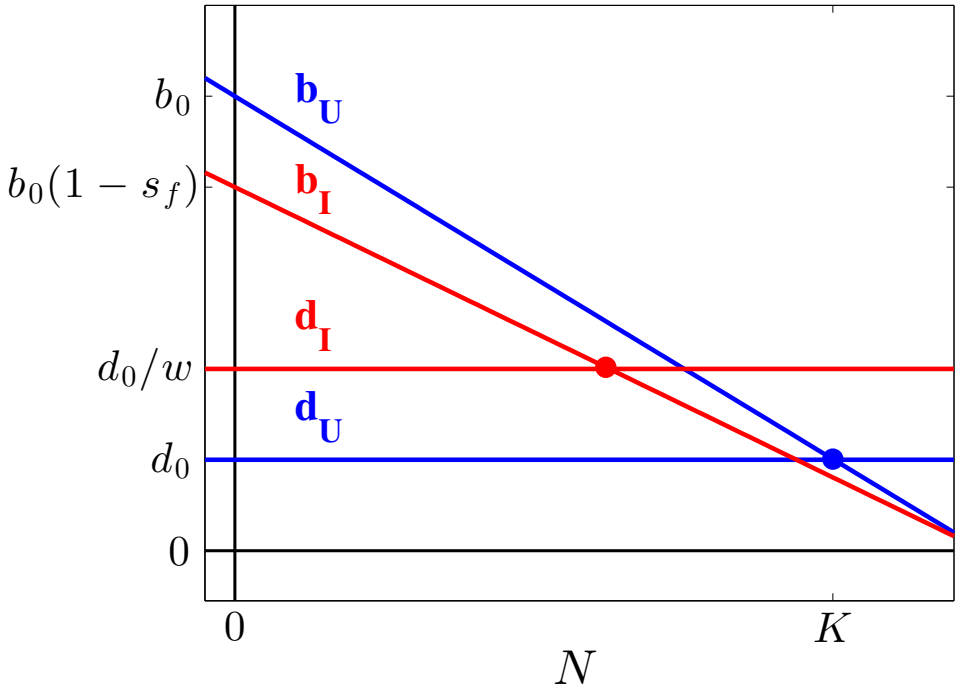

Figure A.1: Per capita density-dependent emergence and death rates for the type of density dependence assumed in Chapter 2. Stable equilibria (filled circles) for all infected (red) or all uninfected (blue) individuals occur where per capita emergence and death rates intersect.

If we substitute the per capita growth rates from Table A.1 into Eq. A.3 and solve for $dp/dt = 0$ and $dN/dt = 0$, we get the six equilibria in Table 2.2. For stability analysis, we evaluate the Jacobian at each of the six equilibria. To make the analysis simpler, we make the change of variables $x = N/K$, such that x is the population number relative to carrying capacity, without loss of generality.

1.
$$J = \begin{bmatrix} -s_f b_0 - D & 0 \\ 0 & b_0 - d \end{bmatrix}, \tag{A.4}$$

which has eigenvalues

$$\lambda = \begin{bmatrix} -s_f\, b_0 - D \\ b_0 - d \end{bmatrix}. \tag{A.5}$$

The second eigenvalue is positive, provided $R_U > 1$, which we assume to be true. Thus, the equilibrium is **unstable**.

2.
$$J = \begin{bmatrix} -s_f d - D & 0 \\ -d\,(s_f + s_h) - D & -b_0 + d \end{bmatrix}, \tag{A.6}$$

which has eigenvalues

$$\lambda = \begin{bmatrix} -s_f\, d - D \\ -b_0 + d \end{bmatrix}. \tag{A.7}$$

As long as $R_U > 1$, both eigenvalues are negative, indicating a **stable** equilibrium. Thus, $R_U > 1$ is necessary to have a stable wild-type population to begin with.

3.
$$J = \begin{bmatrix} -\frac{(s_f\, b_0 + D)(-b_0\, s_h + s_f\, b_0 + D)}{b_0\, s_h} & \frac{(s_f\, b_0 + D)(-b_0\, s_h + s_f\, b_0 + D)(b_0 - d)D}{{b_0}^3 {s_h}^2} \\ 0 & b_0(1 - s_f) - (d + D) \end{bmatrix}, \tag{A.8}$$

with eigenvalues

$$\lambda = \begin{bmatrix} \frac{\left(s_f\ b_0+D\right)\left(b_0(s_h-s_f)-D\right)}{b_0\ s_h} \\ b_0(1-s_f)-(d+D) \end{bmatrix}. \tag{A.9}$$

The second eigenvalue is positive when $R_I > 1$, which we assume throughout, and which is necessary for equilibria 4 and 6 to be positive in N (provided $R_U > 1$). Thus, $R_I > 1$ is sufficient for equilibrium 3 to be **unstable**.

4. The Jacobian evaluated at equilibrium 4 and its eigenvalues are too unwieldy to reproduce here, but the determinant simplifies to Eq. A.10.

$$\Delta = \frac{s_T}{s_h(1-s_f)}\left(R_I - 1\right)\left(s_T - s_h\right) \tag{A.10}$$

A saddle occurs wherever the determinant is negative, which occurs when $s_h > s_T$ and $R_I > 1$. We must assume the former for the p-coordinate to be less than one, and we already assume the latter for both equilibria 4 and 6 to be positive in N. Thus, wherever equilibrium 4 exists and is biologically meaningful, it is **unstable**, and more specifically, a saddle.

5.

$$J = \begin{bmatrix} b_0(s_f - s_h) + D & 0 \\ 0 & b_0(1-s_f) - (d+D), \end{bmatrix}. \tag{A.11}$$

which has eigenvalues

$$\lambda = \begin{bmatrix} b_0\left(s_f - s_h\right) + D \\ b_0(1-s_f) - (d+D) \end{bmatrix}. \tag{A.12}$$

The second eigenvalue is the same as equilbrium 3, and thus we also have that 5 is **unstable** when $R_I > 1$.

6.

$$\begin{bmatrix} \frac{d+D}{1-s_f}(s_T - s_h) & 0 \\ \frac{(s_h - s_f)(d+D)^2(R_I - 1)}{(1-s_f)^2(b_0 - d)} & -b_0(1-s_f) + d + D \end{bmatrix}, \tag{A.13}$$

which has eigenvalues

$$\lambda = \begin{bmatrix} \frac{d+D}{1-s_f}(s_T - s_h) \\ -b_0(1-s_f) + d + D \end{bmatrix}. \tag{A.14}$$

The first eigenvalue is negative when $s_h > s_T$. The second eigenvalue is negative when $R_I > 1$. Since we assume both of these conditions, equilibrium 6 is **stable**.

The stability and locations of the six equilibria are summarized in Figure 2.1.

The difference in p-coordinates between equilibria 3 and 4 gives us a measure of how strongly the invasion threshold depends on population size, or the potential benefit of suppressing the population in decreasing the invasion threshold. The difference is represented by Eq. 2.8. It is evident that when $D = 0$, equilibria 3 and 4 occur at the same value of p, and the invasion threshold will be independent of N.

A.2 Linear increase in per capita death rate, interacting with *Wolbachia*-induced mortality

We now consider the case where per capita emergence rate is constant, and the per capita death rate increases linearly with population size. This type of density dependence is assumed by Keeling et al. (2003), Farkas and Hinow (2010), and Zheng et al. (2014),

Table A.2: Per capita density-dependent emergence and death rates for density-dependent mortality that interacts with *Wolbachia*-induced mortality

	I	U
$b(N)$	$b(1-s_f)$	b
$d(N)$	$(b+D)\frac{N}{K}$	$b\frac{N}{K}$

which is graphically represented in Figure A.2.

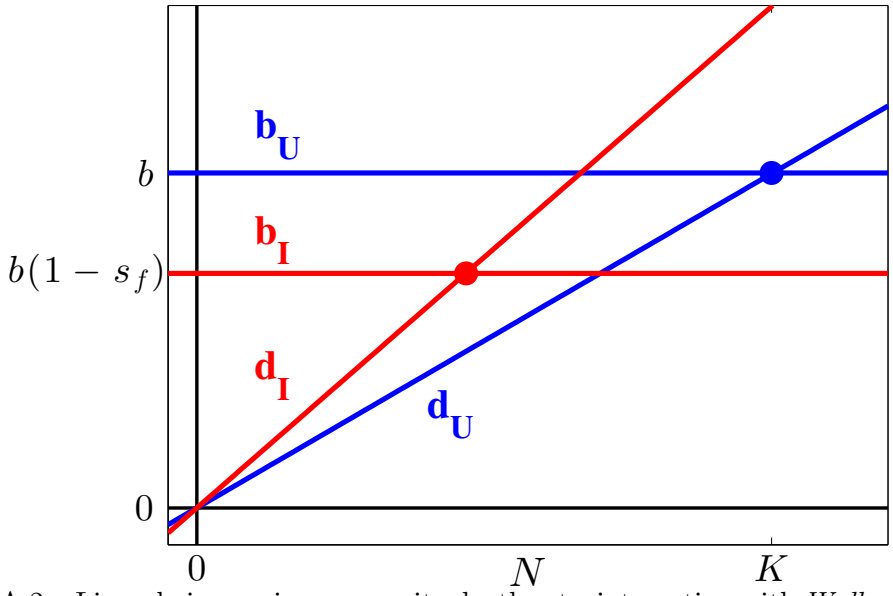

Figure A.2: Linearly increasing per-capita death rate, interacting with *Wolbachia*-induced mortality. Stable equilibria (filled circles) of all infected (red) or all uninfected (blue) individuals occur where per capita emergence and death rates intersect.

Plugging this form of density dependence into Eq. A.3 and then solving for the equilibria of the system gives the six equilibria in Table A.3.

Table A.3: Equilibrium points for linear increase in per capita death rate, interacting with *Wolbachia*-induced mortality. $s_T = (s_f b + D)/(b + D)$.

#	$\boldsymbol{p^*}$	$\boldsymbol{N^*}$
1.	0	0
2.	0	K
3.	$\frac{s_f}{s_h}$	0
4.	$\frac{s_T}{s_h}$	$(1 - s_T)K$
5.	1	0
6.	1	$(1 - s_T)K$

We again consider $x = N/K$ for the stability analysis.

1. $$J = \begin{bmatrix} -bs_f & 0 \\ 0 & b \end{bmatrix}, \tag{A.15}$$

   which has eigenvalues

   $$\lambda = \begin{bmatrix} -bs_f \\ b \end{bmatrix}. \tag{A.16}$$

   One eigenvalue is always positive and the other is always negative, so equilibrium 1 is **unstable**, and more specifically, a saddle.

2.

$$J = \begin{bmatrix} -bs_f - D & 0 \\ -b(s_f + s_h) - D & -b \end{bmatrix}, \tag{A.17}$$

which has eigenvalues

$$\lambda = \begin{bmatrix} -bs_f - D \\ -b \end{bmatrix}, \tag{A.18}$$

both of which are always negative. Thus, equilibrium 2 is **stable**.

3.

$$J = \begin{bmatrix} \frac{bs_f}{s_h}(s_h - s_f) & \frac{Ds_f}{s_h^2}(s_f - s_h) \\ 0 & b(1 - s_f) \end{bmatrix}, \tag{A.19}$$

which has eigenvalues

$$\lambda = \begin{bmatrix} \frac{bs_f}{s_h}(s_h - s_f) \\ b(1 - s_f) \end{bmatrix}, \tag{A.20}$$

the latter of which is positive, indicating that equilibrium 3 is **unstable**.

4.

$$J = \begin{bmatrix} \frac{bs_T}{s_h}(s_T - s_h) & \frac{Ds_T}{s_h^2}(s_T - s_h) \\ \frac{b^2}{b+D}(1 - s_f)(s_T - s_h) & -\frac{b}{b+D}\frac{1 - s_f}{s_h}(bs_h + Ds_T) \end{bmatrix}. \tag{A.21}$$

The eigenvalues are too complicated to display, but we can at least solve for the determinant:

$$\Delta = \frac{b^2}{s_h} s_T (1 - s_f)(s_T - s_h), \tag{A.22}$$

which is negative when $s_h > s_T$, which must be true for the p-coordinate of equilibrium 4 to be less than one. Thus, wherever equilibrium 4 is biologically meaningful, we have that it is **unstable**, and more specifically, a saddle.

5.

$$J = \begin{bmatrix} b(s_f - s_h) & 0 \\ \\ 0 & b(1 - s_f) \end{bmatrix}, \tag{A.23}$$

which has eigenvalues

$$\lambda = \begin{bmatrix} b(s_f - s_h) \\ b(1 - s_f) \end{bmatrix}, \tag{A.24}$$

the latter of which is always positive, indicating that equilibrium 5 is **unstable**.

6.

$$J = \begin{bmatrix} b(s_T - s_h) & 0 \\ \\ b(1 - s_T)(s_h - s_T) & -b(1 - s_f) \end{bmatrix}, \tag{A.25}$$

which has eigenvalues

$$\lambda = \begin{bmatrix} b(s_T - s_h) \\ -b(1 - s_f) \end{bmatrix}, \tag{A.26}$$

both of which are negative, provided $s_h > s_T$, which we have already assumed. Thus, equilibrium 6, the infection-only equilibrium, is **stable**.

The equilibria positions and stabilities are represented in Figure A.3.

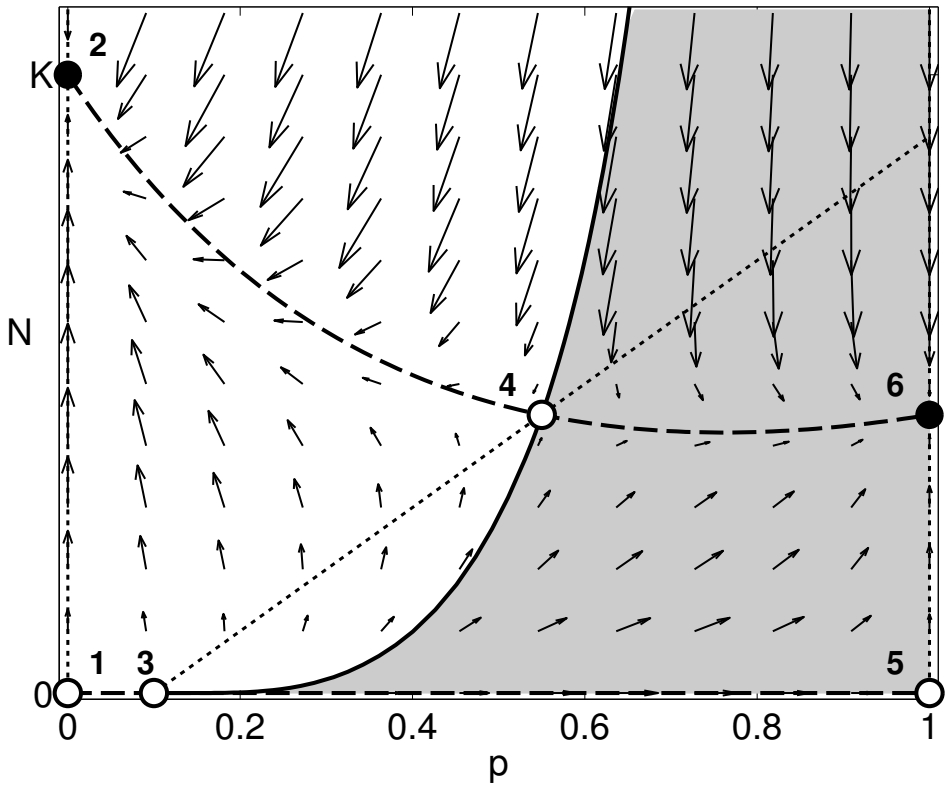

Figure A.3: Phase plane for linearly increasing death rates, interacting with *Wolbachia* mortality, constant emergence rates. The separatrix (solid line) separates the phase space into initial conditions that lead to *Wolbachia* extinction (unshaded region) and *Wolbachia* establishment (shaded region). Equilibria (circles) occur wherever a p-nullcline (dotted lines) intersects an N-nullcline (dashed lines) and are either stable (filled) or unstable (unfilled) as determined by linear stability analysis. Parameter values are chosen to be $b = 1$, $D = 1$, $s_f = 0.1$, $s_h = 1$.

The dependence of the invasion threshold on population size can be expressed, again, as the difference between p-coordinates of equilibria 3 and 4 (Eq. A.27).

$$\delta = \frac{D}{b+D}\left(\frac{1-s_f}{s_h}\right) \tag{A.27}$$

We see, as in the previous form of density dependence, that the invasion threshold depends on initial population size only when $D \neq 0$. Zheng et al. (2014) found this to be the case, although the parameters they used show a weaker dependence on population size. We chose parameters

to illustrate a case when there is a strong dependence on initial population size.

A.3 Linear increase in per capita death rate, independent of *Wolbachia*-induced mortality

We could just as easily select a form of density-dependent per capita death rate in which the density dependence-induced mortality acted independently of *Wolbachia*-induced mortality, as was recently assumed by Souto-Maior et al. (2014). This might be a more appropriate choice if, say, infection with *Wolbachia* caused an average reduction in lifespan of one day, regardless of whether the population was at half or twice carrying capacity. The per capita emergence and death rates would then take the form of Table A.4.

Table A.4: Per capita density-dependent emergence and death rates for density-dependent mortality that is independent of *Wolbachia*-induced mortality

	I	U
$b(N)$	$b(1-s_f)$	b
$d(N)$	$\frac{bN}{K}+D$	$\frac{bN}{K}$

These rates are depicted graphically in Figure A.4.

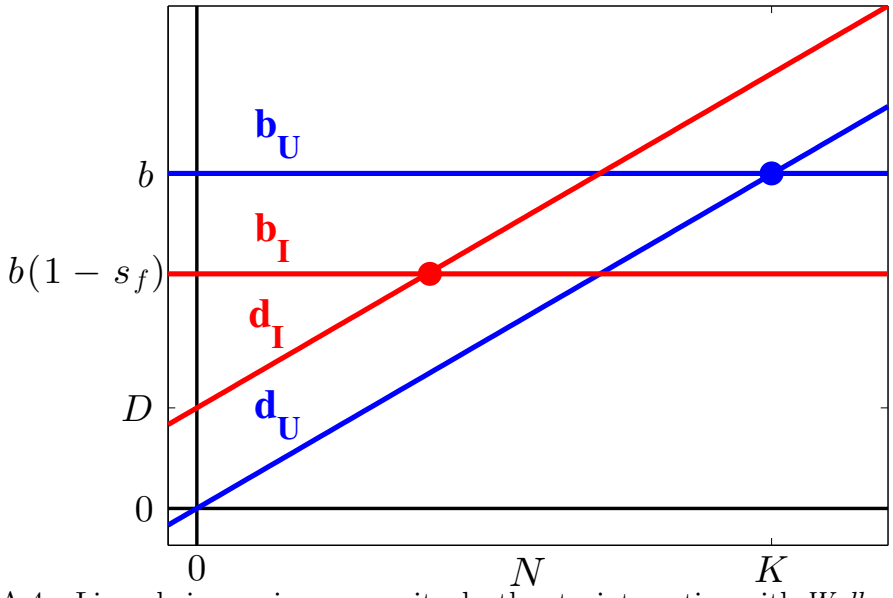

Figure A.4: Linearly increasing per-capita death rate, interacting with *Wolbachia*-induced mortality. Stable equilibria (filled circles) of all infected (red) or all uninfected (blue) individuals occur where per capita emergence and death rates intersect.

Plugging this form of density dependence into Eq. A.3 and then solving for the equilibria of the system gives the six equilibria in Table A.5.

Table A.5: Equilibrium points for linear increase in per capita death rate, independent of *Wolbachia*-induced mortality.

#	$\boldsymbol{p^*}$	$\boldsymbol{N^*}$
1.	0	0
2.	0	K
3.	$\frac{bs_f + D}{bs_h}$	0
4.	$\frac{bs_f + D}{bs_h}$	$\left((1 - s_f) - \frac{D}{b}\right) K$
5.	1	0
6.	1	$\left((1 - s_f) - \frac{D}{b}\right) K$

Linear stability analysis for each point gives the following:

1.
$$J = \begin{bmatrix} -bs_f - D & 0 \\ \\ 0 & b \end{bmatrix}. \tag{A.28}$$

with eigenvalues

$$\lambda = \begin{bmatrix} -bs_f - D \\ \\ b \end{bmatrix}. \tag{A.29}$$

The second eigenvalue is always positive and thus the equilibrium is **unstable**.

2.
$$J = \begin{bmatrix} -bs_f - D & 0 \\ \\ -b(s_f + s_h) - D & -b \end{bmatrix}, \tag{A.30}$$

which has eigenvalues

$$\lambda = \begin{bmatrix} -bs_f - D \\ -b \end{bmatrix}. \tag{A.31}$$

Both eigenvalues are negative, so long as *Wolbachia* does not cause a survival advantage, such that $D < -bs_f$, and the equilibrium is **stable**.

3.

$$J = \begin{bmatrix} \frac{bs_f + D}{s_h}\Big(s_h - \big(s_f + D/b\big)\Big) & 0 \\ 0 & b(1 - s_f) - D \end{bmatrix}, \tag{A.32}$$

which has eigenvalues

$$\lambda = \begin{bmatrix} \frac{bs_f + D}{s_h}\Big(s_h - \big(s_f + D/b\big)\Big) \\ b(1 - s_f) - D \end{bmatrix}. \tag{A.33}$$

The second eigenvalue is positive when $R_I > 1$, and thus the equilibrium is **unstable**.

4.

$$J = \begin{bmatrix} \frac{bs_f + D}{s_h}\Big(s_h - \big(s_f + D/b\big)\Big) & 0 \\ -\Big(b(1 - s_f) - D\Big)\Big(s_h - \big(s_f + D/b\big)\Big) & -\Big(b(1 - s_f) - D\Big) \end{bmatrix}, \tag{A.34}$$

which has eigenvalues

$$\lambda = \begin{bmatrix} \frac{bs_f + D}{s_h}\Big(s_h - \big(s_f + D/b\big)\Big) \\ -\Big(b(1 - s_f) - D\Big) \end{bmatrix}. \tag{A.35}$$

The first eigenvalue is positive as long as $s_h > s_f + D/b$, which must be true for the p-coordinate to be less than one, and thus to be biologically meaningful. The second eigenvalue is negative when $R_I > 1$. Thus, the equilibrium is **unstable**, and more specifically, a saddle.

5.

$$J = \begin{bmatrix} -(b(s_h - s_f) - D) & 0 \\ \\ 0 & b(1 - s_f) - D \end{bmatrix}, \tag{A.36}$$

which has eigenvalues

$$\lambda = \begin{bmatrix} b(s_f - s_h) \\ b(1 - s_f) \end{bmatrix}. \tag{A.37}$$

The second eigenvalue is positive, and thus the equilibrium is **unstable**.

6.

$$J = \begin{bmatrix} -b\Big(s_h - \big(s_f + D/b\big)\Big) & 0 \\ -\Big(b(1 - s_f) - D\Big)\Big(s_h - \big(s_f + D/b\big)\Big) & -\Big(b(1 - s_f) - D\Big) \end{bmatrix}, \tag{A.38}$$

with eigenvalues

$$\lambda = \begin{bmatrix} -b\Big(s_h - \big(s_f + D/b\big)\Big) \\ -\Big(b(1 - s_f) - D\Big) \end{bmatrix}. \tag{A.39}$$

Both eigenvalues are negative when $s_h > s_f + D/b$, as we have already assumed, and when $R_I > 1$. Thus, the equilibrium is **stable**.

The positions and stabilities of the six equilibria are summarized in Figure A.5.

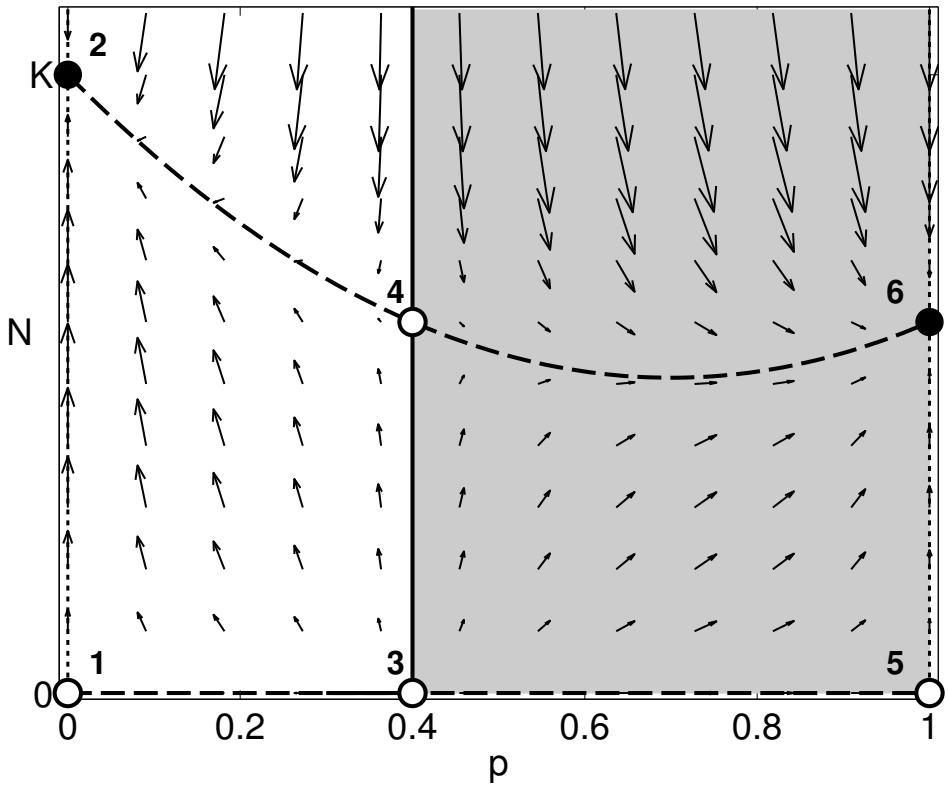

Figure A.5: Phase plane for linearly increasing death rates, independent of *Wolbachia* mortality, constant emergence rates. The separatrix (solid line) separates the phase space into initial conditions that lead to *Wolbachia* extinction (unshaded region) and *Wolbachia* establishment (shaded region). Equilibria (circles) occur wherever a p-nullcline (dotted lines) intersects an N-nullcline (dashed lines) and are either stable (filled) or unstable (unfilled) as determined by linear stability analysis. Parameter values are chosen to be $b = 1$, $D = 0.1$, $s_f = 0.3$, and $s_h = 1$.

The difference in p-coordinates and thus the dependence of the invasion threshold on N is $\delta = 0$, regardless of parameter values, which explains why Souto-Maior et al. (2014) found the invasion frequency threshold to be constant with population size (see their Eq. 3 and 5 and dashed lines in their Figure 1). This is because, if *Wolbachia*-induced mortality acts independently of density-dependent mortality, then N cancels out in Eq. A.3a, and frequency alone can predict the ultimate fate of *Wolbachia*. This does not mean, however, that population size is constant, and density dependence may still affect the timecourse of the invasion, as was the case for density-dependent emergence when $D = 0$ (see Figs. 2.2 and 2.2D in Chapter 2).

Thus, the result that the invasion threshold of *Wolbachia* depends on population size as well as initial frequency requires not only that the infection changes the lifespan of its host ($D \neq 0$), but also that it interacts with any density-dependent mortality assumed in the per capita death rate.

A.4 Nonlinear increase in per capita death rate

We now examine a form of nonlinear density dependence that was assumed by Hancock et al. (2011) in their model for *Ae. aegypti*, although we apply it directly to adult mortality since we do not explicitly model a larval stage.

Table A.6: Per capita density-dependent emergence and death rates for nonlinear density-dependent mortality. w is the relative lifespan of *Wolbachia*-infected individuals, assumed to scale with density-dependent mortality (interacting).

	I	U
$b(N)$	$(1-s_f)b$	b
$d(N)$	$\frac{1}{w}\left(d_0+\alpha N^\beta\right)$	$d_0+\alpha N^\beta$

Note that the form of density dependence in Section A.2 is a special case of this form, where $d_0 = 0$ and $\beta = 1$ (also, we use w here rather than $b/(b+D)$ to represent the relative lifespan of infected individuals). These rates are depicted graphically in Figure A.6.

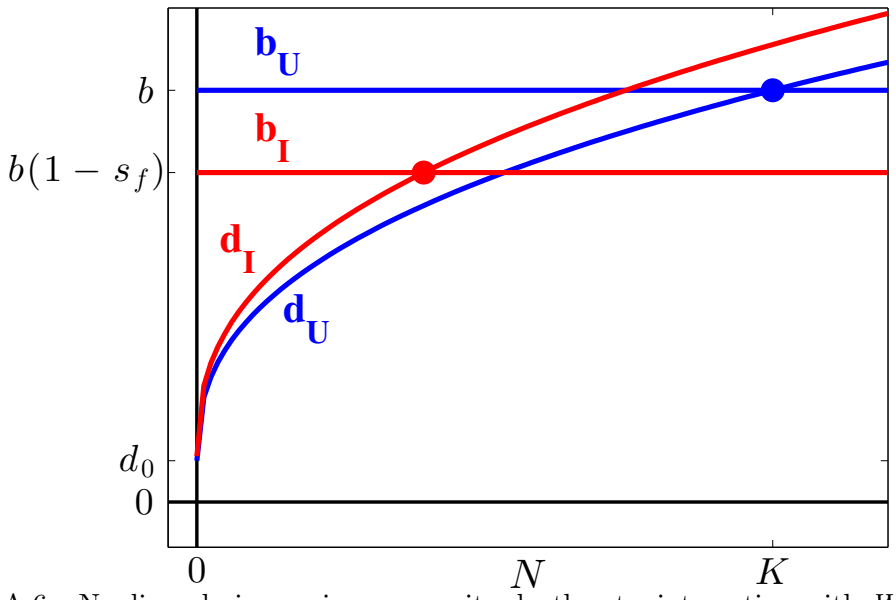

Figure A.6: Nonlinearly increasing per-capita death rate, interacting with *Wolbachia*-induced mortality. Stable equilibria (filled circles) of all infected (red) or all uninfected (blue) individuals occur where per capita emergence and death rates intersect.

The slope of $b(N) - d(N)$ determines how quickly the system returns to carrying capacity for small perturbations, i.e. the strength of density dependence. This slope is proportional to β.

Plugging this form of density dependence into Eq. A.3 and then solving for the equilibria of the system gives the six equilibria in Table A.7.

Table A.7: Equilibriua for nonlinear increase in per capita death rate, interacting with *Wolbachia*-induced mortality. R_I and R_U are the ratio of per capita birth to death rate in the limit as N approaches 0 (equal to $b(1-s_f)/(d_0/w)$ and b/d_0 respectively). They represent the expected number of female offspring produced by an infected and uninfected individual, respectively, when density dependence and CI effects are absent. The total fitness cost is $s_T = 1-w(1-s_f)$.

#	$\boldsymbol{p^*}$	$\boldsymbol{N^*}$
1.	0	0
2.	0	K
3.	$\frac{1}{s_h}\left(s_f + \frac{d_0}{b}\left(\frac{1-w}{w}\right)\right)$	0
4.	$\frac{s_T}{s_h}$	$\left(\frac{R_I-1}{R_U-1}\right)^{1/\beta} K$
5.	1	0
6.	1	$\left(\frac{R_I-1}{R_U-1}\right)^{1/\beta} K$

Linear stability analysis for each point gives the following:

1. $$J = \begin{bmatrix} -bs_f - d_0\left(1-w\right)/w & 0 \\ 0 & b-d_0 \end{bmatrix}. \tag{A.40}$$

   with eigenvalues

   $$\lambda = \begin{bmatrix} -bs_f - d_0\left(1-w\right)/w \\ b-d_0 \end{bmatrix}. \tag{A.41}$$

   The second eigenvalue is always positive and thus the equilibrium is **unstable**.

2.

$$J = \begin{bmatrix} b(1 - s_f - 1/w) & 0 \\ \\ b(1 - s_f - s_h - 1/w) & -\beta(b - d_0) \end{bmatrix}, \tag{A.42}$$

which has eigenvalues

$$\lambda = \begin{bmatrix} b(1 - s_f - 1/w) \\ -\beta(b - d_0) \end{bmatrix}. \tag{A.43}$$

Both eigenvalues are negative, so long as *Wolbachia* does not cause a survival advantage such that $w > 1/(1 - s_f)$, and the equilibrium is **stable**. The strength of density dependence, represented by β, affects how quickly trajectories approach this equilibrium. The stronger density dependence, the more quickly they approach, although the effect of this also depends on the relative magnitude of the first eigenvalue (if it is much smaller than the second eigenvalue, then the effect will be small because the rate of approach will be limited by the first eigenvalue).

3.

$$J = \begin{bmatrix} -\dfrac{1}{bws_h}\Big(bs_f + d_0(1-w)/w\Big)\Big(b(s_f - s_h) + d_0(1-w)/w\Big) & 0 \\ \\ 0 & b(1 - s_f) - d_0/w \end{bmatrix}, \tag{A.44}$$

whose diagonal elements are the eigenvalues. The second eigenvalue is positive when $R_I > 1$, and thus the equilibrium is **unstable**.

4. The Jacobian and its eigenvalues for this equilibrium are too unwieldy to reproduce here, but after some simplifying (see detailed_stability_analysis_type4.mw), the determinant can be written

$$\Delta = -\frac{b\,\beta\,d_0\,s_T}{w}\left(1 - \frac{s_T}{s_h}\right)(R_I - 1) \tag{A.45}$$

The determinant is always negative because we assume $R_I > 1$ and $s_h > s_T$ (both must be true for this equilibrium to be biological, i.e. $p^* < 1$ and $N^* > 0$). Thus, the equilibrium is **unstable**, and more specifically, a saddle.

5.
$$J = \begin{bmatrix} -(b(s_h - s_f) - d_0(1-w)/w) & 0 \\ 0 & b(1-s_f) - d_0/w \end{bmatrix}, \tag{A.46}$$

whose eigenvalues are the diagonal elements. The second eigenvalue is positive when $R_I > 1$, so the equilibrium is **unstable**.

6.
$$J = \begin{bmatrix} b(s_T - s_h) & 0 \\ -b(s_T - s_h)\left(\dfrac{bw(1-s_f) - d_0}{b - d_0}\right)^{1/\beta} & -\beta\left(b(1-s_f) - d_0/w\right) \end{bmatrix}, \tag{A.47}$$

with eigenvalues

$$\lambda = \begin{bmatrix} b(s_T - s_h) \\ -\beta\left(b(1-s_f) - d_0/w\right) \end{bmatrix}. \tag{A.48}$$

Both eigenvalues are negative when $s_h > s_T$ and $R_I > 1$. Thus, the equilibrium is **stable**. When density dependence is strong (β is large), nearby trajectories approach the equilibrium more quickly.

The effect of density dependence on the invasion threshold can once again be quantified by the difference in p-coordinates in equilibria 3 and 4:

$$\delta = \frac{1-w}{s_h}\left(1 - s_f - \frac{d_0}{bw}\right) \tag{A.49}$$

We see again that for the effect to be positive, we must have a lifespan-shortening strain $w < 1$. Incidentally, again, the effect is reversed if $w > 1$ (*Wolbachia* causes an increase in lifespan), though we must still have $w < 1/(1 - s_f)$ for the equilibrium analysis to hold. Interestingly, the strength of density dependence β does not enter into this equation, although its effect can

clearly be seen in Figure A.7, where higher values of β tend to make it easier for *Wolbachia* to spread (more gray area on phase plane). This illustrates the difficulty in defining one quantity to measure the curvature of the separatrix without being able to explicitly solve for it.

The positions and stabilities of the six equilibria are summarized in Figure A.7.

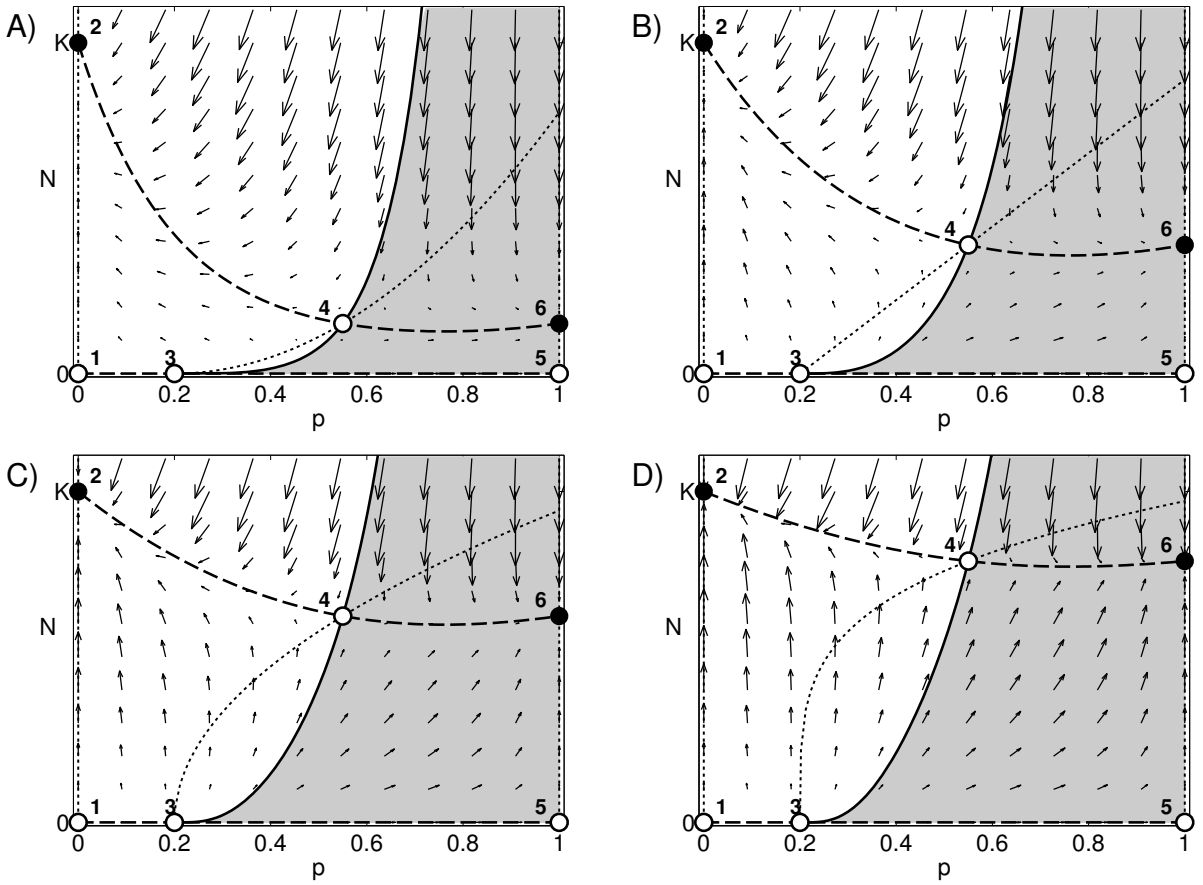

Figure A.7: Phase plane for nonlinearly increasing death rates, independent of *Wolbachia* mortality, constant emergence rates. The separatrix (solid line) separates the phase space into initial conditions that lead to *Wolbachia* extinction (unshaded region) and *Wolbachia* establishment (shaded region). Equilibria (circles) occur wherever a p-nullcline (dotted lines) intersects an N-nullcline (dashed lines) and are either stable (filled) or unstable (unfilled) as determined by linear stability analysis. Parameter values are chosen to be $b = 1$, $d_0 = 0.1$, $s_f = 0.1$, $w = 0.5$, $s_h = 1$, $\beta =$ A) 0.5, B) 1, C) 2 and D) 4.

Appendix B

Eco-evolutionary dynamics of *Wolbachia*: The interactions of multiple releases and density dependence

Let us consider a single release of I_T infected individuals into a population at carrying capacity K. The frequency of infected individuals immediately after release is

$$p_s = \frac{I_T}{I_T + K}. \tag{B.1}$$

Now consider releasing the same total number of mosquitoes split equally into $M > 1$ releases at equal time-intervals τ. Thus, I_T/M infected mosquitoes are added each release. Of interest is the final infection frequency after all M releases, p_m, and how this compares to p_s. We initially represent all fitness cost as fecundity cost rather than lifespan shortening, because as we saw in the main text, when there is no lifespan shortening, frequency alone is sufficient to determine whether *Wolbachia* will become established or extinct. Thus, we have a one-to-one correspondence of final infection frequency and *Wolbachia*'s ability to spread, so it is sufficient to compare p_s and p_m to determine which strategy better facilitates the introgression of *Wolbachia*.

The results for four different scenarios, with and without only two effects: CI + fecundity cost and density-dependent growth, are presented in Table B.1 (also in Table 2.3. The argument for each scenario is explained in detail below.

Table B.1: Comparison of infection frequency following either one (p_s) or multiple (p_m) releases. Results vary based on the presence/absence of only two effects: CI + fecundity cost and density-dependent growth. Because there is no lifespan shortening in all cases, infection frequency alone is an accurate predictor of the eventual fate of *Wolbachia* and so greater infection frequency corresponds to a better chance for *Wolbachia* to spread

		Density Dependence	
		No	Yes
CI + Fecundity Cost	No	A) $p_m = p_s$	B) $p_m > p_s$
	Yes	C) $p_m < p_s$	D) $p_m < p_s$ or $p_m > p_s$

1. In the absence of density dependence or CI + fecundity cost, released infected individuals remain in the population and replace themselves at the same rate as uninfected individuals. Thus, the frequency after the ith release, p_i, is the cumulative number of released individuals iI_T/M divided by the cumulative number of released individuals plus the original uninfected population size K:

$$p_i = \frac{iI_T/M}{iI_T/M + K}. \tag{B.2}$$

   Thus, $p_m = I_T/(I_T + K) = p_s$, which is independent of τ.

2. We present two arguments for why $p_m > p_s$ in this case: a verbal argument and a mathematical proof. The mathematical proof is more rigorous but essentially says the same thing as the verbal argument.

   1. Consider the phase plane for density-dependent population growth in Figure B.1, which shows the example of logistic growth, though the results apply more generally.

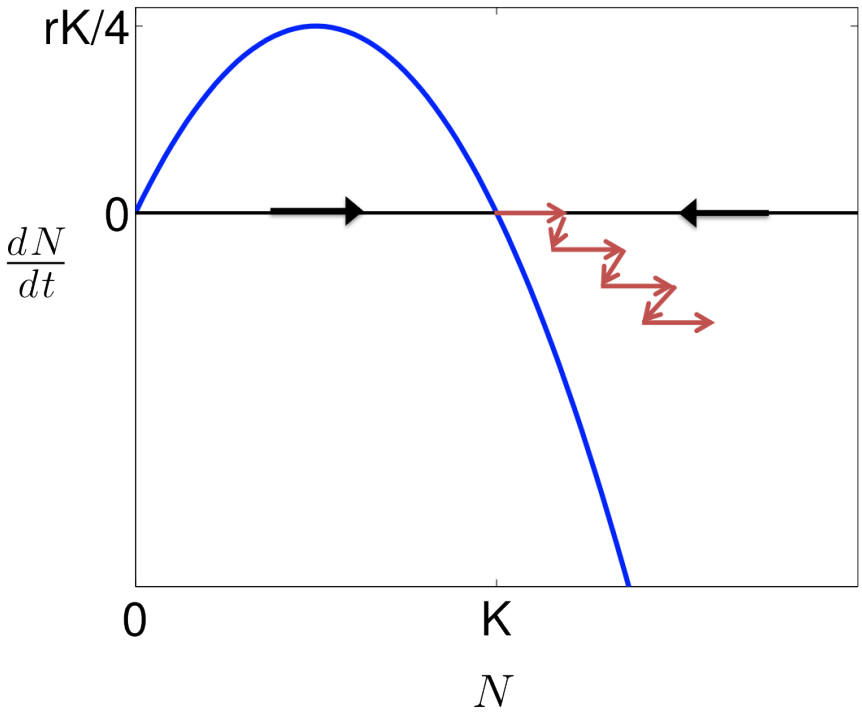

Figure B.1: Phase diagram for logistic growth, showing how population decreases in between releases into a wild-type population initially at carrying capacity. Carrying capacity is represented by the positive stable equilibrium, where the curve for dN/dt crosses the N-axis. The right-pointing red arrows represent the separate releases and the downward-left-pointing red arrows represent the decrease in population size in between releases as the population returns toward carrying capacity.

As seen by the red arrows in Figure B.1, the total population size decreases in between releases as the population returns toward carrying capacity. This decrease will be greater if τ is larger. It is important to note that, because there is no CI or fitness cost in this case, infected individuals are equally fit relative to uninfected individuals, so the infection frequency does not change between releases. That is, the decrease in net per capita growth rate due to increased population size applies equally to both infected and uninfected individuals. Due to the decrease in population size between releases, the I_T/M released individuals after all but the first release make up a larger proportion of the population than they would have if the population size remained the

same, as in scenario A). This causes the cumulative infection frequency at the end of all releases to be greater than the frequency after a single release of all I_T individuals.

2. The mathematical proof is as follows: Consider the population size after the i^{th} release, N_i, the infection frequency p_i, and that the population decreases by a fraction $a_i < 1$ during the time between releases τ. Then,

$$N_{i+1} = a_i N_i + \frac{I_T}{M} \tag{B.3}$$

$$p_{i+1} = \frac{a_i p_i N_i + I_T/M}{N_{i+1}} \tag{B.4}$$

Then, given $N_1 = K + I_T/M$, and $p_1 = I_T/(I_T + MK)$, we find (after some simplifying) that

$$p_2 = \frac{(a_1+1)I_T}{(a_1+1)I_T + a_1 MK} \tag{B.5}$$

$$p_3 = \frac{(a_1a_2 + a_1 + 1)I_T}{(a_1a_2 + a_1 + 1)I_T + a_1a_2 MK} \tag{B.6}$$

$$\vdots \tag{B.7}$$

$$p_m = \frac{(a_1a_2\cdots a_{M-1} + a_1a_2\cdots a_{M-2} + \cdots + a_1 + 1)I_T}{(a_1a_2\cdots a_{M-1} + a_1a_2\cdots a_{M-2} + \cdots + a_1 + 1)I_T + a_1a_2\cdots a_{M-1}MK} \tag{B.8}$$

$$= \frac{\left(1 + \dfrac{1}{a_{M-1}} + \dfrac{1}{a_{M-2}a_{M-1}} + \cdots + \dfrac{1}{a_1a_2\cdots a_{M-1}}\right) I_T}{\left(1 + \dfrac{1}{a_{M-1}} + \dfrac{1}{a_{M-2}a_{M-1}} + \cdots + \dfrac{1}{a_1a_2\cdots a_{M-1}}\right) I_T + MK}. \tag{B.9}$$

Because all M terms (except the first) in the coefficient of I_T are greater than one, the coefficient $A = 1 + \dfrac{1}{a_{M-1}} + \dfrac{1}{a_{M-2}a_{M-1}} + \cdots + \dfrac{1}{a_1a_2\cdots a_{M-1}} > M$. Thus,

$$\frac{M}{A} < 1 \tag{B.10}$$

$$\implies I_T + \frac{M}{A}K < I_T + K \tag{B.11}$$

$$\implies \frac{1}{I_T + \frac{M}{A}K} > \frac{1}{I_T + K} \tag{B.12}$$

$$\implies \frac{I_T}{I_T + \frac{M}{A}K} > \frac{I_T}{I_T + K} \tag{B.13}$$

$$\implies \frac{AI_T}{AI_T + MK} > \frac{I_T}{I_T + K} \tag{B.14}$$

$$\implies p_m > p_s. \tag{B.15}$$

The degree of difference will depend on the specific form of density dependence assumed as well as τ. We can find an upper bound for p_m however, because as $\tau \to \infty$ for any form of density dependence, $a_i \to MK/(I_T + MK)$ for all i. Using the formula for the partial sum of a geometric series in this case, we can write

$$p_{m,\,max} = 1 - \left(\frac{MK}{I_T + MK}\right)^M. \tag{B.16}$$

Thus,

$$p_s < p_m < 1 - \left(\frac{MK}{I_T + MK}\right)^M \tag{B.17}$$

3. For this scenario, we will assume that most of the multiple releases are insufficient to cause the infection frequency to exceed the threshold. Additionally, the population does not respond to changes in size, such that, after a release, the population remains at the new population size until the next release. This allows us to remove the effects of density dependence. Consider the phase plane in Figure B.2:

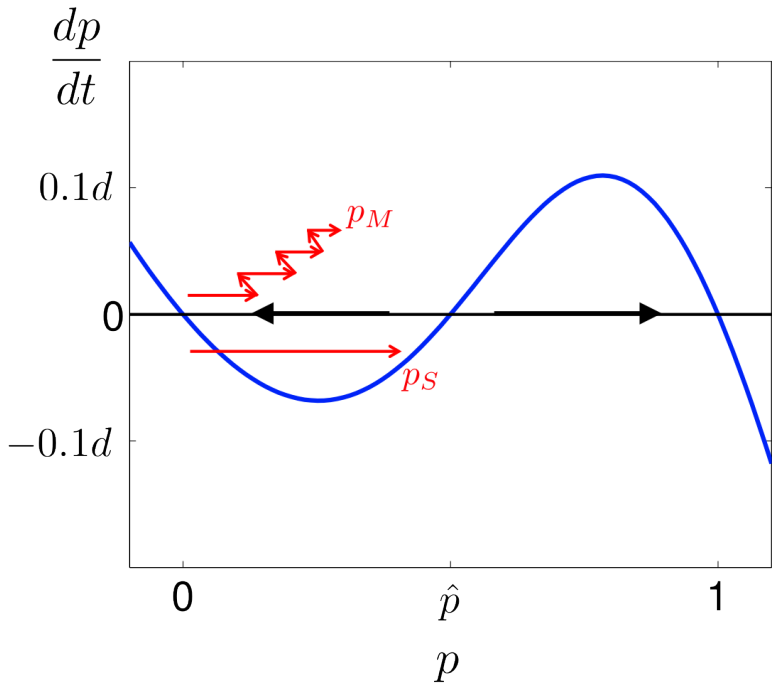

Figure B.2: Phase diagram for bistable dynamics caused by, for example, the frequency-dependent selection of *Wolbachia* due to CI and fitness cost. The unstable equilibrium $\hat{p}$ occurs where dp/dt crosses the p-axis between 0 and 1. The stable equilibria occur at 0 and 1, where perturbations decay back toward equilibrium rather than move away. Releases are shown with right-pointing red arrows, and the decrease in infection frequency between releases is shown by upward-left-pointing red arrows.

Analogous to case B), the multiple releases are battling uphill, this time against the fitness cost of *Wolbachia* rather than increased mortality, which drives the infection frequency toward 0. This causes the frequency after multiple releases to be lower than if they were released all at once.

Mathematically, if we consider that the infection frequency changes by a fraction a_i during the time τ after the i^{th} release, we can write

$$N_i = i\frac{I_T}{M} + K \tag{B.18}$$

$$p_{i+1} = \frac{a_i p_i N_i + I_T/M}{N_{i+1}} \tag{B.19}$$

which, given $N_1 = K + I_T/M$ and $p_1 = I_T/(I_T + MK)$, yields

$$p_m = \frac{a_1 a_2 a_{M-1} + a_1 a_2 a_{M-2} + \cdots + a_1 + 1}{M} p_s. \tag{B.20}$$

Whenever all $a_i < 1$, as in Figure B.2, the numerator in (B.20) will be less than M and $p_m < p_s$. This is a conservative estimate, however. Some releases in the multiple release scenario might lead to an increase in frequency over the time interval τ, specifically whenever the frequency threshold $\hat{p}$ is exceeded. However, as long as $a_1 a_2 \cdots a_{M-1} + a_1 a_2 \cdots a_{M-2} + \cdots + a_1 + 1 < M$, some of the a_i may be greater than one and p_m will still be less than p_s.

One can imagine exceptions in which $p_m > p_s$. For example, when the frequency threshold is low, one might be able to split the infected individuals into a small number of releases such that the first release is enough to exceed the threshold. Then one can wait a long time τ, allowing CI to increase the infection frequency ($a_1 > 1$) before releasing the next batches, such that the frequency after all releases is greater than for a single release. We focus here on the relevant scenario where it takes the majority of the multiple releases to exceed the frequency threshold and satisfies $a_1 a_2 \cdots a_{M-1} + a_1 a_2 \cdots a_{M-2} + \cdots + a_1 + 1 < M$.

Some examples using the frequency-only model with complete CI and no lifespan shortening (Eq. B.21) are shown in Figures B.3-B.5.

$$\frac{dp}{dt} = d\frac{p(1-p)(p-s_f)}{1 - s_f p - p(1-p)} \tag{B.21}$$

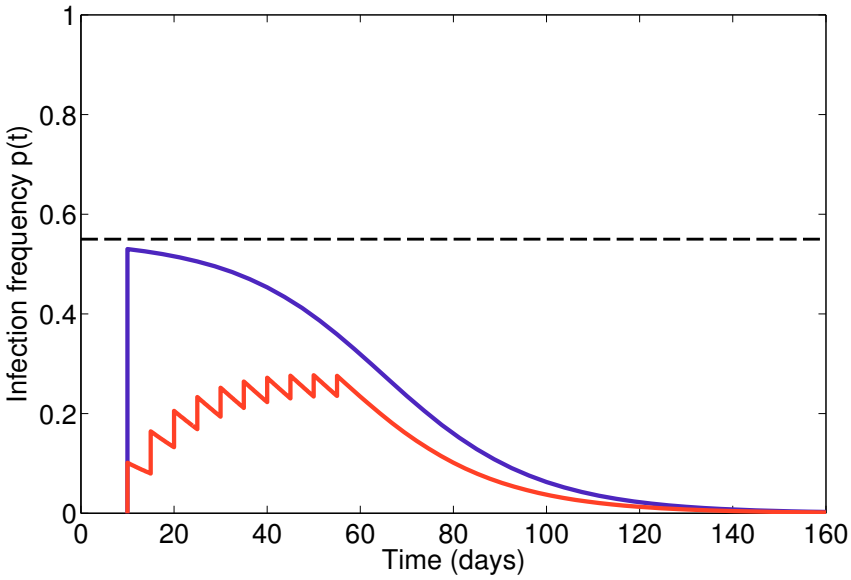

Figure B.3: Infection frequency following single release (blue, dark) and multiple release (red, light) of the same total number of released infected individuals. $p_s = 0.53$, $M = 10$, $\tau = 5$, $s_f = 0.55$. The frequency threshold (dashed line) is $\hat{p} = s_f$.

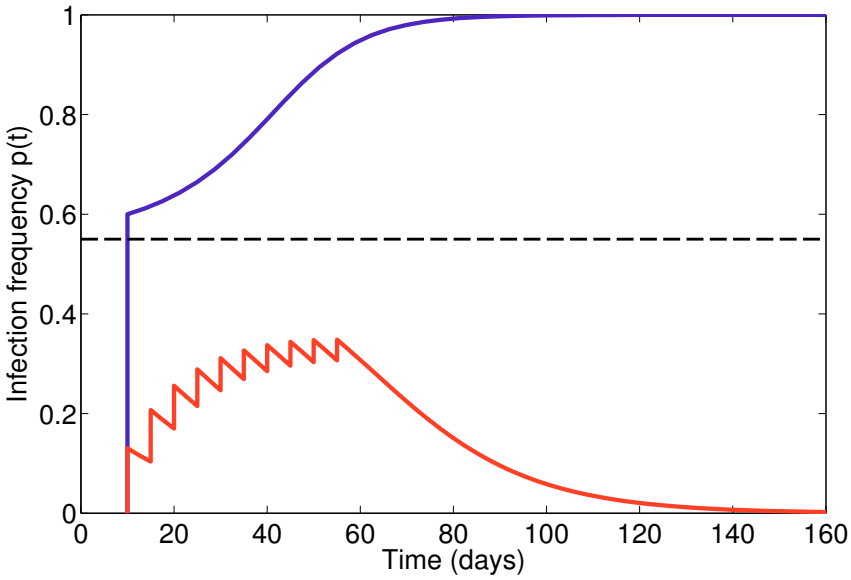

Figure B.4: Infection frequency following single release (blue, dark) and multiple release (red, light) of the same total number of released infected individuals. $p_s = 0.6$, $M = 10$, $\tau = 5$, $s_f = 0.55$. The frequency threshold (dashed line) is $\hat{p} = s_f$.

Figure B.5 shows the effect of different values of M and τ for the same total number of released individuals. Note that Figures B.3 and B.4 are similar to Figure 2 in Hancock et al. (2011), and we have chosen similar parameter values and time scale to compare. The comparison will be more evident in scenario D) where we also consider density dependence.

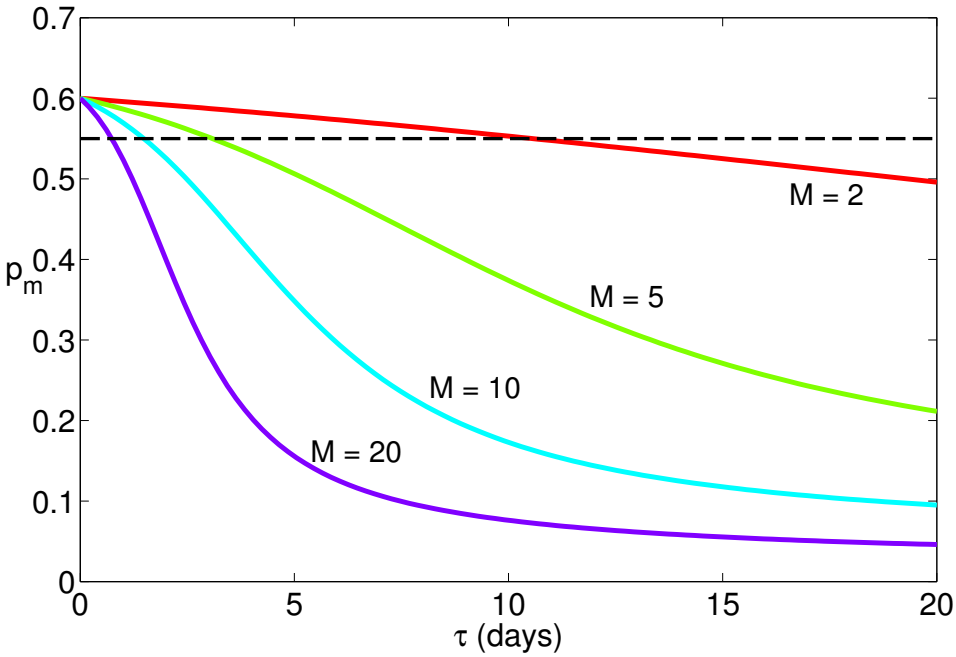

Figure B.5: The infection frequency p_m following the final release for various M and τ values. Other parameters are the same as Figure B.4: $p_s = 0.6$, $s_f = 0.55$. The frequency threshold (dashed line) is $\hat{p} = s_f$. Without lifespan shortening, the final frequency relative to the threshold determines whether *Wolbachia* will spread such that points above the dashed line indicate eventual establishment and points below the dashed line represent eventual extinction.

In Figure B.5, as τ approaches zero, all release strategies approach the single release frequency p_s, which is the maximum attainable frequency given the same total number of released insects. Figure B.5 is similar to Figure B1 in Appendix B of Hancock et al. (2011), which looks at the minimum number of insects required to achieve release as a function of M and τ. The main difference in Figure B.5 is that all points are for the same number of released insects. Figure B.5 illustrates that single release is better than any multiple release in this scenario.

4. For the final case it is difficult, if not impossible, to construct an analytical argument. We therefore rely on simulations to show a variety of outcomes and demonstrate that it is difficult to reach one single conclusion about whether multiple or single release is better.

In our simulations we use density dependence type 4 (see Section A.4), though we expect the results to apply broadly across different forms of density dependence. Even without lifespan shortening, which further complicates matters because frequency alone can no longer determine the outcome, we find that the results depend highly on values for M and τ, as seen in Figure B.6.

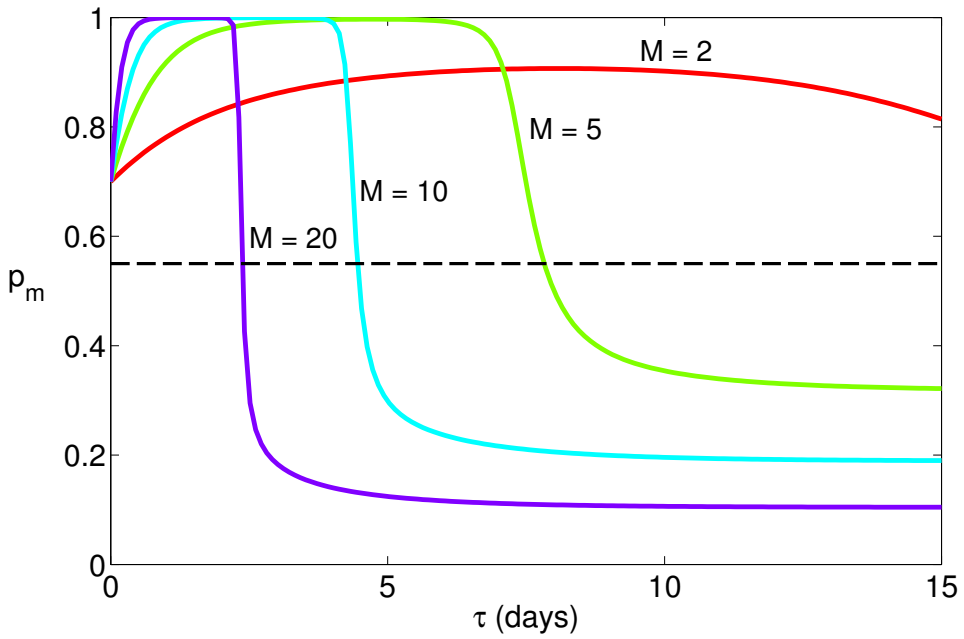

Figure B.6: The infection frequency p_m following the final release for various M and τ values. $p_s = 0.7$, $b = 1$, $d_0 = 0.1$, $\beta = 0.5$, $s_f = 0.55$. The frequency threshold (dashed line) is $\hat{p} = s_f$. Without lifespan shortening, the final frequency relative to the threshold determines whether *Wolbachia* will spread such that points above the dashed line indicate eventual establishment and points below the dashed line represent eventual extinction.

In Figure B.6, we see that there are a range of M and τ values for which the final frequency is above that for a single release. The benefit of many releases falls off quickly however, after some critical τ, beyond which the infection frequency falls too much between releases for establishment to occur. Single release in Figure B.6 causes establishment of *Wolbachia*. Figure B.7 illustrates an example when single release leads to extinction and multiple

release (of the same total number of individuals) in some cases leads to establishment.

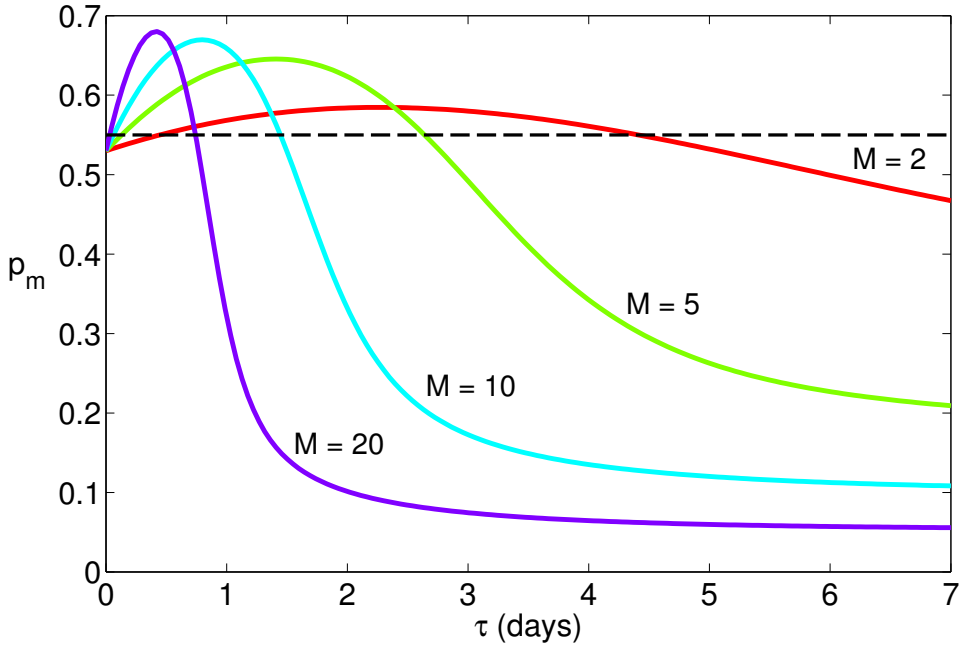

Figure B.7: The infection frequency p_m following the final release for various M and τ values. $p_s = 0.53$, $b = 1$, $d_0 = 0.1$, $\beta = 0.5$, $s_f = 0.55$. The frequency threshold (dashed line) is $\hat{p} = s_f$. Without lifespan shortening, the final frequency relative to the threshold determines whether *Wolbachia* will spread such that points above the dashed line indicate eventual establishment and points below the dashed line represent eventual extinction.

We now look at the case with lifespan shortening.

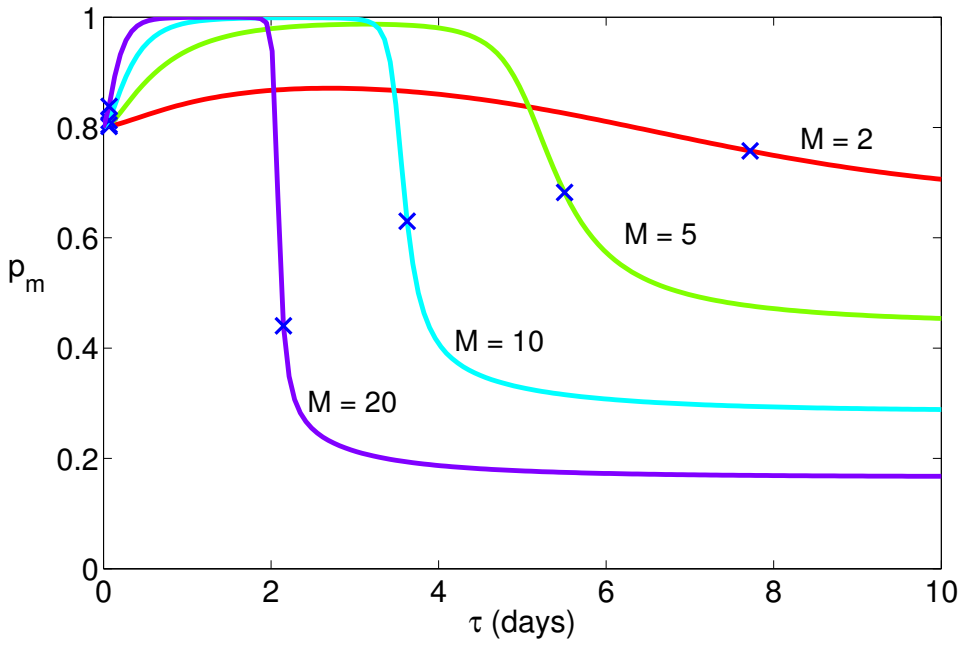

Figure B.8: The infection frequency p_m following the final release for various M and τ values. $p_s = 0.8$, $b = 1$, $d_0 = 0.1$, $\beta = 0.5$, $s_f = 0.05$, $s_v = 0.5$, where $s_v = 1 - w$. Points in between the blue xs for each curve cause establishment of *Wolbachia*. Single release with the same number of individuals causes extinction.

For the case of high survival fitness ($s_v = 0.5$), single release to achieve an initial frequency of 0.8 does not spread due to the large density-dependent response of the population, and the proportionately higher death rate of newly released infected individuals, which was also found by Hancock et al. (2011). Here, multiple releases are better for achieving spread, but only for a range of M and τ values, indicated by the regions between blue xs (we have no dashed line because the invasion threshold is no longer determined only by infection frequency, and cannot be solved for, as discussed in the main text for the case of lifespan shortening). Notice that the left-most xs are surprisingly close to the single release approximation ($\tau \to 0$). This indicates that a very small τ (< 0.1) can cause establishment of *Wolbachia* when single release ($\tau = 0$) does not. This is likely due to how quickly density dependence acts and the assumptions that changes in frequency

are occurring continuously (i.e. start immediately after release). We believe this to be a consequence of some of the simplifying assumptions in the model and not necessarily biological. We do believe that the result that each number of releases has an associated optimal number of time in between releases is biological, however. This is caused by the tradeoff between splitting the total released number into smaller releases, each less likely to exceed the *frequency* threshold but also less likely to experience high density-dependent mortality.

Finally, when lifespan shortening is small, splitting the number of infected individuals into multiple releases may still be more efficient, but the effect appears less so than when lifespan shortening is large, as seen in Figure B.9. This mostly agrees with Hancock et al. (2011). Their appendix B also looks at the trade-off between various M and τ values though theirs is for different numbers of mosquitoes whereas we hold the number of mosquitoes in each scenario constant. The difference between the two strategies is greater when fitness cost, and thus the invasion threshold, are high. However, whether single or multiple release is more advantageous will largely depend on the M and τ values chosen. We have shown analytically how the case with both density dependence and CI + fitness cost causes the interaction of two effects, each of which alone causes one or the other to be a better strategy (see Table B.1). This creates some optimal parameter values where multiple releases are better, although they may not be practical for real release scenarios.

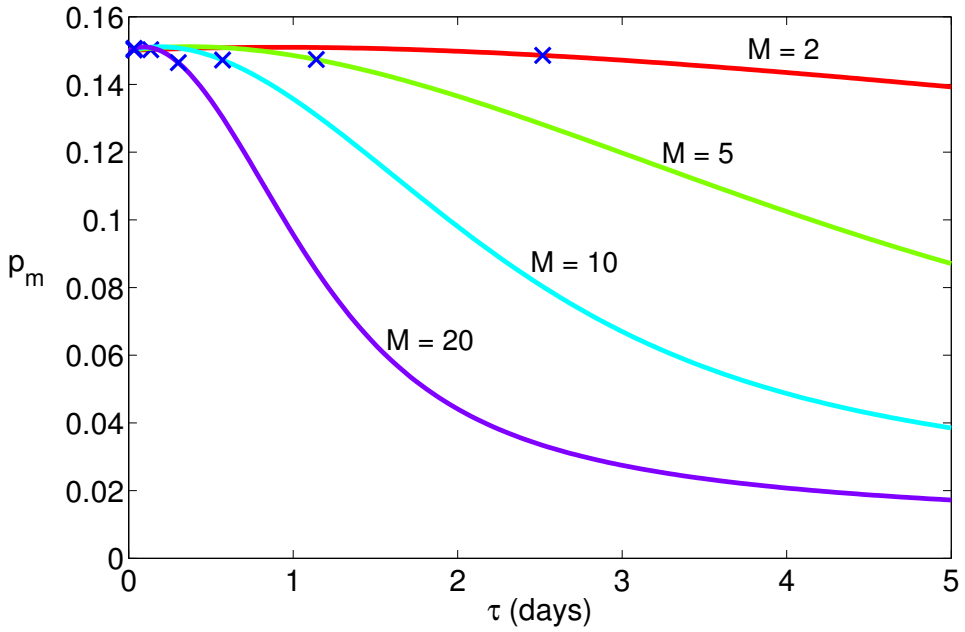

Figure B.9: The infection frequency p_m following the final release for various M and τ values. $p_s = 0.15$, $b = 1$, $d_0 = 0.1$, $\beta = 0.5$, $s_f = 0.05$, $s_v = 0.1$, where $s_v = 1 - w$. Points in between the blue xs for each curve cause establishment of *Wolbachia*. Single release with the same number of individuals causes extinction.

Appendix C

Eco-evolutionary dynamics of underdominance

We develop two models of single-locus underdominance in a well-mixed population that assume a 1:1 sex ratio and random mating. The first is a population dynamics model that allows for changing population size and density-dependent per capita growth rates. The second is a frequency-only model that assumes that the population size is constant. We then compare results from the two models and discuss similarities to *Wolbachia*.

C.1 Population dynamics model

We consider a diploid population of individuals that are either wild-type (aa), heterozygous (Aa), or homozygous (AA) for a novel allele A. We assume that Aa females experience a fitness cost to longevity (s_{vAa}) and fecundity (s_{fAa}), and that AA females experience a lower fitness cost to longevity (s_{vAA}) and fecundity (s_{fAA}), such that $s_{fAa} > s_{fAA}$ and $s_{vAa} > s_{vAA}$.

We consider N_{aa}, N_{Aa}, and N_{AA} to be the number of females of each genotype in the population, such that the total female population size is $N = N_{aa} + N_{Aa} + N_{AA}$. We can model the number of females of each genotype over time with the system of continuous-time ordinary differential equations in Eq. C.1:

$$\dot{N}_{aa} = \Big(b(N)(1-p_A) - d(N)\Big)N_{aa} + b(N)(1-s_{fAa})\left(\frac{1-p_A}{2}\right)N_{Aa} \tag{C.1a}$$

$$\dot{N}_{Aa} = b(N)p_A N_{aa} + \left(\frac{b(N)(1-s_{fAa})}{2} - \frac{d(N)}{1-s_{vAa}}\right)N_{Aa} + b(N)(1-s_{fAA})(1-p_A)N_{AA} \tag{C.1b}$$

$$\dot{N}_{AA} = b(N)(1-s_{fAa})\frac{p_A}{2}N_{Aa} + \left(b(N)(1-s_{fAA})p_A - \frac{d(N)}{1-s_{vAA}}\right)N_{AA}, \tag{C.1c}$$

where

$$p_A = \frac{\frac{1}{2}N_{Aa} + N_{AA}}{N} \tag{C.2}$$

is the frequency of allele A in the population. The coefficients in Eq. C.1 correspond to the probabilities of the various mating pairs combined with the probability of each offspring genotype arising from each mating pair. Density-dependent emergence and death rates $b(N)$ and $d(N)$ depend only on total female population size and not on the genotype distribution. We will focus on the type of density dependence assumed in the main text (Eq. 2.5 in the main text).

C.2 Frequency-only model

We now use a Moran process to model the frequency of each genotype in the population, assuming that the population size is constant. That is, $p_{aa}(t) + p_{Aa}(t) + p_{AA}(t) = 1$. To do this, we assume that each death is immediately followed by the emergence of a new adult. Deaths occur at the rate

$$r = d_{aa}p_{aa} + d_{Aa}p_{Aa} + d_{AA}p_{AA} \tag{C.3}$$

$$= d\,p_{aa} + \left(\frac{d}{1 - s_{vAa}}\right)p_{Aa} + \left(\frac{d}{1 - s_{vAA}}\right)p_{AA}, \tag{C.4}$$

where d is the constant per capita death rate of wild-type females.

The probability that the death of an i-genotype female is followed by the emergence of a j-genotype female is

$$\left(\frac{d_i p_i}{\sum_k d_k p_k}\right)\left(\frac{b_j p_j}{\sum_k b_k p_k}\right), \tag{C.5}$$

where $i, j, k \in \{aa, Aa, AA\}$, and $b_{aa} = b$, $b_{Aa} = b(1 - s_{fAa})$, and $b_{AA} = b(1 - s_{fAA})$.

The change in frequency of a genotype i can then be modeled by the rate of events multiplied by the probability of an event that increases p_i minus the probability of an event that decreases p_i:

$$\frac{dN_i}{dt} = r\left(\frac{b_i p_i\left(\sum_{j\neq i} d_j p_j\right)}{\left(\sum_j b_j p_j\right)\left(\sum_j d_j p_j\right)} - \frac{d_i p_i\left(\sum_{j\neq i} b_j p_j\right)}{\left(\sum_j b_j p_j\right)\left(\sum_j d_j p_j\right)}\right) \tag{C.6a}$$

$$= \frac{1}{\sum_j b_j p_j}\left[b_i p_i\left(\sum_{j\neq i} d_j p_j\right) - d_i p_i\left(\sum_{j\neq i} b_j p_j\right)\right], \tag{C.6b}$$

where we have used the fact that $r = \sum_j d_j p_j$.

C.3 Results

The time series for two different release scenarios with two different parameter sets are shown in the main text (Fig. 3). We will focus here on the first parameter set: $s_{fAa} = 0.4$, $s_{vAa} = 0.8$, $s_{fAA} = 0.1$, $s_{vAA} = 0.3$ when releasing into carrying capacity. The trajectories in 3-D phase space are shown for both models in Figs. C.1 and C.2.

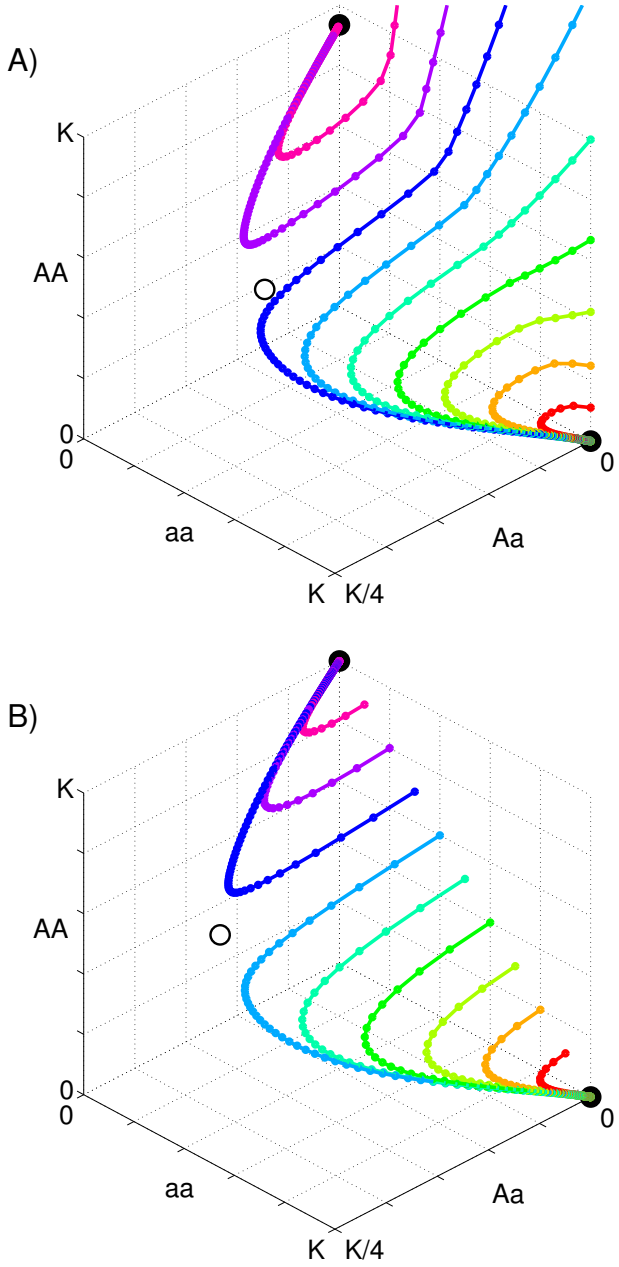

Figure C.1: Differences in population dynamics model (A) and frequency-only model (B) for release of AA homozygous females into a wild-type (aa) population at carrying capacity K. Initial frequencies are 0.1 (red, lower right), 0.2, ..., 0.9 (magenta, top center). Trajectories start at back right and go to a stable equilibrium of all AA (top center) or all aa (bottom right), depending on initial conditions. The unfilled circle is the unstable equilibrium. Parameter values are $b = 1$, $d = 0.1$, $s_{fAa} = 0.4$, $s_{vAa} = 0.8$, $s_{fAA} = 0.1$, $s_{vAA} = 0.3$.

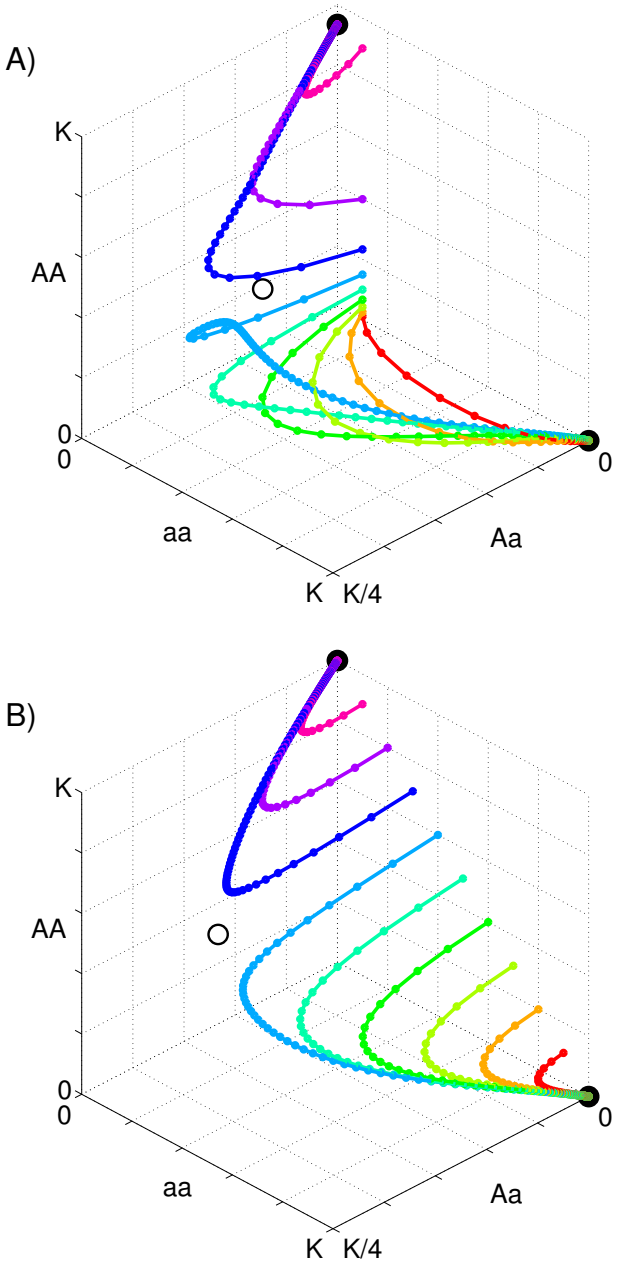

Figure C.2: Differences in population dynamics model (A) and frequency-only model (B) for release of AA homozygous females into a wild-type (aa) population that was suppressed to 10% of carrying capacity prior to release. Initial frequencies are 0.1 (red, lower right), 0.2, ..., 0.9 (magenta, top center). Trajectories start at back right and go to a stable equilibrium of all AA (top center) or all aa (bottom right), depending on initial conditions. The unfilled circle is the unstable equilibrium. Parameter values are $b = 1$, $d = 0.1$, $s_{fAa} = 0.4$, $s_{vAa} = 0.8$, $s_{fAA} = 0.1$, $s_{vAA} = 0.3$.

The solutions to the frequency-only model lie in the triangular section of the plane $N_{aa} + N_{Aa} + N_{AA} = K$ where $N_{aa}, N_{Aa}, N_{AA} \geq 0$, and the frequency-only model results are identical in Figs. C.1 and C.2, since the frequency-only model does not distinguish among different release scenarios. As in *Wolbachia*, we see that the invasion threshold is higher than predicted by the frequency-only model when releasing into a population at carrying capacity. In Fig. C.1, the $p_0 = 0.7$ trajectory (dark blue) leads to allele A being lost from the population dynamics model but becoming established in the frequency only model (see Fig. 2.3A). While it is not clear from Fig. C.2, there is a narrow range of initial frequencies in the case of releasing into a suppressed population for which the opposite is true: the population dynamics model predicts establishment where the frequency-only model predicts extinction (see Fig. 2.3B). It is not clear why the difference between the models for releases into a suppressed population is much smaller for underdominance than for *Wolbachia*.

Appendix D

Markov chain transition probabilities

D.1 Transition probabilities

We consider the continuous-time stochastic process $\{X(t), t \geq 0\}$ where $X(t)$ represents the life stage of an individual at time t. Thus, X has state space $\{1, 2, ..., 7\}$. We define $P_{ij}(t, t+\Delta t)$ as the probability that an individual is in stage j after a time interval Δt given that it is in stage i at time t:

$$P_{ij}(t, t + \Delta t) = \Pr\{X(t + \Delta t) = j \,|\, X(t) = i\}, \tag{D.1}$$

We start with the time-homogeneous case, meaning P_{ij} does not depend on t and $P_{ij}(t, t+\Delta t) = P_{ij}(\Delta t)$. We refer to the 7×7 matrix $\boldsymbol{P}(t)$ with elements P_{ij} as the transition matrix.

The forward Kolmogorov equation states that

$$\frac{d\boldsymbol{P}(t)}{dt} = \boldsymbol{P}(t)\boldsymbol{Q}. \tag{D.2}$$

where $\boldsymbol{Q}$ is the instantaneous transition rate matrix, with elements defined

$$q_{ij} = \lim_{\Delta t \to 0} \frac{P_{ij}(\Delta t) - P_{ij}(0)}{\Delta t}. \tag{D.3}$$

We have two rate matrices for each model: $\boldsymbol{Q}_f$ when food is present, and $\boldsymbol{Q}_v$ when food is absent. According to the descriptions in Section 4.2, the rate matrices for each model when food is available are

Model 1:

$$\boldsymbol{Q}_f = \begin{bmatrix} -(r+\mu_f) & r & 0 & 0 & 0 & 0 & \mu_f \\ 0 & -(r+\mu_f) & r & 0 & 0 & 0 & \mu_f \\ 0 & 0 & -(r+\mu_f) & r & 0 & 0 & \mu_f \\ 0 & 0 & 0 & -(r+\mu_f) & r & 0 & \mu_f \\ 0 & 0 & 0 & 0 & -(r+\mu_f) & r & \mu_f \\ 0 & 0 & 0 & 0 & 0 & 0 & 0 \\ 0 & 0 & 0 & 0 & 0 & 0 & 0 \end{bmatrix} \tag{D.4}$$

Model 2:

$$\boldsymbol{Q}_f = \begin{bmatrix} -r & r & 0 & 0 & 0 & 0 & 0 \\ 0 & -r & r & 0 & 0 & 0 & 0 \\ 0 & 0 & -r & r & 0 & 0 & 0 \\ 0 & 0 & 0 & -r & r & 0 & 0 \\ 0 & 0 & 0 & 0 & -r & r & 0 \\ 0 & 0 & 0 & 0 & 0 & 0 & 0 \\ 0 & 0 & 0 & 0 & 0 & 0 & 0 \end{bmatrix} \tag{D.5}$$

Model 3:

$$\boldsymbol{Q}_f = \begin{bmatrix} -r_1 & r_1 & 0 & 0 & 0 & 0 & 0 \\ 0 & -r_1 & r_1 & 0 & 0 & 0 & 0 \\ 0 & 0 & -r_1 & r_1 & 0 & 0 & 0 \\ 0 & 0 & 0 & -r_2 & r_2 & 0 & 0 \\ 0 & 0 & 0 & 0 & -r_2 & r_2 & 0 \\ 0 & 0 & 0 & 0 & 0 & 0 & 0 \\ 0 & 0 & 0 & 0 & 0 & 0 & 0 \end{bmatrix}. \tag{D.6}$$

The rate matrix when food is absent is the same for all three models:

$$\boldsymbol{Q}_v = \begin{bmatrix} -\mu_v & 0 & 0 & 0 & 0 & 0 & \mu_v \\ 0 & -\mu_v & 0 & 0 & 0 & 0 & \mu_v \\ 0 & 0 & -\mu_v & 0 & 0 & 0 & \mu_v \\ 0 & 0 & 0 & -\mu_v & 0 & 0 & \mu_v \\ 0 & 0 & 0 & 0 & -\mu_v & 0 & \mu_v \\ 0 & 0 & 0 & 0 & 0 & 0 & 0 \\ 0 & 0 & 0 & 0 & 0 & 0 & 0 \end{bmatrix}. \tag{D.7}$$

The matrix differential equation in Eq. D.2 with initial condition $\boldsymbol{P}(0) = \boldsymbol{I}$ (which simply states that the probability of being in the current state given that the individual is in the current state is one), has the solution

$$\boldsymbol{P}(t) = e^{\boldsymbol{Q}t}. \tag{D.8}$$

Using Maple v. 16 to evaluate the matrix exponential of each of the rate matrices, we can thus determine the probability of any transition $P_{ij}(\Delta t)$. If we consider equally spaced observation times $\vec{t} = (0, \Delta t, 2\Delta t, \ldots, n\Delta t)$, then the joint probability of any observed state sequence $\vec{x} = (x_0, x_1, x_2, \ldots, x_n)$ is

$$\Pr\{\vec{X} = \vec{x}\} = P_{x_0 x_1}(\Delta t) P_{x_1 x_2}(\Delta t) \cdots P_{x_{n-1} x_n}(\Delta t). \tag{D.9}$$

This is due to the fact that the memoryless property of Markov chains states that that each transition probability depends only on the current state, meaning they are all independent. Each factor in D.9 comes from the element of the transition matrix $\boldsymbol{P}(\Delta t)$ corresponding to the observed transition.

D.2 Food Dynamics

If we assume that the time until food in a container is depleted is a random variable T, then we have, by the law of total probability

$$\begin{aligned}\Pr\{X(t+\Delta t)=j \,|\, X(t)=i\} = & \\ \Pr\{X(t+\Delta t)=j \,|\, X(t)=i, T\le t\}\Pr\{T\le t\} & \\ +\Pr\{X(t+\Delta t)=j \,|\, X(t)=i, t<T\le t+\Delta t\}\Pr\{t<T\le t+\Delta t\} & \\ +\Pr\{X(t+\Delta t)=j \,|\, X(t)=i, T>t+\Delta t\}\Pr\{T>t+\Delta t\} &\end{aligned} \tag{D.10}$$

For an exponentially distributed waiting time $T \sim \text{Exp}(\lambda)$, the first term on the right hand side of Eq. D.10 is equal to

$$P_{ij,v}(\Delta t)(1-e^{-\lambda t}), \tag{D.11}$$

where $P_{ij,v}$ is the element of $\boldsymbol{P}_v(t) = \exp(\boldsymbol{Q}_v t)$ corresponding to transition $i \to j$. The $(1-e^{-\lambda t})$ term comes from the cumulative distribution function of T, which describes the probability that $T \le t$.

Similarly, the third term on the right hand side of Eq. D.10 is equal to

$$P_{ij,f}(\Delta t)e^{-\lambda(t+\Delta t)}, \tag{D.12}$$

where $P_{ij,f}$ comes from $\boldsymbol{P}_f = \exp(\boldsymbol{Q}_f t)$.

The second term on the right hand side of Eq. D.10 is more difficult to evaluate. However, if we consider $T = t + s$ on the interval $[t, t+\Delta t]$, then any transition $i \to j$ that is not death must occur by time $t + s$, such that $X(t+s) = j$. This is because, once food is depleted, immature *Ae. aegypti* can only die or stay in the same state. In addition, the individual must

then remain in state j (i.e. not die) until the end of the interval. Thus, the probability of observing $i \to j$ ($j < 7$) during the interval $[t, t+\Delta t]$, given that $T = t+s$, is the joint probability $\Pr\{X(t+s) = j | X(t) = i, T = t+s\} \Pr\{X(t+\Delta t) = j \,|\, X(t+s) = j, T = t+s\}$. This probability is equal to $P_{ij,f}(s)P_{jj,v}(\Delta t - s)$. Using the law of total probability for all the values of s at which this can occur, we have

$$\begin{aligned}
\Pr\{X(t+\Delta t) = j \,|\, X(t) = i, t < T \le t+\Delta t\} \Pr\{t < T \le t+\Delta t\} \\
&= \int_0^{\Delta t} P_{ij,f}(s) P_{jj,v}(\Delta t - s) \Pr\{t+s < T \le t+s+ds\} ds \\
&= \int_0^{\Delta t} P_{ij,f}(s) \left(1 - \exp^{-\mu_v(\Delta t - s)}\right) \lambda e^{-\lambda(t+s)} ds. \qquad \text{(D.13)}
\end{aligned}$$

In simplifying the last expression, we have used the fact that $P_{jj,v}(\Delta t - s) = \left(1 - \exp^{-\mu_v(\Delta t - s)}\right)$ in all three versions of the model and the probability density function of an exponentially distributed random variable $\Pr\{s < T \le s + ds\} = \lambda e^{-\lambda s} ds$.

Thus, we can solve for all transition probabilities other than death by substituting Eqs. D.11–D.13 into Eq. D.10:

$$\begin{aligned}
P_{ij}(t, \Delta t) = P_{ij,v}(\Delta t)(1 - e^{-\lambda t}) \qquad \text{(D.14)} \\
&+ \int_0^{\Delta t} P_{ij,f}(s) \left(1 - e^{-\mu_v(\Delta t - s)}\right) \lambda e^{-\lambda(t+s)} ds \\
&+ P_{ij,f}(\Delta t) e^{-\lambda(t+\Delta t)}
\end{aligned}$$

and then use the fact that $\sum_j P_{ij} = 1$ to solve for death:

$$P_{i7} = 1 - \sum_{j=1}^{6} P_{ij}. \qquad \text{(D.15)}$$

Note that the transition probabilities are now time-inhomogeneous, meaning they depend on t

as well as the time between observations Δt.

Appendix E

Markov chain Monte Carlo methods

E.1 Background

Using Bayes' rule, we can write

$$p(\Theta \mid x) \propto p(x \mid \Theta)\, p(\Theta) \tag{E.1}$$

for the posterior distribution of parameters given the likelihood $p(x \mid \Theta)$ and prior distribution $p(\Theta)$. Note that we have dropped the vector notation used in Section 4.2.1 as almost all quantities in this section are vector-valued, either indexed by house, treatment, replicate or number of parameters. For our mixed-effects model we can split the parameters into our rate parameters, $\theta = (r_{ij},\, \mu_{ij},\, \lambda_{ij})$, fixed effects $\phi = (\nu_i,\, \sigma_H^2,\, \sigma_\varepsilon^2)$ and random effects $\psi = (H_j)$:

$$\begin{aligned} p(\theta, \phi, \psi \mid x) &\propto p(x \mid \theta, \phi, \psi)\, p(\theta, \phi, \psi), \\ &\propto p(x \mid \theta)\, p(\psi \mid \phi)\, p(\phi)\, p(\theta). \end{aligned} \tag{E.2}$$

The posterior distribution is denoted by $p(\theta, \phi, \psi \mid x)$, the hyper-prior by $p(\psi \mid \phi)$, and the prior distribution of fixed-effect parameters by $p(\theta)$. The joint likelihood over all buckets is $p(x \mid \theta) = \prod_i \prod_j \prod_k p(x_k \mid \theta_{ij})$, where $p(x_k \mid \theta_{ij})$ is given by Eq. 4.2 for individual k in house j and bucket i. Given the joint posterior distribution, our estimates for individual fixed effects will then come from the marginal posterior distributions

$$p(\phi_\ell \mid y) = \int \cdots \int p(\theta, \phi, \psi \mid y)\, d\theta\, d\psi\, d\phi_1\, \cdots d\phi_{\ell-1}\, d\phi_{\ell+1} \cdots d\phi_{n_f}, \tag{E.3}$$

where n_f is the number of fixed effects.

E.2 Metropolis-Hastings

When it is impossible to calculate the posterior distribution directly, we can use a computational method known as Markov chain Monte Carlo (MCMC) to estimate it by drawing many samples

that eventually converge to the posterior distirbution (Tierney, 1994). One such technique is the Metropolis-Hastings algorithm (Metropolis et al., 1953; Hastings, 1970), which is the following (note that we use parenthetical superscript notation $\theta^{(t)}$ throughout to denote $\theta(t)$ for readability, not a power):

0. Choose initial parameter values $\theta^{(0)}$, set iteration counter $t = 0$, and choose chain length N.

1. Propose new values θ^* from a proposal probability distribution $q\big(\theta^* | \, \theta^{(t)}\big)$.

2. Evaluate $\alpha = \dfrac{p(\theta^* | \, y)\, q(\theta^{(t)} \, | \, \theta^*)}{p(\theta^{(t)} \, | \, y)\, q(\theta^* | \, \theta^{(t)})} = \dfrac{p(y \, | \, \theta^*)\, p(\theta^*)\, q(\theta^{(t)} \, | \, \theta^*)}{p(y \, | \, \theta^{(t)})\, p(\theta^{(t)})\, q(\theta^* | \, \theta^{(t)})}$ (from Eq. E.1, where the proportionality constant $p(y)$ cancels out in the ratio).

3. Draw a random number $u \sim \text{Uniform}(0, 1)$.

4. Set $\theta^{(t+1)} = \theta^*$ if $\alpha > u$. Otherwise, set $\theta^{(t+1)} = \theta^{(t)}$.

5. Iterate $t = t + 1$ and stop if $t = N$. Otherwise, repeat from step 1.

The autocorrelated random-walk $\theta^{(t)}$ will eventually converge to samples from the posterior distribution. Whether it does so efficiently is a more difficult question and depends on problem specifics such as the initial parameter values, chain length, and shapes of the proposal and target posterior distributions (Chib and Greenberg, 1995). Generally, the chains are run for an initial "burn-in" period to reduce dependence on the initial conditions. The chains are also run long enough after the burn-in period to reduce the effect of the autocorrelation between closely spaced points (Plummer et al., 2006). Finally, there is a tradeoff between accepting proposed values (climbing the posterior distribution) and rejecting proposed values (exploring parameter space), such that the ideal proportion of proposed values that are accepted is between 25% for high-dimensional systems and 45% for one-dimensional systems (Gelman et al., 1996).

A common choice for the proposal distribution $q(\theta^* \, | \, \theta^{(t)})$ is a normal distribution centered at $\theta^{(t)}$. Any symmetric distribution about $\theta^{(t)}$ simplifies the expression for α since $q(\theta^* \, | \, \theta^{(t)}) = q(\theta^{(t)} \, | \, \theta^*)$, causing these terms to cancel in the ratio. Then, the proposal variance can be

adjusted to obtain the desired acceptance ratio (Chib and Greenberg, 1995). However, specifying this variance for all parameters in high-dimensional problems can be difficult. Our model has 93 parameters in version 2, and 124 parameters in versions 1 and 3. We thus turn to another MCMC method, Gibbs sampling, to reduce the amount of tuning required.

E.3 Gibbs Sampling

Gibbs sampling was developed by Geman and Geman (1984) and Gelfand (1990), and samples from the posterior distribution by repeatedly sampling from and updating the full conditional distributions of the parameters. The full conditional distribution of a parameter is

$$p(\theta_i \,|\, \theta_1, \ldots, \theta_{i-1}, \theta_{i+1}, \ldots, \theta_p, y). \tag{E.4}$$

The algorithm is

0. Choose initial parameter values $\theta^{(0)}$, set iteration counter $t = 0$, and choose chain length N.

1. Sample $\theta_1^{(t+1)} \sim p(\theta_1 \,|\, \theta_2^{(t)}, \ldots, \theta_p^{(t)}, y)$

2. Sample $\theta_2^{(t+1)} \sim p(\theta_2 \,|\, \theta_1^{(t+1)}, \theta_3^{(t)}, \ldots, \theta_p^{(t)}, y)$

$\vdots$

p. Sample $\theta_p^{(t+1)} \sim p(\theta_p \,|\, \theta_1^{(t+1)}, \ldots, \theta_{p-1}^{(t+1)}, y)$

$p+1$. Iterate $t = t + 1$ and stop if $t = N$. Otherwise, repeat from step 1.

This method also converges to the posterior distribution and has the advantage of not requiring a proposal distribution, but it requires that all of the full conditionals can be derived, which is not always the case. Because we derived the likelihood (Eq. 4.2) from Markov transition probabilities rather than assume its form, we are unable to determine a conjugate prior for the

full model, i.e. a prior that when multiplied by the likelihood yields a posterior with the same distribution. This prevents us from being able to find the full conditionals for the full model. However, we can derive the full conditionals for a submodel, update the submodel parameters using Gibbs sampling, and then use Metropolis-Hastings to sample the remaining parameters. This greatly reduces the dimension of the required proposal distribution and aids in ensuring convergence to the posterior distribution.

Consider the posterior distribution of the full model

$$p(\log\theta, \phi, \psi \mid x) \propto p(x \mid \log\theta)\, p(\log\theta \mid \phi, \psi)\, p(\psi \mid \phi)\, p(\phi). \tag{E.5}$$

We are unable to determine the full conditionals for $\log\theta$ due to the complicated form of the likelihood function. We can, however, determine the full conditionals for the sub-model

$$p(\phi, \psi \mid \log\theta) \propto p(\log\theta \mid \phi, \psi)\, p(\psi \mid \phi)\, p(\phi), \tag{E.6}$$

which represents all but the first factor on the right-hand side of Eq. E.5, if we choose the following conjugate priors for $p(\phi)$:

$$\nu_i \sim \mathcal{N}(0, \sigma_\nu^2) \tag{E.7a}$$

$$\sigma_H^2 \sim \text{InvGamma}(a_H, b_H) \tag{E.7b}$$

$$\sigma_\varepsilon^2 \sim \text{InvGamma}(a_\varepsilon, b_\varepsilon). \tag{E.7c}$$

As an example, we go through the derivation of the full conditional $p(\nu_i \,|\cdot)$ in Eq. E.8.

$$
\begin{aligned}
p(\nu_i \,|\, \cdot) = p(\nu_i \,|\, \rho_{ij}, H, \sigma_\varepsilon^2) &\propto \Big(\prod_{j=1}^{n_H} p(\rho_{ij} \,|\, \nu_i, H_j, \sigma_\varepsilon^2) \Big)\, p(\nu_i) \\
&\propto \exp\left(-\frac{1}{2\sigma_\varepsilon^2} \sum_{j=1}^{n_H} \big(\rho_{ij} - (\nu_i + H_j)\big)^2 \right) \exp\left(-\frac{\nu_i^2}{2\sigma_\nu^2} \right) \\
&\propto \exp\left(-\left(\frac{n_H}{2\sigma_\varepsilon^2} + \frac{1}{2\sigma_\nu^2} \right) \nu_i^2 + \left(\frac{\sum_j (\rho_{ij} - H_j)}{\sigma_\varepsilon^2} \right) \nu_i \right) \\
&\propto \exp\left(-\left(\frac{n_H}{2\sigma_\varepsilon^2} + \frac{1}{2\sigma_\nu^2} \right) \left(\nu_i - \frac{\sum_j (\rho_{ij} - H_j)}{n_H + \sigma_\varepsilon^2/\sigma_\nu^2} \right)^2 \right) \\
&\implies \nu_i \,|\, \cdot \sim \mathcal{N}\left(\frac{\sum_j (\rho_{ij} - H_j)}{n_H + \sigma_\varepsilon^2/\sigma_\nu^2}, \left(\frac{n_H}{\sigma_\varepsilon^2} + \frac{1}{\sigma_\nu^2} \right)^{-1} \right), \qquad \text{(E.8a)}
\end{aligned}
$$

where n_H is the number of houses in the experiment. All of the full conditionals for the submodel are listed in Eq. E.9, where n_B is the number of buckets in each house and $n_T = n_H n_B$ is the total number of buckets in the experiment. Note that the i-summations go from 1 to n_B and the j-summations go from 1 to n_H.

$$
\begin{aligned}
\nu_i \,|\, \cdot &\sim \mathcal{N}\left(\frac{\sum_j (\rho_{ij} - H_j)}{n_H + \sigma_\varepsilon^2/\sigma_\nu^2},\ \left(\frac{n_H}{\sigma_\varepsilon^2} + \frac{1}{\sigma_\nu^2} \right)^{-1} \right) && \text{(E.9a)} \\
H_j \,|\, \cdot &\sim \mathcal{N}\left(\frac{\sum_i (\rho_{ij} - \nu_i)}{n_B + \sigma_\varepsilon^2/\sigma_H^2},\ \left(\frac{n_B}{\sigma_\varepsilon^2} + \frac{1}{\sigma_H^2} \right)^{-1} \right) && \text{(E.9b)} \\
\sigma_H^2 \,|\, \cdot &\sim \text{InvGamma}\left(\frac{n_H}{2} + a_H,\ \frac{\sum_j H_j^2}{2} + b_H \right) && \text{(E.9c)} \\
\sigma_\varepsilon^2 \,|\, \cdot &\sim \text{InvGamma}\left(\frac{n_T}{2} + a_\varepsilon,\ \frac{1}{2}\sum_j \sum_i (\rho_{ij} - \nu_i - H_j)^2 + b_\varepsilon \right) && \text{(E.9d)}
\end{aligned}
$$

Once we sample from the full conditionals of the submodel, we can find the posterior density (relative to the normalizing constant) of the sampled ϕ and ψ (Eq. E.6), multiply by

our likelihood $p(x \mid \log\theta)$ to estimate the posterior of the full model, and update $\log\theta$ using Metropolis-Hastings. We summarize our algorithm, which incorporates both Gibbs sampling and Metropolis-Hastings, below:

0. Choose initial parameter values $\theta^{(0)}$, set iteration counter $t = 0$, choose proposal variances for log-rates $\sigma^2_{\log\theta}$, and choose chain length N.
1. Sample $\nu_1^{(t+1)} \sim p(\nu_1 \mid \nu_2^{(t)}, H_1^{(t)}, \ldots, \sigma_H^{2(t)}, \sigma_\varepsilon^{2(t)}, \log(\theta)^{(t)})$
2. Sample $\nu_2^{(t+1)} \sim p(\nu_2 \mid \nu_1^{(t+1)}, H_1^{(t)} \ldots, \sigma_H^{2(t)}, \sigma_\varepsilon^{2(t)}, \log(\theta)^{(t)})$

$\vdots$

13. Sample $\sigma_\varepsilon^{2(t+1)} \sim p(\sigma_\varepsilon^2 \mid \nu_1^{(t+1)}, \nu_2^{(t+1)}, \ldots, H_9^{(t+1)}\sigma_H^{2(t+1)}, \log(\theta)^{(t)})$
14. Define $\beta\big(\log(\theta)\big) \equiv p(x \mid \theta) + \log\Big(p\big(\log(\theta) \mid \psi^{(t+1)}\big)\, p(\psi^{(t+1)} \mid \phi^{(t+1)})\, p(\phi^{(t+1)})\Big)$
15. Propose new values $\log(\theta)^* \sim \mathcal{N}\big(\log(\theta)^{(t)}, \sigma^2_{\log\theta}\big)$
16. Evaluate $\alpha = \exp\Big(\beta\big(\log(\theta)^*\big) - \beta\big(\log(\theta)^{(t)}\big)\Big)$
17. Draw a random number $u \sim \text{Uniform}(0, 1)$.
18. Set $\log(\theta)^{(t+1)} = \theta^*$ if $\alpha > u$. Otherwise, set $\log(\theta)^{(t+1)} = \log(\theta)^{(t)}$.
19. Iterate $t = t + 1$ and stop if $t = N$. Otherwise, repeat from step 1.

Appendix F

Transgenic Pests and Human Health: A Short Overview of Social, Cultural, and Scientific Considerations[1]

Tim Antonelli, Amanda Clayton, Molly Hartzog, Sophia Webster, Gabriel Zilnik[2]

1. This chapter is published in the book *Genetic Control of Malaria and Dengue*: Antonelli, T., Clayton, A., Hartzog, M., Webster, S. & G. Zilnik, 2015. Transgenic Pests and Human Health: A Short Overview of Social, Cultural, and Scientific Considerations. Pp. 1–30, *in* Z. N. Adleman, ed. Genetic Control of Malaria and Dengue. Elsevier.

2. All authors contributed equally to this work.

F.1 Introduction

The global problems of dengue fever and malaria are multi-faceted, complex issues that span many disciplines, including human health, ecology, economics and urban development, health and environmental policy, social work, and risk analysis. Effective disease control and prevention therefore requires integrated research from all of these disciplines in order to understand the problem from as many angles as possible and within its social and cultural contexts. This type of interdisciplinary approach that integrates perspectives from the natural sciences, social sciences, and humanities was recently endorsed by the American Academy of Arts and Sciences as critical for developing effective solutions for the world's problems.[1] Adopting this approach, we introduce the ethical, regulatory, social, and economic aspects of control programs for dengue fever and malaria, relating to both currently used control techniques as well as the emerging technologies involving genetically modified organisms (GMOs).

The goal of this chapter is not to offer a definitive stance on whether or not GM technologies should be used to control mosquito-borne diseases, but rather to offer a cursory look at the complex issues that span multiple disciplines, governmental and non-governmental organizations, and community interests. In conclusion, we argue that a discussion of whether or not to implement GM technologies should be conducted within the larger discussion of national, regional, and global disease control strategies. These control plans should consider an integration of multiple control strategies and adapt to suit differing social and cultural contexts based on the area under consideration.

F.2 Current State of GMOs

In 1996 agriculture experienced a genetic revolution. Before the planting season, the United States Environmental Protection Agency (EPA) had approved the commercial sale of what would become the most widespread transgenic cultivars. Recombinant DNA technology has revolutionized biological sciences with practical impacts in fields ranging from medicine to

agriculture.[2] New crops and modified organisms would soon come to be known as genetically modified organisms (GMOs). Crops carried genes from bacteria conferring resistance to Roundup^{TM} (glyphosate) weed killer and to certain insect species. Bacteria were engineered to produce human insulin. With regard to pest management the impact of transgenics remains acutely felt in agriculture. Entire agricultural systems were constructed around new transgenic cultivars; new industries were born, while old ones failed. Land Grant institutions around the country helped research the impacts of these new varieties. Fields from the applied life sciences produced thousands of articles in biochemistry, molecular biology, conservation biology, ecology, evolution, plant science, weed science, environmental resource management and many more regarding the efficacy and safety of transgenic cultivars.[3] Yet, this technology has its detractors. Many groups such as Union of Concerned Scientists and Gene Watch point to issues with regulatory systems in assessing safety or environmental concerns related to transgenic organisms.

Controlling pests with transgenic technology is predominantly accomplished with δ-endotoxins (Cry toxins) from strains of *Bacillus thuringiensis*. Commonly known as Bt crops, the plants have a host of attractive features. Most notable is the narrow spectrum of pests that each Cry toxin affects. At the time of this writing, varieties of Bt crops primarily target lepidopteran, dipteran, and coleopteran pests. Furthermore, a single gene encodes each Cry toxin making the combination of toxins, known as stacking, relatively straightforward.[4] Growers have found these crops extremely useful; in 2014, transgenic Bt crops constituted 84% of cotton and 80% of corn grown in the United States.[5] Developing countries such as India, China, South Africa, Brazil, and Argentina have seen explosive growth in transgenic crop adoption. Those five countries accounted for nearly 50% of transgenic crops (including herbicide tolerant cultivars) grown worldwide in 2011.[6] However, these crops are not without their drawbacks. While the primary pests of these crops have been controlled, a surge of secondary piercing-sucking pests such as stink bugs and aphids has become a problem in some regions of the world.[7] Consequently, the increase in insecticide use to control secondary pests may offset the decreased insecticide

applications for the primary pests now controlled by Bt. Thus, detailed knowledge of the pest assemblage is useful when approaching transgenic control through direct modification. Similarly, in thinking about genetically-modified mosquitoes to combat dengue and malaria, detailed knowledge of the transmission cycle and host assemblage is required to know how the system might respond to genetic control of a single species.

While transgenic crops are widespread in much of North America and Asia, this is not necessarily the case around much of the globe. For example, many nations in Europe restrict transgenic cultivars and in some cases have even seen a decline in field trials of these cultivars.[6] Concern over the safety of these crops remains intense, but as it stands now, no credible scientific evidence has been presented demonstrating adverse effects associated with consumption of transgenic crops.[8] However, the moral and ethical arguments against transgenic crops seem to have the most traction and these arguments are more difficult to resolve with scientific data alone. Below we discuss some of the ethical implications surrounding transgenic insects, which are derived from literature surrounding transgenic cultivars.

F.3 Dengue Fever and Malaria

The WHO provides fact sheets (available online) on both dengue and malaria that are straightforward and highly informative. Here we provide a summary and comparison of the two diseases focusing on their global prevalence, symptom severity, and vector characteristics. We also discuss briefly the availability and efficacy of existing treatment and prevention methods for both diseases. Table F.1 displays a summary of the key facts for both diseases discussed below.

F.3.1 Dengue Fever

Dengue is caused by at least four independent viruses that are all transmitted primarily by the mosquito *Aedes aegypti*. The most typical form of the disease is commonly called dengue fever and its symptoms include fever, rash, headache, and joint and retro-orbital pain. The severe form of the disease, called severe dengue or dengue hemorrhagic fever (DHF), can result in

Table F.1: Key facts about dengue and malaria[9–11]

	Dengue	**Malaria**
Vector	*Aedes aegypti, Aedes albopictus* (secondary)	about 20 species from the *Anopheles* genus
Strains	4 virus serotypes from the *Flavivirus* genus	4 parasite species from the *Plasmodium* genus
Severity	contracting a second serotype results in a higher likelihood of experiencing severe dengue	prevalence and severity varies with parasite (*Plasmodium falciparum* is the most common and deadly)
Immunity	contracting one serotype provides permanent immunity to that strain and temporary immunity to the others	partial immunity is accumulated over time and provides protection against severe disease
Diagnosis	ELISA tests for antigens (IgM & IgG), PCR	rapid diagnostic tests for antigens, microscopy, PCR
Symptoms	**Classic**: fever, rash, headache, muscle aches, retro-orbital pain, vomiting **Severe**: internal hemorrhaging, severe abdominal pain and vomiting, respiratory distress	**Classic**: fever, headache, chills, vomiting **Severe**: anemia, respiratory distress, cerebral malaria, organ failure
Mortality	without treatment: about 20% mortality rate with treatment: less than 1% mortality rate	about 584,000 deaths in 2013 90% of deaths were from Africa, mostly among children
Global Burden	WHO[9]: 50-100 million cases per year Bhatt et al.[12]: about 390 million cases per year, including asymptomatic	WHO[10]: about 200 million cases in 2013
Risk Groups	children, elderly, immuno-compromized	children, elderly, immuno-compromized; tourists & immigrants
Vaccines	In development but not yet available	In development but not yet available
Treatment	**Classic**: fluids, pain medication, rest **Severe**: fluid replacement therapy, blood transfusion	antimalarial medications (parasite resistance is a continuing issue)
Common Vector Control	container control, indoor residual spraying (IRS) of insecticides, larvicide packets in collected water	long-lasting insecticide-treated nets (LLINs), indoor residual spraying (IRS) of insecticides

vomiting, internal hemorrhaging and even death.[13]

The WHO estimates that there are 50-100 million dengue infections each year, mostly in tropical regions, though a more recent estimate is nearer to 400 million due to the large number of asymptomatic and unreported cases.[12] Despite its high incidence, dengue fever is one of seventeen diseases classified as a neglected tropical disease (NTD).[14] In terms of human health impact, NTDs are often compared to the big three: malaria, HIV/AIDS, and tuberculosis, which receive significantly more attention in funding, research, and social welfare projects than the seventeen NTDs. The disproportionate attention is partly a result of the big three being outlined specifically in the Millennium Development Goals, where NTDs are included only in the other diseases category. However, while NTDs typically carry a low mortality rate, they are both promoted by and promote poverty, are highly debilitative, and disproportionately impact women and children. Perhaps most importantly, NTDs can increase the severity and prevalence of the big three through co-infection and co-endemicity.[15,16] As a result, Hotez et al. encourage the development of a global plan for the big three that includes control of seventeen NTDs as a powerful tool in the process.[17]

F.3.2 Malaria

Malaria is a parasitic disease spread by about 20 different species of Anopheles mosquitoes in tropical and subtropical climates throughout the world. According to the WHO, malaria is more prevalent in areas with species of Anopheles that have longer lifespans or that have breeding habits leading to increased mosquito populations.[10] Because malaria is spread by so many species of mosquitoes, the direct suppression of the mosquito populations responsible for transmission is complicated. However, because all Anopheles species bite at night, one of the simplest and most effective forms of malaria prevention is to use long-lasting insecticide-treated bed nets (LLINs) to keep humans from being bitten while sleeping.

Symptoms of malaria include fever, headache, chills, and vomiting. Severe complications can involve anemia, respiratory distress, and cerebral malaria in children and other forms of organ

failure in adults. However, as with dengue, severe and fatal complications from malaria are generally avoidable via effective vector control practices and fast access to medical treatment.[11] Antimalarial medications are able to both treat and prevent malaria but parasitic resistance to medications is an ongoing issue.[10] Recent WHO estimates indicate that there were about 200 million cases of malaria in 2013, about 584,000 of which resulted in death.[10] Over 90% of these deaths occurred in Africa, mostly among children where, according to the WHO, "a child dies every minute from malaria."[10] Although the death toll of malaria is still high globally and especially among children in Africa, the occurrence of malaria cases and deaths has decreased by around 50% since 2000.[10]

F.3.3 Dengue and Malaria Control

Currently, the most commonly used techniques for dengue control include chemical control in the form of either larvicide in water sources, or adulticide applied via indoor residual spraying (IRS) or aspiration packs; and cultural control in the form of recruiting communities to empty containers of standing water that may serve as larval rearing sites. For malaria, cultural control in the form of using LLINs during sleep is the most common form of vector control. This form of control is highly effective for malaria prevention, but does not successfully prevent dengue fever because *Ae. aegypti* bite during the day. The other main form of malaria vector control is the implementation of IRS to reduce adult Anopheles populations. Antimalarial medications can also be taken preemptively to prevent malaria transmission and their use is recommended by the WHO for travelers, pregnant women, and children under 5 years old in high transmission areas.[10]

Emerging techniques to control both diseases using GMOs can be broadly categorized as either population suppression, which seek to reduce the numbers of mosquitoes, or population replacement, which seeks to replace the disease-carrying population with a transgenic strain incapable of transmitting disease (for a more detailed description of these strategies, see Chapter 1 of WHO/TDR, 2014).[18] GMO technology is controversial, however, especially in the United

States and Europe, where a heated debate continues surrounding genetically modified foods.

F.4 Things to consider before implementing GMO control methods

Table F.2 lists key issues to consider before implementing GMO control methods. In the following sections, we focus primarily on the simpler system of dengue transmission and control. While malaria is a more complex system, the points we raise should still apply to using GMO methods for the prevention of malaria. Issues of regulation, public opinion, and ethics pertaining to the use of GMOs as a control technique are likely similar for both diseases, as these issues relate more to the emerging technologies of genetic modification rather than to the specific diseases to which these technologies are applied.

Table F.2: Considerations for potential use of GM technologies for disease control

- Economic burden of dengue or malaria in the area under consideration
- Burden on quality of life
- Burden on healthcare system in time of epidemic
- Local community's perception of disease risk
- Local community's willingness to participate in cultural control
- Local community's values and belief systems regarding environmental protection and care
- Efficacy and public acceptance of currently used control measures, locally and in neighboring areas
- Financial cost, quality of life cost, and ethical cost of candidate technologies for mosquito control
- Benefits of disease prevention over disease treatment in the area under consideration
- Other culturally-specific considerations in the area under consideration

F.4.1 Allocating Resources between Treatment and Control

It is important to prioritize treatment strategies to mitigate severe health problems resulting from disease transmission. General improvements to healthcare infrastructures along with other forms of economic development would likely decrease instances of malaria and dengue as well as many other communicable diseases. For any control methods implemented to reduce transmission of dengue or malaria, it is important that local communities are consulted and actively engaged in policy decisions and implementation.

Dengue treatment is usually simple and highly effective at reducing death rates if infected individuals are able to obtain timely access to necessary treatment facilities.[9] However, researchers and policymakers working with the virus note that healthcare infrastructures in low and middle income countries are often incapable of handling the influx of cases that occurs during an epidemic.[9,19] The response to this problem seems to have often been to push for increased dengue prevention rather than to try and tackle healthcare infrastructure issues directly.[20] Although the control and prevention of dengue is vital to reducing the negative impacts of the virus in the long run, it is important that researchers and policymakers not overlook the immediate importance of ensuring individual access to dengue treatment.

The WHO handbook on dengue management states that "emergency preparedness and response are often overlooked by programme managers and policy-makers," and that "while plans have frequently been prepared in dengue-endemic countries, they are seldom validated."[21 (pp 123–124)] However, this problem could be due to a lack of resources rather than a lack of diligence. Because each area will typically only experience an epidemic every few years, it may be difficult to maintain the resources needed to treat high case loads of dengue. We suggest that mobile dengue response units be formed at the international level with neighboring countries pooling resources to maintain effective response teams. This is an area in which NGOs like the Red Cross, NIH, or WHO could step in to provide the necessary resources and expertise to be able to respond to the needs of a larger area.

The effective treatment of dengue will not eliminate disease incidence or transmission. Pre-

vention of the disease will still only be possible through preemptive vector control practices or the development of an effective vaccine. However, the effective control and prevention of dengue is likely to take an extensive amount of time and resources. In the interim, steps should be taken as quickly as possible to ensure that all areas are capable of treating cases of dengue and severe dengue in order to reduce serious health complications and fatalities to the lowest possible levels. There is no justification for accepting high death rates from dengue while long-term solutions are being developed when short-term treatment solutions are currently available for implementation.

F.4.2 Economic Development

Although the risk of dengue transmission is present and possibly increasing in parts of Europe and the US due to increased global temperatures and the presence of *Aedes* mosquitoes in these regions, the vast majority of countries at the highest risk levels are low- to middle-income countries. While this is likely to be in part due to the fact that many low- and middle-income countries are located in tropical and subtropical climate regions, there are several infrastructural factors that are likely to contribute to a nations level of dengue risk as well. Improving upon these infrastructural issues would likely not only reduce incidences of dengue but would also have other health benefits for the individuals in the affected areas.

Because *Ae. aegypti* breed in open water containers, one of the main infrastructural obstacles to preventing the spread of dengue lies in poor water and sewage availability. According to the WHO, "Dengue afflicts all levels of society but the burden may be higher among the poorest who grow up in communities with inadequate water supply and solid waste infrastructure, and where conditions are most favourable for multiplication of the main vector, *Ae. aegypti*,".[21] This is because areas without reliable waste disposal or piped water tend to have issues with water drainage and/or are forced to collect water in open containers for household use. These open pools of water then act as viable oviposition sites for the *Ae. aegypti* mosquito.[22] Improving waste disposal and piped water availability would also lead to many health benefits for affected

communities that spread far beyond reduced incidences of dengue fever, such as a reduction in hookworm and gastrointestinal diseases which are also prevalent in areas most affected by dengue.[23]

As noted above, *Ae. aegypti* bite during the day, which makes bed nets an ineffective control method against the mosquitoes. Infrastructural improvements to household construction, particularly regarding the availability of screened windows, air conditioning, and enclosed walls and roofs, would therefore further reduce dengue risk by preventing *Ae. aegypti* from entering households and biting inhabitants during the day.[22,24] Such household improvements are costly however and would necessitate either higher household incomes or subsidization by outside sources like governmental or non-governmental organizations.

Making permanent improvements to the healthcare infrastructures in dengue endemic countries would increase the ability of these countries to handle epidemics and minimize severe disease complications and deaths. These infrastructural improvements would also have health benefits extending outside of dengue outcomes by increasing the ability of healthcare infrastructures to treat a wide range of diseases requiring intravenous fluid replacement therapies or other simple medical interventions.[25] Improving transportation infrastructures by building roads and increasing the availability of affordable public transportation would further increase the accessibility of healthcare facilities, thereby reaching a wider spectrum of individuals in need of treatment.

There is ample research linking health outcomes to educational and other economic outcomes.[26–28] Limited healthcare access due to low income levels leads to worsened health outcomes which can keep individuals from obtaining a formal education or from working, thus leading to even lower incomes. A poverty trap is thus formed wherein low incomes lead to poor health outcomes which contribute to even lower incomes.[27] However, infrastructural improvements and other development programs that increase the access of low income individuals to healthcare have the potential to stop or even reverse the cycle of these poverty traps since healthier individuals are more likely to be able to obtain a formal education and/or to partici-

pate in the labor market.[26,28]

F.4.3 Community Engagement

Community engagement for dengue control emerged in the 1980s as a new attempt at sustainable control for the mosquito vector *Ae. aegypti*. It is envisioned as a bottom-up control strategy, one that is carried out by citizens of the community and guided by local leaders rather than government officials. However, especially in the initial stages, collaboration between the government and local leaders is an integral part of community engagement. This strategy is in contrast to a top-down approach, that is, a program run entirely by the government and health officials without input from or expectations of the local community. In some cases attempts at community engagement end up looking very similar to the traditional government-run control, especially once funding for a trial program has ceased. If implemented correctly, the sense of leadership and ownership in resources and ideas should make a community more responsive and engaged in addressing the dengue problem even after outside support is withdrawn.[29]

Community engagement for control of *Anopheles* mosquitoes, which transmit malaria, uses some similar and some different techniques for the mosquitos different behaviors and feeding habits. Rather than focusing on emptying containers with standing water in and around homes, as is done for *Ae. aegypti*, community engagement focuses on distributing and educating about bed nets. Both mosquitoes may be controlled through insecticidal spraying of homes however, especially when it is carried out properly by the household and by the vector control employees.

In the 1980s the World Health Organization (WHO) put funding into community engagement trial programs and initially gave funding to Thailand to conduct trials using the new strategy. However, these initial programs were not very successful because they did not involve true community engagement. The program was government directed, still maintained as top-down control, and participating citizens were simply told what to do, so when the support was withdrawn the community programs fell apart.[29]

The trials in the 1980s taught important lessons: community engagement programs will not

be sustainable unless there are continued economic incentives and the programs will not receive funding from the limited government health dollars once they have been successful. However, even with continued programmatic incentives and government funding, there are still other factors that underscore the success of a community-based program. If the economic incentives disappear after the external funding ends, the incentive of improved health and fewer cases of dengue should continue to motivate community participation in control programs but it may not be enough, especially during times when dengue is absent from an area and other health concerns take precedence.

While community based programs are intended to ultimately give control to members of the community, relying solely on the community presents problems itself. Even when incentives are present, members of the community must be convinced that removing larval habitats is in their best interests and that controlling *Ae. aegypti* is a priority. Some reinforcement and involvement from the government must always be maintained to ensure that the community is educated and continuing to implement the control measures. The shift from governmental control to local control will take time because the community may see the task as one for which the government is responsible.[29]

Since the 1980s, community based programs to control dengue have been implemented in many areas around the world. Some of these programs have been successful and sustained over periods of years after funding has ceased, while others continue to look like the initial trials in Thailand where the programs deteriorate after funding and other incentives are removed. Today, some of the most successful community based programs are present in Cuba, where local Cubans appear to have truly embraced the cause and believe in suppressing dengue through educating community members, removing larval habitats, and going door to door during epidemic periods to check for symptoms of dengue. In 1981, the first and largest DHF epidemic presented itself in the Americas. In response, the Cuban government trained and mobilized over 15,000 workers to go house to house educating citizens about dengue and mosquito vector control, in addition to extensive pesticide application.[30]

Initially, the 1980s success of Cuban programs depended on top-down control with enforcement through anti-mosquito breeding laws. People were educated on how to prevent mosquitoes from breeding in and around their homes and were fined by inspectors who were sent to frequently check individual households and enforce the laws.[29] Today, numerous studies suggest that the top-down control is no longer needed even when outside incentives are not present. For example, a 2007 study conducted in Santiago de Cuba focused on the sustainability of a community-based approach for two years after external funding was withdrawn.[31] The sustainability was evaluated through direct observation, questionnaires, group interviews, and routine entomological surveys using the Breteau and entomological house indices. Two years after the external support was removed, people living in neighborhoods who had received the intervention continued to correctly apply larvicides and store water properly; as a result, larval indices continued to decline. Comparatively, larval and house indices of people living in the control area, who had not received community engagement support and education, increased.[31] This study provides evidence that the community-based approaches in Cuba are sustainable and effective at reducing *Ae. aegypti*.

Thailand still heavily maintains governmentally run, top-down control programs for reducing and eliminating *Ae. aegypti*. Although successful, this type of continued government intervention is more expensive than the approaches in Cuba in which, over time, the external support is removed and the community takes over responsibilities the government had previously assumed.

A study in Taiwan, where dengue cases have been limited, examined the impacts and stress that volunteers in community health experience and suggests that the volunteers experience a lack of support in the role they are expected to fulfill, as well as a lack of proper education and work overload.[32–33] These types of concerns and considerations are important for community engagement as the volunteers are expected to dedicate time to extra duties outside of their everyday jobs and families needs. Although the participants in this study are volunteers, in other community based programs the people do not necessarily volunteer to participate, especially during trial periods where governmental or outside support is maintaining that the

community follows through with the tasks requested of them. A careful balance between giving the community too much responsibility versus not giving enough is difficult to achieve and what a successful program looks like will differ dramatically between countries and even local areas. New techniques, such as the use of transgenic mosquitoes to control vector populations, may help to reduce the burden of community health volunteers. However, before release, it is important to gather the input from public opinion studies in the communities using community engagement to understand the attitudes, concerns, and ideas that people have surrounding transgenic insect releases.[34]

Considering the current programs that use traditional non-transgenic approaches, a good community engagement strategy is one that (1) is sustainable over decades and evolves to meet the rising number of dengue cases each year, (2) empowers citizen to be involved, but does not place too much responsibility on the community so that engagement disappears after incentives or lawful actions are no longer there, and (3) is widely accepted and does not involve forcing a community to be a part of a control program that goes against its beliefs and values.

If transgenic mosquitoes are released to suppress dengue, the programs are likely to change in terms of the levels of involvement required from the government and community. First, the removal and monitoring of larval habitats by private homeowners would still be useful in reducing cases, but if released mosquitoes are able to suppress wild populations to non-transmissible levels, likely less monitoring would be required. Secondly, the amount of insecticidal spraying inside and outside of homes would be reduced. This would reduce the need for homeowners to vacate during spraying as well as reduce the risk of chemical exposure. Thirdly, engagement would be more frontloaded in the sense that government and community collaboration would take place before the transgenic mosquitoes are released. GMO educational events and gathering public opinion would be essential to gain a sense of the public acceptance or denial of the GMO technology. After this, the next step would be to understand the reasons why people accept or deny transgenic mosquitoes as a method to suppress dengue. All of this collaboration would be done before the release of mosquitoes, and hence most of the community engagement

would be done before the program actually begins and with less community involvement needed after implementation. This is in contrast to the current programs in which community participation is oftentimes required and even increases overtime as governments or outside sources pull funding.

Box 1: Community Engagement

Community engagement, involvement, and development to reduce mosquito borne diseases all refer to the concept of giving a community leadership and ownership of ideas and resources after education and collaboration from the government. Community engagement (bottom-up/horizontal control) is intended to be a sustainable method that is less costly and more effective at reducing dengue than programs run solely by the government (top-down control).

Ideally, the initial steps of community engagement involve governmental vector control employees educating and collaborating with local communities and then slowly the community takes over responsibility for some of the tasks the government once performed. More than this, the strategy is ideally sustainable because the communities have a desire to reduce the mosquitoes and believe in the methods they have been taught. Sustainability is key to the strategy because the initial money the government or outside source of funding had will eventually be used up and the initial incentives to perform the tasks may no longer be present. Thus, the success of trials for community engagement are difficult to assess unless long term studies are carried out years after the funding and incentives are removed.

To date, the most successful community engagement programs appear to be in Cuba, where Cubans have embraced the techniques needed to suppress dengue such as removing larval habitats, going door to door to check for dengue symptoms, and educating other citizens about suppression and control techniques.

F.4.4 Values and Ethics of Control Measures

Here we offer an "informed laypersons" ethical framework for considering the release of genetically modified mosquitoes. Entire careers and numerous volumes have been dedicated to the study of bioethics. We hope this will serve, at the very least, as a spark for further exploration of relevant ethical and social concepts and issues surrounding the use of transgenic mosquitoes for public health. The principles we believe to be most pertinent to the discussion are outlined with some hypothetical examples drawn from literature and adapted to the modification of pest species. Table F.3 offers a brief overview of the principles discussed, namely: stewardship, animal welfare, justice as fairness, and precaution.

Stewardship

The stewardship principle states that humans are entrusted to care for and promote the good quality of air, water, soil, ecosystems, biodiversity, and the earth as a whole.[35] Illustrating this role, Resnik states a steward is like a property manager and "should ensure that the property is not damaged and should make improvements on the property."[35] This includes, first and foremost, the residents of the property. Field trials for transgenic insects intended to control disease should be conducted in an area where the disease is a recognized public health concern. Mechanisms should be put in place to protect these residents and especially those who are affected by the disease during the field trial. This protection would include informing the community about the trials and providing free healthcare for the targeted disease. These mechanisms would help to ensure that the benefits significantly outweigh the risks to the community and to the residents environment.[36] All life depends on environmental resources for survival; thus stewardship argues it is no longer defensible to solely consider the natural resource needs of humans. The principle of stewardship moves the ethical discussion toward a biocentric view that nature has its own moral worth.[35,37] Control measures that may conflict with the notions of stewardship include chemical pesticides, environmental management, and transgenic technology.

Table F.3: Brief outline of ethical principles

Principle	**Short Definition**	**Potential Questions to Address**
Stewardship	The environment must be cared for in such a way as to provide natural resources for future generations.	What could the future environmental impact look like? How would this technology change the impact of controlling this pest?
Animal Welfare	Animals have rights in so much that "because it is an animal" is not an acceptable justification for actions taken against them.	Is genetic modification of this species necessary? Does genetic modification unreasonably or unnecessarily interfere with biological drivers of this species?
Justice as Fairness	A fair decision is one in which maximizes liberty for all and the distribution of effects follows that the least advantaged individuals in a society will receive the greatest benefits.	Who benefits from this technology and who bears the associated risks? How are benefits and risks divided among those directly involved with the technology? Is the distribution of risks and benefits fair (as defined by Rawls)?
Precaution	With the acknowledgement that zero risk is an impossible standard, reasonable risks to the environment, health, and safety of participants must be considered prior to initiating a control program.	What are the plausible environmental, health, and safety risks of this technology? Would further research significantly alter the impact or reduce the probability of adverse effects?

Long-term damage to natural resources has occurred from short- and long-term applications of chemical insecticides such as DDT to control disease vectors.[35,38] In the years immediately following World War II, unrestricted pesticide use posed dangers to nature and humans which drew increasing public and academic attention.[38–40] Given the preponderance of evidence demonstrating the damage unrestricted pesticide use can cause to the environment, one would be hard-pressed to find environmental scientists that would endorse such use. Still, one can strongly argue for judicious application of pesticides if they are used to promote a universally recognized goal of high priority, such as human health.[35]

Animal Welfare

Animal biotechnology has often been considered in the light of the modification of vertebrates. Ethicists have developed a number of ethical theories that allowed for the modification of animals under certain conditions.[41,42] Discourse centered predominantly on domesticated animals, their ecological relationships with the natural environment, and their relationships to humans. Mosquitoes, and invertebrates in general, present a new and challenging test for these ethical theories developed in response to the potential of transgenic farm animals.

How should animals be treated? Do humans have "dominion" over life, the right to do as we please? Modern arguments that humans do have to make ethical decisions in treating animals arise from Peter Singers 1975 utilitarian treatise *Animal Liberation*. Can a dog, cow, or fish suffer? If yes, then in the interest of maximizing happiness, humans are obligated not to inflict upon them any unnecessary suffering.[43] Animals deserve our respect, but how much respect they deserve is still debated.

Finding strict utility insufficient, other authors have attempted to formulate a more deontological—or constrained—view of how we should treat animals. For instance, some have argued that all sentient animals possess intrinsic value, with sentience being defined as the ability to feel.[41,44] By Intrinsic value we mean an animal has value aside from any use or aesthetic value humans derive from it. We should treat animals as if what we do to them matters to them.

Violating an animals intrinsic value is permissible only if a serious animal or human interest (life or death) is threatened and no alternative measures are available.[44]

Yet another concept is *telos*, a creature's "end" or "purpose." Aristotle defined *telos* as the full, flourishing development of existence. In application to mosquitoes, it would constitute the nature of the mosquito or, more abstractly, the "mosquitoness" of the mosquito. Animals have needs and interests, and those needs and interests that matter most are inviolable.[41] For instance, it would be wrong to isolate a social animal from social interactions. Contrast this with the previous statement: we should treat animals well because what we do to them matters to them. Can *telos* be changed? Should humans manipulate an animal's *telos*? Let us examine a thought experiment we modified from Michael Hauskeller:[45 (p 59)]

> *Scientists genetically design a human. This person lacks the possibility to live a fully human life. Traits have been knocked out so that they cannot use their hands the way humans do, their nose the way humans do, their eyes the way humans do, and so on. Simultaneously, the desire to live a fully "human" existence is removed so they would not know that anything is missing from their existence.*

Is this morally acceptable? Have the scientists caused this person harm? After all, this person does not know or care that these things have been done to them. Yet, "We could still deplore their state and say that harm has been done to them, because we perceive the gap between what they now are and what they are meant to be," says Hauskeller.[45 (p 59)] Alternatively, if we would not do this to a human, is it permissible to do this to an animal?

Critics are particularly suspicious of the extensions beyond utilitarian arguments for animal welfare. For instance, if animals have intrinsic value, then what of bacteria, viruses, and other pathogens?[35] If yes, then is it wrong to eradicate tuberculosis, HIV, or dengue? We find this to be an interesting, but fundamentally frail argument. Examination of potential consequences inhabits any ethical discussions, but because a principle may be uncomfortable or have negative outcomes for humanity is not a reason for rejection. Even if pathogens had intrinsic value, eradication could be justifiable because of the level of morbidity and mortality caused by pathogens.

In other words, eradication of pathogens is justified despite their intrinsic value. In practical application, conflicts will arise between competing ethical principles. Resolving those conflicts reasonably and fairly is part and parcel in deciding what actions to take.

Justice as Fairness

How does one decide what is just or fair with regards to dengue and malaria control? Aristotle outlined the formal definition of justice: equals should treat each other as equals.[46] We adopted Rawls' concept of justice as fairness, which outlines two principles: (i) equal liberties for all, and (ii) the difference principle.[46] Under the first, everyone in a society would be entitled to maximum liberty insofar as everyone had equal liberty. The difference principle ensures people have equality of opportunities, but restricts social and economic inequalities to ones that benefit the least advantaged members of society. Justice as fairness does not only apply to individuals, but it is equally applicable to organizations. Rawls[46 (p 3)] wrote, "A theory however elegant and economical must be rejected or revised if it is untrue; likewise laws and institutions no matter how efficient or well-arranged must be reformed or abolished if they are unjust."

Two areas of justice concern control programs. Procedural justice regards the process of making fair societal decisions, and distributive justice seeks a fair distribution of risks and benefits. How we determine the process of making fair decisions includes several underlying principles such as public participation in decisions that affect them, transparency in public decisions, and that people have equal protection under the law. Legal and political systems are responsible for carrying out procedural justice.[46] Determining how risks and benefits are distributed is a complex issue with social and cultural considerations. One way to make that determination is to use "veil of ignorance" thought experiment.[46] Under the veil, members of a group would negotiate the distribution of risks and benefits in a society not knowing what the negotiators socioeconomic position in the society would be. Rawls argues this would provide a powerful incentive to formulate an equitable distribution of risks and benefits. For example, one would most likely not place a majority of the risk from insecticide exposure on individuals

without access to healthcare because, after the negotiation, they might occupy that place in society.

This has straightforward applications to the control of mosquitoes and vector-borne disease. How should communities and nations organize their infrastructure to treat those affected by dengue or malaria? Access to healthcare options needs to be universally promoted. New control strategies need to balance risks and benefits equitably among society. Those that have the least ability to mitigate suffering from disease should receive the greatest benefit from control. Communities have a right to make informed public decisions on control strategies that directly impact their interests.

Precaution

How should a society weigh the risks and benefits of a control measure? Science can only give estimates of probabilities of what may occur based on the best evidence available at the time. This is because science works not by proving hypotheses, but by rejecting alternative hypotheses.[47] It arrives at explanations of natural processes through narrowing down probable outcomes until only one or a handful remain. This means that the scientific method does not have the capability to precisely predict what will happen in the future only the likelihood of what could happen. Still, when weighing the risks of control strategies, the worst advice is to "be careful".[48] This also happens to be a mischaracterization of the precautionary principle.

There lies some difficulty in defining the precautionary principle due to the often vague language used in official documents.[49–51] The practical approach to the precautionary principle is embodied in Principle 15 of the Rio Declaration:[52]

> *In order to protect the environment, the precautionary approach shall be widely applied by States according to their capabilities. Where there are threats of serious or irreversible damage, lack of full scientific certainty shall not be used as a reason for postponing cost-effective measures to prevent environmental degradation.*

While this may still seem vague, a number of authors have attempted to clarify the principle.

Scientific evaluation of the probability of risks should be employed to determine to what extent a reasonable risk of environmental harm exists.[49] Individual nations have the right to determine the level of acceptable risks to take, in so far as taking those risks does not unfairly place burdens on neighboring states or individuals least able to bear such risks.

The precautionary principle has engendered a heated debate in the scientific community. On one end it is seen as irrational, incoherent, and paralyzing to discovery, research and exploration. Conversely, proponents argue that it is a policy tool for making practical decisions in spite of scientific uncertainty. When appropriately defined and applied with careful weighing of reasonable risks, the precautionary principle can allow regulators and policy makers to take informed, rational approaches to protect the environment and human health without paralyzing scientific discovery.[35,51]

The precautionary principle will have the most potential to affect proposed systems with gene drives such as homing endonucleases, killer-rescue, and *Wolbachia*.[53–55] These approaches have the potential to spread to areas or countries with bans or moratoriums on transgenic technology. Therefore, any drive system will need to prepare for this encroachment and be able to reverse or cancel the spread of the system into unwanted areas. Furthermore, where the system is designed for eradication of the species there are the possibility of ecological knock-on effects. These effects may not be predictable or even known until the control strategy is underway. While these examples are not reasons in-of-themselves not to pursue a strategy, it would seem reasonable to prepare a method to recall the transgene. This agrees with Macer (2003) who states that the precautionary principle makes us "reasonably cautious" because it aligns with the principle of "do no harm," although no human action is completely without risk. Thus, there should be continual re-evaluation of the risks involved, and a plan to abort the program should be in place.[34] For genetically modified mosquitoes, this could be accomplished with additional drive systems or a rescue construct.[55,56]

An Ethical, Cultural, and Social Framework

The development of any framework is difficult. Stepping back to examine why something is done or how it ought to be done has eye-opening ramifications. If rushed, the creators of such a framework will have difficulty defending it to the public. This process will certainly yield diverse results depending on the situation. We suggest the principles outlined above as a framework with which to approach questions regarding transgenic pests and human health, fully aware that they may often create situations of conflict. Part of creating a framework is resolving conflict between principles or potentially making a value judgment as to which principle supersedes another. But a given framework should not be viewed as relativistic and thus dismissed as unprincipled; rather, it should produce similar results in similar situations. Thus, in deciding how to resolve conflicts between principles one must outline why one principle must take precedence over another. Ethicists and philosophers could be brought into the conversation as there are many tools within their disciplines in which to deal with conflicting principles in a logically defensible manner. We accept that no two situations or communities are exactly the same, but we argue that making a good-faith effort to utilize a framework will result in a publicly defensible approach to disease mitigation and mosquito control.

F.4.5 Regulation, Deliberation, and Public Communication of Biotechnology

Current US Regulation of Biotechnology

Current regulation of GMOs within the U.S. is delegated under the Coordinated Framework for the Regulation of Biotechnology (CFRB). This framework employed existing legislation and regulatory organizations to regulate biotechnology. In one sense, this is a result of a definitional question; the regulation of GE plants, microorganisms, food, and animals are divided among

These include the Toxic Substances Control Act (TSCA), Federal Insecticide, Fungicide, and Rodenticide Act (FIFRA), Federal Food Drug and Cosmetic Act (FFDCA), and the Federal Plant Pest Act (FPPA) (Kuzma, Najmaie & Larson, 2009).

These include the Food and Drug Administration (FDA), the Environmental Protection Agency (EPA), and the U.S. Department of Agriculture (USDA) (Kuzma, Najmaie & Larson, 2009).

the EPA, FDA, and USDA based on whether they are defined as "plant pests," "pesticides," "toxic chemicals," or "investigational new animal drugs."[57]

Regulatory Controversy and Oxitec

British biotech company, Oxitec, made the first release of GM mosquitoes for dengue control in 2009 on the Caribbean Island of Grand Cayman, with another trial in the summer of 2010.[58] The following year, Oxitec completed another release in Malaysia, supported by the Malaysian government.[59] While the 80% drop in the *Ae. aegypti* mosquito population in Grand Cayman was considered a major success by Oxitec, these releases have not come without controversy, with Science claiming "strained ties" between Oxitec and the Bill and Melinda Gates Foundation.[58] While anti-GMO activists have warned against potential risks of releasing GE mosquitoes, Nature Biotechnology cited disagreements having to do with regulatory processes; that is, some disagree with the speed at which Oxitec seemed to conduct releases, and the way in which these releases were communicated with the local communities. Oxitec founder Luke Alphey stated that flyers were distributed in Grand Cayman and government officials went door-to-door answering questions; however, many remain critical of the unorthodox press release via a YouTube video at the conclusion of the trials.[60] In addition to Oxitec's arguably sparse public communication efforts, other scientists were critical of Oxitec's procedure of conducting field trials and making information public before going through the peer review system.[60] Later, the Oxitec mosquitoes were released in Brazil to seemingly little public controversy, while the discussion of possible releases in the Florida Keys in the United States sparked a public petition against the releases.[61]

Debates regarding Oxitec's procedure of field releases and public communication strategy has directly spilled over into discussions regarding the regulation of GM pests. Most notably, R. Guy Reeves et al. offered a critique of the current regulatory system in the US, Cayman Islands, and Malaysia.[62] They strongly criticized the use of categorical exclusions (CEs) based on the 2008 Environmental Impact Statement (EIS) on GE insects. A CE is a request for

exemption from drafting a full environmental assessment (EA), with the argument that a new EA would be redundant and unnecessary. According to Reeves et al., CEs for GM insects are largely granted based on the 2008 EIS.[62] The 2008 EIS covered four species of GE insects: pink bollworm moth (*P. gossypiella*), Mediterranean fruit fly (*Ceratitis capitata*), Mexican fruit fly (*Anastrepha ludens*), and oriental fruit fly (*Bactrocera dorsalis*). They argue that the 2008-EIS is "scientifically deficient on the basis that (1) most consideration of environmental risk is too generic to be scientifically meaningful; (2) it relies on unpublished data to establish central scientific points; and (3) of the approximately 170 scientific publications cited, the endorsement of the majority of novel transgenic approaches is based on just two laboratory studies in only one of the four species covered by the document."[62] Furthermore, Reeves et al. argue that the continual reliance on the 2008 EIS, especially given what they see as scientific deficiencies, suggests that US regulators fail to acknowledge critical technological differences among different GE insects. In conclusion, they argue for a public engagement approach that includes public access to pre-release materials as well as a "high quality multi-disciplinary approach" in order for these new technologies to succeed.[62]

In a response, Alphey and Beech pointed to Reeves et al.'s argument for transparency in the pre-release process, stating the "argument has some merit, but needs to be balanced against significant practical difficulties. Technology developers have legitimate rights to protect proprietary information; governments understand this and provide statutory protections."[63] In addition, Alphey and Beech question Reeves et al.'s basis that regulatory decisions should be based primarily on peer reviewed scientific works, asserting that this argument "depends on three assumptions: that journal peer-review is a superior guarantee of quality than any other method, that no data from any other source can be of adequate quality to warrant consideration, and that regulators themselves are incapable of adequately assessing the quality and significance of data provided to them. Each of these assumptions is naïve at best."[63] Alphey and Beech believe that regulatory bodies should have access to a wider range of information aside from peer-reviewed studies and that peer-review should not be the benchmark for quality regulatory

data.[63]

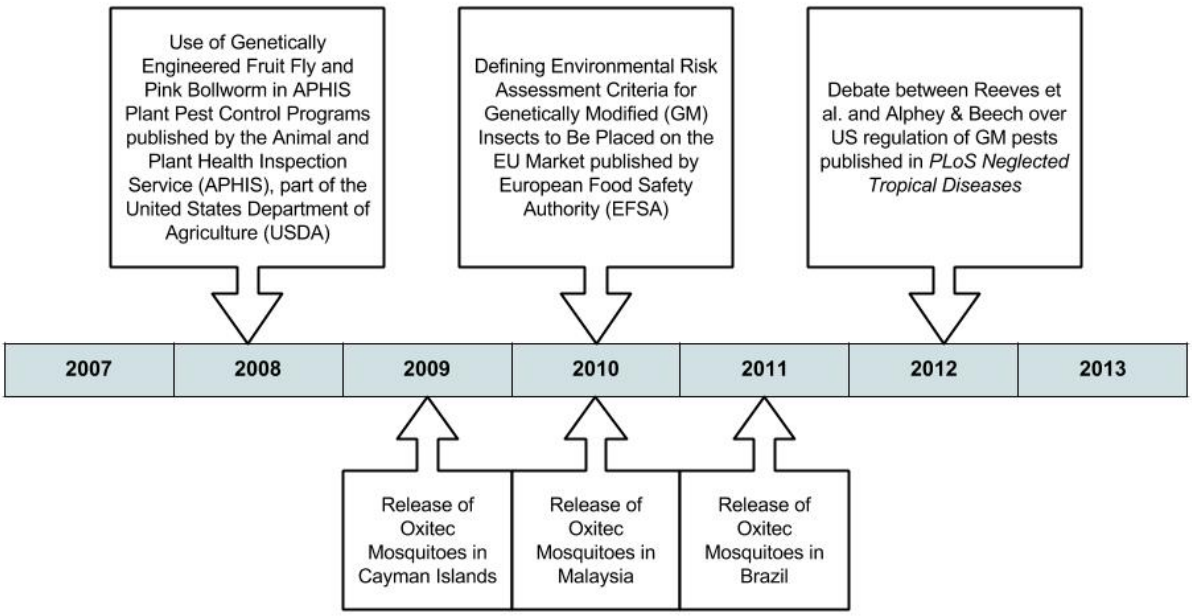

Figure F.1: Timeline of Oxitec mosquito releases and relevant regulation

As it currently sits, the controversy surrounding the Oxitec field releases seems to primarily circulate around social issues, both the social practices of the scientific community and what is seen as appropriate social interactions among scientists, regulators, and lay communities. As Alphey and Beech point out, Reeves et al. "confuse the concepts of transparency, independence, and scientific quality."[63] On the other hand, Alphey and Beech seem to reify these concepts themselves, not acknowledging that there may be a diversity of values surrounding each of these concepts, depending on the given situation.

Biotechnology and the Public Sphere

Regulation for biotechnologies like transgenic mosquitoes require a sensitivity to the academic and scientific traditions, or how knowledge is constructed and verified, of the nation at hand.

Jasanoff calls these traditions "civic epistemologies."[64] As Jasanoff defines it, a civic epistemology includes the citizens' and government's ideology regarding the roles that science and technology play in the nation. These frameworks are usually implicit, operating in the background of political and technical discussions. Discussions regarding the common values of a nation and how science and technology further or hinder these values can help bring this epistemological framework to the foreground, helping to bring the governing body to a stronger consensus on how to regulate these technologies.

This philosophy of debate perhaps best aligns with the concept of the public sphere, originally developed by Jrgen Habermas.[65] The Habermasian public sphere is intended to be an inclusive social space where issues are introduced, developed, and debated among a group of equal-standing citizens who are brought together by a common interest. However, it should not be taken for granted that all voices are given an equal and appropriate platform. Governing bodies must give due consideration to the voices that arise not only in governmental institutions, but also within common arenas such as public school associations, religious institutions, and other community organizations and NGOs.[66] These organizations are distinct from interest groups and lobbyists.[66] Explicit attention to the civic epistemologies of a nation, especially as it is defined in non-institutionalized community organizations, can help to bring attention to marginalized epistemologies, or counterpublics,[67] in order to enable a more inclusive form of participatory democracy, leading to a more desirable oversight framework that incorporates differing values, ethics, morals, and concerns of the affected citizens.[57]

Models of Public Communication

Sensitivity to the way in which a new technology is presented and discussed within a given community or communities is not merely to quibble over "rhetoric." This idea assumes a definition of "rhetoric" as "mere words" or "mere style" that is added as an extra flourish and has no effect on the core message. However, the academic tradition of rhetoric, stretching back to the work of Aristotle in Ancient Greece, studies the structure and effects of argumentation

and persuasion through the three appeals (*ethos*, or credibility and character; *pathos*, or emotion; and *logos*, or logic). While many may initially believe that only logos applies to science, many rhetoricians have illustrated how *ethos*, or credibility and character, has been a major driver in scientific communication. *Ethos* plays an especially strong role when scientists are called upon as policy advisors; several historical examples have been documented where scientists were both successful and unsuccessful in developing what was seen as an acceptable *ethos*, including J. Robert Oppenheimer in the case of nuclear warfare, Rachel Carson in the case of pesticides, and the Nongovernmental International Panel on Climate Change (IPCC).[68] When managed carefully and appropriately, a speakers ethos can help to garner trust among public communities.[69] In addition, rhetoricians have shown*pathos* is embedded in science communication, perhaps unconsciously, through arrangement, style, and diction in public communication about biotechnology.[70] This is not to say that *pathos* appeals should be flagged and avoided at all costs, as this would be an impossible task. Rather, a more productive use of rhetoric would be to give due attention to the values and emotions that are implicit in our communication and foreground these in public communication and deliberation. Foregrounding these values and emotions would open up a site of public deliberation that fairly considers the desires of the relevant stakeholders.

However, the model of public communication that has been used for some time by the scientific community has not accounted for this kind of open deliberation. In the past several decades, a deficit model of communication has been used widely by governmental agencies and biotech industries. This model is based on the Shannon-Weaver[71] model of communication that consists of a sender, receiver, noise, and feedback loop. This model comes with a number of problematic assumptions regarding the role of the audience and the role of the communicator. First of all, the traditional model of public communication of science assumes a one-way, linear mode of discourse flowing from the expert speaker to a lay audience, with a singular and transparent means of communication.[69] In this model, the audience is usually perceived as ignorant at best, hostile at worst, and in all cases in need of "simple, clear" information

in order to understand reason.[72] This model problematically assumes that pure information can be communicated and received without any alteration to the message; however, language studies scholars have argued that language choice inherently and unavoidable directs attention to certain aspects of a situation, while deflecting others.[73] Appeals to transparency are often made in the deficit model of communication, but the appeal to "transparency" hides the role of language in shaping how we understand science, nature, illness, the human condition, and so on, by ignoring how language unavoidably shapes meaning, ultimately governing what is admitted for discussion into the public sphere (Hartzog and Katz, unpublished manuscript). However, it is not only within the public sphere that style inherently directs what is discussed and how it is discussed. Even in the laboratory, the rhetorical figures of analogy, metaphor, and metonymy have been shown, through ethnographic research, to direct experimental research within the physics laboratory.[74]

Given that messages can never truly be sent through a "clear" channel, a model of communication that values multiple interpretations of information will create a more trustworthy, respectful, and productive discursive landscape for understanding and talking about this technology in regulatory debates. Several alternative models have been proposed by humanists and social scientists, including a rhetorical model of communication[69] and a "genetic" model of communication that understands specialist and public discourses as a "double helix," with one influencing the other.[75] Both the rhetorical and helical model of public communication emphasize a communication that is focused on influence rather than information. In other words, instead of the one-way information transfer model, these models emphasize recursivity, where scientists and stakeholders use a common language to engage in a back-and-forth dialog that influences one another's positions. In addition, the rhetorical model in particular emphasizes the complexities surrounding the speakers, audiences, languages, histories, and intentions around a

Analogy is a model of argument where one thing is compared to another thing that are essentially dissimilar. For example, discussing a budget in terms of going on a diet. Metaphor is a rhetorical figure that offers a way of "talking about one thing in terms of another." For example, talking about the human brain in terms of a computer. Metonymy is another rhetorical figure that can be defined as "a form of substitution in which something that is associated with x is substituted for x." For example, describing a group of on-duty Secret Service agents as "suits" (Jasinski, 2001).

given situation. Therefore, a close critique of various texts and spoken exchanges, is valued in order to understand what enabled productive/unproductive communication or miscommunication.

Public Opinion of Transgenics

Little research has been done on the public opinion of transgenic mosquitoes for dengue control. However, past research shows that public opinion of genetic modification of living organisms varies.[76] One public opinion survey found that the opinion of a representative sample of the US population varies slightly based on how the technology is presented, whether the technology is described as a "transgenic mosquito," a "genetically modified mosquito," a "genetically engineered mosquito," or "sterile mosquito."[77] Support for the release of "genetically modified," "genetically engineered" or "transgenic" mosquitoes was generally lower than support for the release of "sterile" mosquitoes. However, respondents exposed to all labels generally indicated that they believed the technology to be safer than insecticides.[77]

This change in opinion due to change in the label used is not surprising given past research of this nature. For example, research in H1N1/swine flu coverage illustrates that the latter term generally elicits a more emotional response and connection to the human experience with the flu, while the former distanced the flu from the human experience by emphasizing its scientific aspects.[78] In research concerning the global warming/climate change debate, preference in terminology aligned closely to party preference.[79,80] Sensitivity to the effects of language on public opinion should not be used simply in order to mislead the community into complacency. Rather, future research in public opinion of transgenic technologies should take into account how the technology is presented as one factor that affects public response. This information can then be used create a more accurate assessment of a communitys level of accepted risk regarding control measures, which can, in turn, inform regulatory decisions within the community.

In addition to studies of public opinion, future research should take into consideration how transgenic technologies are incorporated into the cultural norms of various communities. In

the case of transgenic mosquitoes, for example, this would include an understanding of the community control practices and how these are integrated into the citizens' daily lives. Arnold Pacey[81] offers a critique of what happens when technology is transferred from one culture to another (e.g. from the lab to the field), ultimately arguing for an experiential study of technology in society. That is, a focus on the knowledge and practices of the communities which use and/or are affected by the technologies developed by scientists and engineers. He expresses a deep need to discuss and justify technology using the discourse of these publics, rather than keeping the technologies close to the scientific communities until ready for release.

This cultural sensitivity is especially crucial in many cultural control methods. For example, the removal of vector breeding containers that was proposed to be an effective method of reducing vector populations, but this depends in part on active community involvement.[29] While it had been proposed that community intervention was effective, many of the studies suffered from a lack of methodological rigor (see Community Participation). It remains disputed if community involvement will decrease over time as enthusiasm for the new control methods fades.[31,82] Careful consideration of the sociological composition in a community is needed to avoid the potential pitfalls of community involvement research that could lead to a loss of trust for implementation of new control measures.

F.5 Conclusion

Every community charged with controlling malaria and/or dengue faces unique challenges regarding its available resources, political infrastructure and cultural values in implementing any control technique or treatment plan. We fully acknowledge that there can be no single most effective way to control vector-borne disease across so many different scenarios, and that any such decision rests entirely within the policymakers and public health officials of the community in question. What we have attempted here is to outline the various considerations that we believe should be taken into account when considering how best to control dengue, regardless of the decision reached. These considerations include the effectiveness of currently used control

measures, the potential use of transgenic control methods, risks and benefits of each, and diagnosis and treatment options including access to clean water and health care, public opinion, and bioethics.

While there remains no cure for dengue, the current treatment option of fluid replacement is simple and its availability should be prioritized, especially because it can benefit the treatment of a myriad of health issues beyond dengue. Likewise, accessibility to currently effective malaria treatment should be prioritized. Alongside the availability of treatment, proper emphasis must be given to informing people on how to correctly diagnose each disease, the timing of which is crucial for proper treatment. With fluid replacement for dengue and anti-malarial drugs, combined with early diagnosis, mortality rates from both diseases can be drastically reduced. For overcrowding of hospitals during dengue epidemics, we suggest the development of response units in endemic regions that can be mobilized when necessary to avoid the diversion of hospital resources.

Vector control remains a critical component in the integrated strategy to suppress malaria and dengue; however, current methods should be continually reassessed to monitor their effectiveness while other options, including GMO use, should be considered. We have outlined one ethical framework that we believe to be most widely applicable to the multitude of societies performing or considering vector control. By enumerating several relevant ethical principles (stewardship, animal welfare, justice as fairness, and precaution), we hope to shed light on how to proceed with discussions surrounding this controversial new technology. These principles as well as inclusive public discussions are particularly important considering the gaps in current regulations regarding the use of GMOs. Such discussions across both the expert and non-expert spheres are required in order for new policy to reflect both the most efficient form of vector control as well as the societys values and concerns.

The fight against malaria and dengue is far from over, but we hope to inform and encourage open discussion regarding the various forms of treatment and vector control, so that communities may take steps toward further reducing disease in the most efficient and responsible means

possible.

REFERENCES

1. American Academy of Arts & Sciences. The heart of the matter. Cambridge, 2013.

2. National Research Council (US) Committee on Genetically Modified Pest-Protected Plants. Genetically modified pest-protected plants: science and regulation. Washington, DC, 2000.

3. Snell C, Bernheim A, Berg J-B, et al. Assessment of the health impact of GM plant diets in long-term and multigenerational animal feeding trials: a literature review. Food Chem Toxicol 2012; 50: 1134-48.

4. Lereclus D, Delecluse A, Lecadet M-M. Diversity of Bacillus thuringiensis toxins and genes. In: Entwistle P, Cory JS, Bailey MJ, Higgs S, eds. Bacillus thuringiensis, an environmental biopesticide: theory and practice, John Wiley & Sons Ltd., 1993: 37-69.

5. USDA. Recent trends in GE adoption. United States Department of Agriculture, 2014. http://www.ers.usda.gov/data-products/adoption-of-genetically-engineered-crops-in-the-us/recent-trends-in-ge-adoption (accessed Aug 30, 2014).

6. Marshall A. Existing agbiotech traits continue global march. Nat Biotechnol 2012; 30: 207.

7. Wang S, Just D, Pinstrup-Andersen P. Bt-cotton and secondary pests. Int J Biotechnol 2008; 10: 113-21.

8. Nicolia A, Manzo A, Veronesi F, Rosellini D. An overview of the last 10 years of genetically engineered crop safety research. 2014; published online Feb 17. http://informahealthcare.com/doi/abs/10.3109/07388551.2013.823595 (accessed Aug 30, 2014).

9. WHO. Dengue and severe dengue: Fact sheet No. 117. Geneva: World Health Organization, 2014. http://www.who.int/mediacentre/factsheets/fs117/en/ (accessed

July 8, 2014).

10. WHO. Malaria: Fact Sheet No. 94. Geneva: World Health Organization, 2015. http://www.who.int/mediacentre/factsheets/fs094/en/ (accessed July 9, 2015).

11. CDC. Malaria. Centers for Disease Control and Prevention, 2014 http://www.cdc.gov/malaria/index.html (accessed Aug 30, 2014).

12. Bhatt S, Gething PW, Brady OJ, et al. The global distribution and burden of dengue. Nature 2013; 496: 504-7.

13. Kyle JL, Harris E. Global spread and persistence of dengue. Annu Rev Microbiol 2008; 62: 71-92.

14. WHO. Research priorities for the environment, agriculture and infectious diseases of poverty. Geneva: World Health Organization, 2013.

15. Hotez PJ, Yamey G. The evolving scope of PLoS Neglected Tropical Diseases. PLoS Negl Trop Dis 2009; 3: e379.

16. Hotez PJ. A plan to defeat neglected tropical diseases. Sci Am 2010; 302: 90-6.

17. Hotez PJ, Molyneux DH, Fenwick A, Ottesen E, Sachs SE, Sachs JD. Incorporating a rapid-impact package for neglected tropical diseases with programs for HIV/AIDS, tuberculosis, and malaria. PLoS Med 2006; 3: e102.

18. WHO/TDR. Guidance Framework for testing genetically modified mosquitoes. Geneva: World Health Organization, 2014.

19. Gubler DJ. Epidemic dengue/dengue hemorrhagic fever as a public health, social and economic problem in the 21st century. Trends Microbiol 2002; 10: 100-3.

20. Tun-Lin W, Lenhart A, Nam VS, et al. Reducing costs and operational constraints of dengue vector control by targeting productive breeding places: a multi-country non-inferiority cluster randomized trial. Trop Med Int Health 2009; 14: 1143-53.

21. WHO. Dengue: guidelines for diagnosis, treatment, prevention and control. Geneva: World Health Organization, 2009.

22. Morrison AC, Zielinski-Gutierrez E, Scott TW, Rosenberg R. Defining challenges and proposing solutions for control of the virus vector Aedes aegypti. PLoS Med 2008; 5: e68.

23. Bleakley H. Disease and development: evidence from hookworm eradication in the American south. Q J Econ 2007; 122: 73-117.

24. Reiter P, Lathrop S, Bunning M, et al. Texas lifestyle limits transmission of dengue virus. Emerg Infect Dis 2003; 9: 86-9.

25. WHO. Emerging infectious diseases?: World Health Day 1997 information kit. Geneva: World Health Organization, 1997.

26. Bleakley H. Health, human capital, and development. Annu Rev Econom 2010; 2: 283-310.

27. French D. Causation between health and income: a need to panic. Empir Econ 2012; 42: 583-601.

28. Strauss J, Thomas D. Health, nutrition, and economic development. J Econ Lit 2008; 36: 766-817.

29. Gubler DJ, Clark GG. Community involvement in the control of Aedes aegypti. Acta Trop 1996; 61: 169-79.

30. Armada Gessa JA, Gonzalez RF. Application of environmental management principles in the programme for eradication of Aedes (Stegomyia) aegypti (Linneus, 1762) in the Republic of Cuba, 1984. New Delhi: WHO Regional Office for South-East Asia, Dengue Newsletter 1987; 3:111-119.

31. Toldeo Romani ME, Vanlerberghe V. Achieving sustainability of community-based dengue control in Santiago de Cuba. Soc Sci Med 2007; 64: 976-88.

32. Chang S-F, Huang J-H, Shu P-Y. Characteristics of dengue epidemics in Taiwan. J Formos Med Assoc 2012; 111: 297-9.

33. Gau Y-M, Buettner P, Usher K, Stewart L. Burden experienced by community health volunteers in Taiwan: a survey. BMC Public Health 2013; 13: 491.

34. Macer D. Ethical, legal and social issues of genetically modified disease vectors in public health. World Health Organization, 2003.

35. Resnik DB. Environmental health ethics. Cambridge University Press, 2012.

36. Resnik DB. Ethical issues in field trials of genetically modified disease-resistant mosquitoes. Dev World Bioeth 2014; 14: 37-46.

37. Worrell R, Appleby MC. Stewardship of natural resources: definition, ethical and practical aspects. J Agric Environ Ethics 2000; 12: 263-77.

38. Carson R. Silent spring. Houghton Mifflin Harcourt, 2002.

39. Bosch R Van Den. The pesticide conspiracy. University of California Press, 1989.

40. Perkins JH. Insects, experts, and the insecticide crisis: the quest for new pest management strategies. Plenum Press, 1982.

41. Rollin BE. The moral status of research animals in psychology. Am Psychol 1985; 40: 920-6.

42. Verhoog H, Matze M, Bueren EL van, Baars T. The role of the concept of the natural (naturalness) in organic farming. J Agric Environ Ethics 2003; 16: 29-49.

43. Singer P. Animal liberation: towards an end to mans inhumanity to animals. 1977.

44. Verhoog H. The concept of intrinsic value and transgenic animals. J Agric Environ Ethics 1992; 5: 147-60.

45. Hauskeller M. Biotechnology and the integrity of life: taking public fears seriously. Ashgate Publishing, Ltd., 2007.

46. Rawls J. A theory of justice. Harvard University Press, 1971.

47. Platt JR. Strong Inference: Certain systematic methods of scientific thinking may produce much more rapid progress than others. Science 1964; 146: 347-53.

48. Comstock G. Ethics and genetically modified foods. In: Gottwald F-T, Igensiep HW, Meinhardt M, eds. Food ethics. Springer Science & Business Media, 2010: 49-66.

49. Resnik DB. Is the precautionary principle unscientific? Stud Hist Philos Sci Part C Stud Hist Philos Biol Biomed Sci 2003; 34: 329-44.

50. Peterson M. The precautionary principle is incoherent. Risk Anal 2006; 26: 595-601.

51. Dorman P. Evolving knowledge and the precautionary principle. Ecol Econ 2005; 53: 169-76.

52. United Nations. Rio declaration on environment and development. Rio de Janeiro: United Nations Environment Programme, 1992.

53. Windbichler N, Menichelli M, Papathanos PA, Thyme SB, Li H, Ulge UY, et al. A synthetic homing endonuclease-based gene drive system in the human malaria mosquito. Nature 2011; 473: 212-5.

54. Gould F, Huang Y, Legros M, Lloyd AL. A killer-rescue system for self-limiting gene drive of anti-pathogen constructs. Proc Biol Sci 2008; 275: 2823-9.

55. Sinkins SP, Gould F. Gene drive systems for insect disease vectors. Nat Rev Genet 2006; 7: 427-35.

56. Burt A. Site-specific selfish genes as tools for the control and genetic engineering of natural populations. Proc Biol Sci 2003; 270: 921-8.

57. Kuzma J, Najmaie P, Larson J. Evaluating oversight systems for emerging technologies: a case study of genetically engineered organisms. J Law Med Ethics 2009; 37: 546-86.

58. Enserink M. GM Mosquito trial strains ties in Gates-funded project. Science/AAAS News Sci Insid 2010. http://news.sciencemag.org/2010/11/gm-mosquito-trial-strains-ties-gates-funded-project (accessed Aug 30, 2014).

59. Enserink M. GM Mosquito release in Malaysia surprises opponents and scientists again. Science/AAAS News Sci Insid 2011. http://news.sciencemag.org/asia/2011/01/gm-mosquito-release-malaysia-surprises-opponents-and-scientistsagain (accessed Aug 30, 2014).

60. Subbaraman N. Science snipes at Oxitec transgenic-mosquito trial. Nat Biotechnol 2011; 29: 9-11.

61. Maxmen A. Florida abuzz over mosquito plan. Nature 2012; 487: 286.

62. Reeves RG, Denton JA, Santucci F, Bryk J, Reed FA. Scientific standards and the regulation of genetically modified insects. PLoS Negl Trop Dis 2012; 6: e1502.

63. Alphey L, Beech C. Appropriate regulation of GM insects. PLoS Negl Trop Dis 2012; 6: e1496.

64. Jasanoff S. Designs on nature: science and democracy in Europe and the United States. Princeton University Press, 2007.

65. Habermas J. The structural transformation of the public sphere: an inquiry into a category of bourgeois society. MIT Press, 1991.

66. Hauser GA. Vernacular dialogue and the rhetoricality of public opinion. Commun Monogr 1998; 65: 83-107.

67. Fraser N. Rethinking the public sphere: a contribution to the critique of actually existing democracy. Soc Text 1990; 25: 56-80.

68. Walsh L. Scientists as prophets: a rhetorical genealogy. Oxford University Press, USA, 2013.

69. Katz S, Miller C. The low-level radioactive waste siting controversy in North Carolina: toward a rhetorical model of risk communication. In: Herndl CG, Brown SC, editors. Green culture: environmental rhetoric in contemporary America. University of Wisconsin Press; 1996, p. 111-40.

70. Katz SB. Language and persuasion in biotechnology communication. 2002; published online Jan 24. http://www.agbioforum.org/v4n2/v4n2a03-katz.htm (accessed Aug 30, 2014).

71. Shannon CE, Weaver W. The mathematical theory of communication. University of Illinois Press, 1967.

72. Bucchi M. Handbook of public communication of science and technology. Routledge, 2008.

73. Burke K. Language as symbolic action: essays on life, literature, and method. University of California Press, 1966.

74. Graves HB. Rhetoric in(to) science: style as invention in inquiry. Hampton Press, 2005.

75. Bucchi M. Can genetics help us rethink communication? Public communication of science as a "double helix." New Genet Soc 2004; 23: 269-83.

76. Brossard D, Shanahan J. The media, the public and agricultural biotechnology. CABI, 2007.

77. Shipman M. First-ever national survey on genetically engineered mosquitoes shows mixed support. 2012.

78. Angeli E. Metaphors in the rhetoric of pandemic flu: electronic media coverage of H1N1 and swine flu. J Tech Writ Commun 2012; 42. No. 3: 203-22.

79. Schuldt JP, Konrath SH, Schwarz N. "Global warming" or "climate change"?: whether the planet is warming depends on question wording. Public Opin Q 2011; 75: 115-24.

80. Whitmarsh L. What's in a name? Commonalities and differences in public understanding of "climate change" and "global warming." Public Underst Sci 2008; 18: 401-20.

81. Pacey A. Meaning in technology. MIT Press, 2001.

82. Spiegel J, Bennett S, Hattersley L, Hayden MH, Kittayapong P, Nalim S, et al. Barriers and bridges to prevention and control of dengue: the need for a social-ecological approach. Ecohealth 2005; 2: 273-90.